The Astrophysical Journal, 811:32 (42pp), 2015 September 20 doi:10.1088/0004-637X/811/1/32

THE 2010 ERUPTION OF THE RECURRENT NOVA U SCORPII: THE MULTI-WAVELENGTH LIGHT CURVE

Ashley Pagnotta[1], Bradley E. Schaefer[2], James L. Clem[2], Arlo U. Landolt[2], Gerald Handler[3], Kim L. Page[4], Julian P. Osborne[4], Eric M. Schlegel[5], Douglas I. Hoffman[6], Seiichiro Kiyota[7], and Hiroyuki Maehara[8]
[1] Department of Astrophysics, American Museum of Natural History, New York, NY 10024, USA; pagnotta@amnh.org
[2] Department of Physics and Astronomy, Louisiana State University, Baton Rouge, LA 70803, USA
[3] Nicolaus Copernicus Astronomical Center, Bartycka 18, 00-716 Warsaw, Poland
[4] Department of Physics and Astronomy, University of Leicester, Leicester LE1 7RH, UK
[5] Department of Physics and Astronomy, University of Texas at San Antonio, San Antonio, TX 78249, USA
[6] Infrared Processing and Analysis Center, California Institute of Technology, Pasadena, CA 91125, USA
[7] 7-1 Kitatasutomi, Kamagaya, Chiba 273-0126, Japan
[8] Kwasan Observatory, Kyoto University, Yamashina-ku, Kyoto 607-8471, Japan
Received 2015 June 5; accepted 2015 August 4; published 2015 September 17

ABSTRACT

The recurrent nova U Scorpii most recently erupted in 2010. Our collaboration observed the eruption in bands ranging from the *Swift* XRT and UVOT *w2* (193 nm) to *K*-band (2200 nm), with a few serendipitous observations stretching down to *WISE W2* (4600 nm). Considering the time and wavelength coverage, this is the most comprehensively observed nova eruption to date. We present here the resulting multi-wavelength light curve covering the two months of the eruption as well as a few months into quiescence. For the first time, a U Sco eruption has been followed all the way back to quiescence, leading to the discovery of new features in the light curve, including a second, as-yet-unexplained, plateau in the optical and near-infrared. Using this light curve we show that U Sco nearly fits the broken power law decline predicted by Hachisu & Kato, with decline indices of -1.71 ± 0.02 and -3.36 ± 0.14. With our unprecedented multi-wavelength coverage, we construct daily spectral energy distributions and then calculate the total radiated energy of the eruption, $E_{\rm rad} = 6.99^{+0.83}_{-0.57} \times 10^{44}$ erg. From that, we estimate the total amount of mass ejected by the eruption to be $m_{\rm ej} = 2.10^{+0.24}_{-0.17} \times 10^{-6} M_{\odot}$. We compare this to the total amount of mass accreted by U Sco before the eruption, to determine whether the white dwarf undergoes a net mass loss or gain, but find that the values for the amount of mass accreted are not precise enough to make a useful comparison.

Key words: novae, cataclysmic variables – stars: individual (U Scorpii)

Supporting material: machine-readable tables

1. U SCORPII

The 2010 eruption of the recurrent nova (RN) U Scorpii was predicted by Schaefer (2005) and discovered independently by B. G. Harris and S. Dvorak as part of an intense monitoring campaign coordinated by our group at Louisiana State University (LSU) and the American Association of Variable Star Observers (AAVSO; Schaefer et al. 2010a, 2010b; Simonson & MacRobert 2010). The discovery triggered a worldwide invocation of both pre-planned (target of opportunity) and serendipitous observing programs. This was the tenth observed eruption of U Sco (Schaefer 2010), and became by far the best observed nova eruption to date. The eruption began on JD 2455224.32 ± 0.12, peaked on JD 2455224.69 ± 0.07 (T_0) at $V = 7.5$ mag, and returned to quiescence 67 days later (Schaefer et al. 2010b).

We present multi-wavelength photometry of the complete eruption obtained by our extensive collaboration of both professional and amateur astronomers. U Sco was observed in all wavelengths from radio to gamma-rays during the 2010 eruption, with detections from IR to soft X-ray. The fast time variations of the light curve are discussed in detail in Schaefer et al. (2011); here we focus on the overall shape and spectral energy distribution (SED). We construct daily SEDs and use them to get a new estimate of the total amount of mass ejected during the eruption, $m_{\rm ej}$, following the method described in Shara et al. (2010). It is critical to get a good measurement of $m_{\rm ej}$ and compare it to estimates of the total amount of mass accreted during the time interval preceding the eruption to ascertain whether the white dwarf (WD) in the system is gaining or losing mass over the course of the eruption cycle. If the WD, which is already near the Chandrasekhar limit (Hachisu et al. 2000; Thoroughgood et al. 2001), is in fact gaining mass and is composed primarily of carbon and oxygen, it must eventually become a Type Ia supernova (SN Ia). Determining whether RNe can become SNe Ia takes us one step closer to solving the long-standing SN Ia progenitor problem and improving the cosmological measurements that rely on SN Ia standard candle distances.

2. OBSERVATIONS

A full list of observers and observation details for the multi-wavelength light curve in this paper is presented in Table 1. The observations were largely coordinated by our group at LSU and were carried out at telescopes all over the world and from a number of orbiting observatories. The discovery occurred on 2010 January 28 (with the first image taken by B. J. Harris at HJD 2455224.94) and, upon confirmation, we immediately notified our collaboration and began observing U Sco nearly constantly. The BVR_cI_cJHK observations by Pagnotta using the SMARTS 1.3 m at CTIO and $UBVR_cI_c$ observations by Handler using the SAAO 0.5 m form the backbone of our optical/near-IR light curve and can be seen in Figure 1, where the observations within a tenth of a phase of eclipse have been removed to better show the overall trend.

Table 1
Observer Details

Observer	Telescope	Location	Filters
Pagnotta	CTIO 1.3 m	Cerro Tololo, Chile	*BVRIJHK*
Handler	SAAO 0.5 m	Sutherland, South Africa	*UBVRIy*
Clem	CTIO 1.3 m	Cerro Tololo, Chile	Strömgren *y*
Landolt	KPNO 2.1 m	Kitt Peak, Arizona	Strömgren *y*
Maehara	Kwasan 0.25 m	Kyoto, Japan	Strömgren *y*
Kiyota	0.25 m Schmidt–Cassegrain	Ibaraki, Japan	Strömgren *y*
...	*Swift* UVOT	…	*w*1 (260 nm), *w*2 (193 nm)
...	*Swift* XRT	…	0.3–10 keV
...	*WISE*	…	*W*1 (3400 nm), *W*2 (4600 nm)

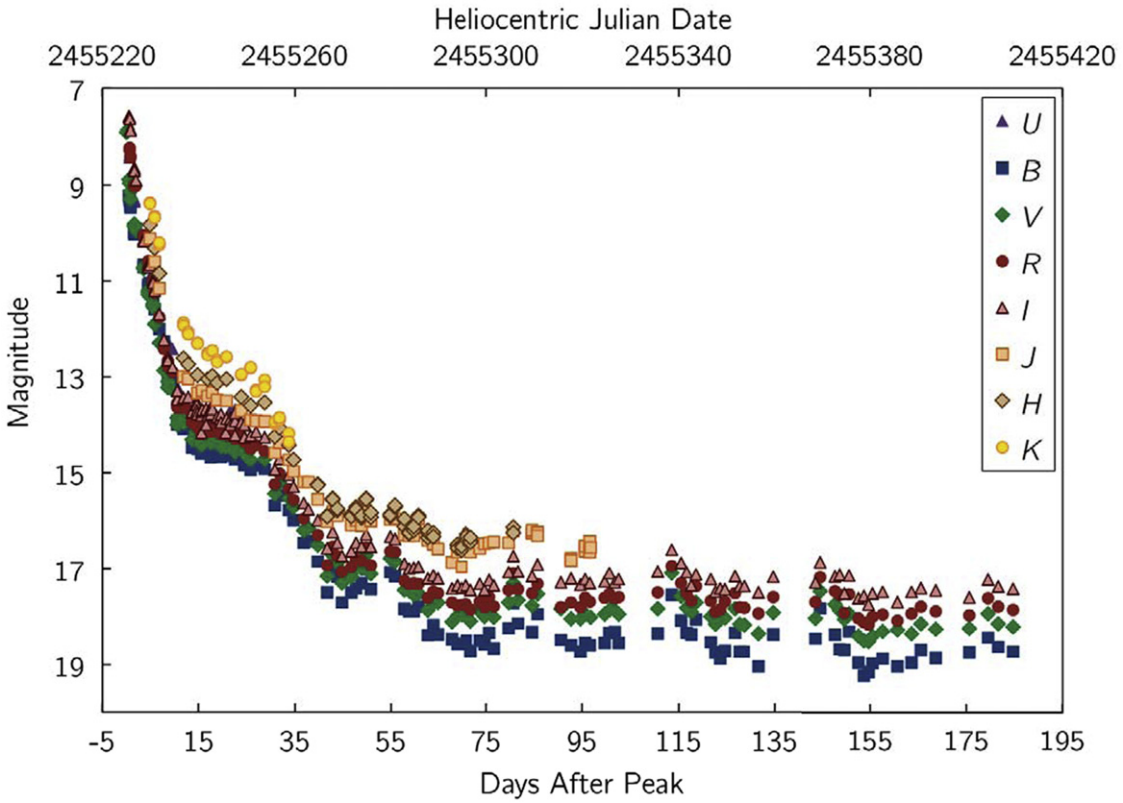

Figure 1. U Sco $UBVR_cI_cJHK$ Full Light Curve from the CTIO 1.3 m and SAAO 0.5 m Telescopes. A *U*-band filter was available for the SAAO 0.5 m but not the CTIO 1.3 m, so the *U*-band data cover only the first month. Due to decreasing signal-to-noise in the near-IR as U Sco faded, the *J*, *H*, and *K* observations end on days 97, 81, and 34 after peak, respectively. This figure shows all of our non-Strömgren out-of-eclipse observations from CTIO and SAAO, lasting until 2010 July 31. The observations within a tenth of a phase of eclipse have been removed to better show the overall trend of the light curve. We followed U Sco far past its return to quiescence to ensure that all late-time phenomena would be observed.

Regular observations were made by the *Swift* XRT and UVOT instruments and analyzed by Page on behalf of the *Swift* Nova-CV Group; they provide the UV and X-ray light curves presented here. U Sco was observed in the hard X-ray and gamma-ray regime by *INTEGRAL*, the *Swift* BAT, *RXTE*, the Fermi GBM, and the MAXI detectors on the International Space Station, but was not detected in hard X-rays by any instrument (Manousakis et al. 2010; E. Kuulkers & K. Mukai 2010, private communication; H. Krimm 2010, private communication; J. Rodi 2010, private communication; T. Mihara and the MAXI team 2015, private communication). The GMRT and ATCA observatories looked at U Sco in radio, but there were no positive detections (G. C. Anupama & N. G. Kantharia 2010, private communication; S. Eyres & T. O'Brien 2010, private communications). Additionally, there were a few serendipitous observations made by the *WISE* satellite during its infrared survey mission.

The U Sco 2010 optical/near-IR eruption light curve can loosely be broken down into five different parts: the initial fast decline (days 0–14 after peak), the first plateau (days 14–32), the subsequent fall (days 32–41), the second plateau (days 41–54), and the jittery return to quiescence (days 54–67). Figure 2 shows a subset of the data from Figure 1, namely the out-of-eclipse observations taken during the course of the actual eruption, to make it easier to distinguish the overall shape of the light curve as well as the different parts. The initial fast decline lasted for approximately two weeks, from the peak until the start of the plateau on day 14. The start of the plateau occurs at approximately the same time it did in previous eruptions and coincides with the detection of the supersoft

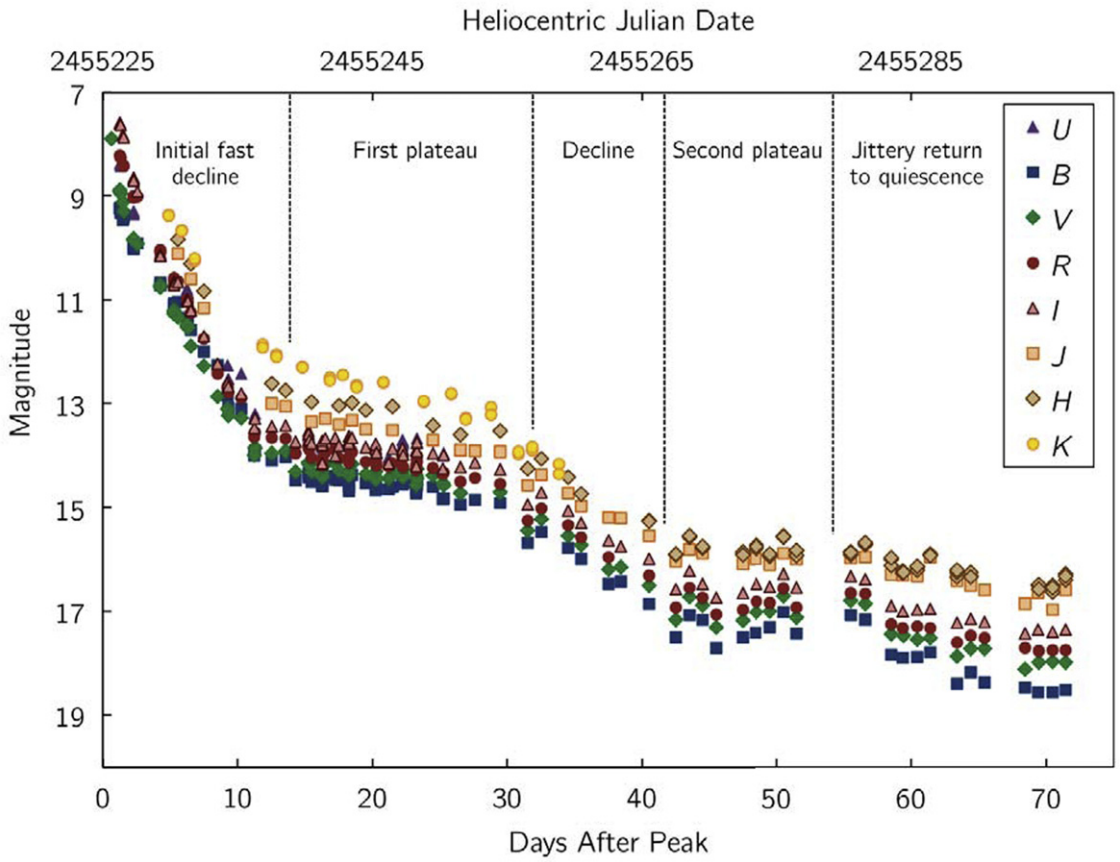

Figure 2. Zoomed-in version of the U Sco *UBVR$_c$I$_c$JHK* Eruption Light Curve from the CTIO 1.3 m and SAAO 0.5 m Telescopes for phases 0.1–0.9. This plot ends at day 71 (after peak), showing just the actual eruption of U Sco and a few days of quiescence. The eruption light curve can be divided into five main parts: the initial fast decline (days 0–14), the first plateau (days 14–32), the subsequent decline (days 32–41), the second plateau (days 41–54), and the jittery return to quiescence (days 54–67). This marks the first time that U Sco has been systematically followed past day 30, and therefore the first time the second plateau has been observed (Pagnotta et al. 2010).

X-rays by *Swift* and the reappearance of the optical eclipses (Schlegel et al. 2010d; Schaefer et al. 2011). These three events are correlated with the thinning of the expanding nova shell, as described by Hachisu et al. (2008): once the shell has become optically thin, it no longer blocks the actual U Sco binary (the two stars and the re-forming accretion disk), and both the X-rays and the eclipses are revealed. Some of the X-rays are reprocessed by circumstellar material to longer wavelengths, and this provides the source of the extra light that causes the UV, optical, and near-IR plateaus. The first plateau lasts for approximately 18 days, during which the eclipses are shallower than during quiescence and the secondary eclipse is visible (Schaefer et al. 2011). At the end of the plateau, the UV, optical, and near-IR light curves resume their drop-off, at a rate slower than the initial decline.

The second plateau begins on approximately day 41 after peak and lasts until day 54. During this second plateau, the average *V*-band magnitude is 17.01, and it varies between 16.71 and 17.30, hovering approximately 1 mag above the quiescent level of $V = 18.0$. This second plateau of U Sco was not seen in any previous eruption, because none of them were followed regularly past day 30. Concurrent fast time series photometry of U Sco showed aperiodic optical dips with amplitudes of up to 0.6 mag (Schaefer et al. 2011). These dips are linked to eclipses of the central light source due to turbulence in the still re-forming accretion disk, but we are unaware of any theoretical link between them and the second plateau. On approximately day 54 the second plateau ended and U Sco resumed fading, returning to quiescence on day 67.

The optical/near-IR colors are relatively constant throughout the eruption. The notable exception to this color constancy is shortly after peak: initially U Sco was brighter in *V* than in *B*, but around HJD 2455228 this switched, and *B* was brighter for approximately 7 days, until HJD 2455235 when the colors switched back and *V* remained brighter than *B* for the rest of the eruption, which is the usual state of the system in quiescence.

The *Swift* UVOT (Roming et al. 2005) regularly monitored the eruption in the ultraviolet bands *w*1 (260.0 nm) and *w*2 (192.8 nm), and also took occasional snapshots in the *u* (346.5 nm) and *m*2 (224.6 nm) bands. The shape of the UV light curve is very similar to that of the optical/near-IR light curve; this can be seen in Figure 3, which compares the *Swift* *w*1 light curve to the idealized *V*-band light curve, which was constructed from more than 35,000 fast time series observations (Pagnotta et al. 2010). The eclipses that are visible in the optical and near-IR data are visible in the UV as well, as was originally noted in Ness et al. (2012). Figure 4 shows a phased *Swift w1* light curve that clearly shows the primary eclipse and shows indications of the secondary eclipse, although there is a lot of scatter. The *Swift* XRT, which is sensitive to the energy range 0.3–10 keV, also observed U Sco regularly. The X-ray light curve compared to the idealized *V*-band light curve can be seen in Figure 5, as well as in Ness et al. (2012) and Orio et al. (2013), which discuss different aspects of the X-ray emission.

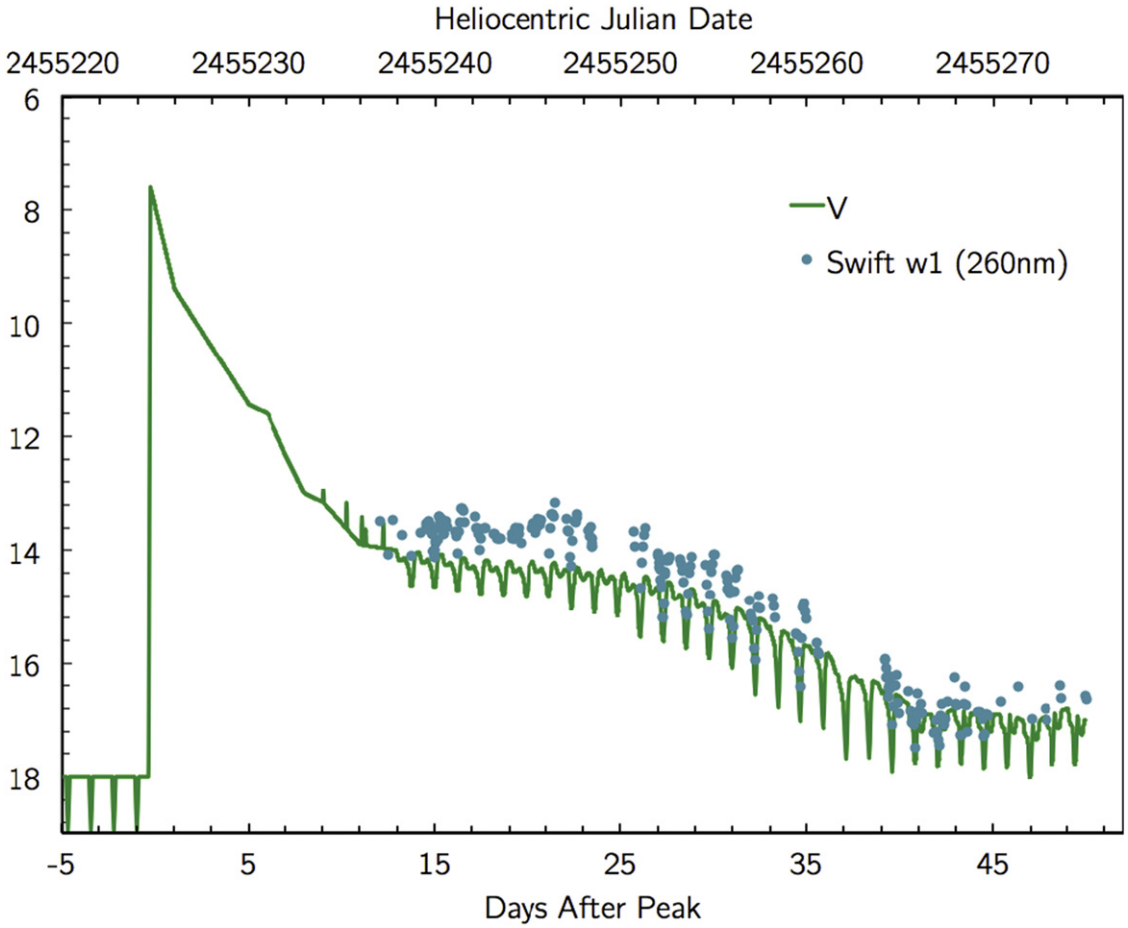

Figure 3. UV vs. *V*-band comparison. The *Swift* *w*1 (260 nm) light curve is plotted along with the idealized *V*-band light curve (Pagnotta et al. 2010). The shape of the UV light curve closely tracks that of the optical, with the UV also showing primary eclipses on U Sco's orbital period.

The eclipses start to reappear in the XRT light curve at approximately the same time they do in optical, near-IR, and UV, however they are not as well defined until around day 30 (Osborne et al. 2010; Schaefer et al. 2010c; E. M. Schlegel et al. 2015, in preparation), perhaps due to the presence of aperiodic X-ray dips early on in the eruption (Ness et al. 2012).

The *WISE* infrared survey mission (Wright et al. 2010) was operating during the eruption and serendipitously observed U Sco ten times from HJD 2455252.5 to 2455253.3 in bands *W*1 (3400 nm) and *W*2 (4600 nm). (For clarity, we use lowercase *w*1 and *w*2 for the *Swift* bands and uppercase *W*1 and *W*2 for the *WISE* bands throughout this paper.) We extracted these observations from the *WISE* All-Sky Single Exposure (L1b) Source Table.[9]

Table 2 shows the average daily magnitudes in all bands, with missing days or observations that occurred during eclipse filled in using the interpolation and extrapolation methods described in Section 4 and denoted in the tables with daggers (†) and double daggers (‡) on the interpolated and extrapolated values, respectively. There are only two days with *WISE* observations; we have listed them in the table but have not extrapolated backward and forward, because there are not enough data to be confident in the comparison between *W*1, *W*2, and *V*-band. Tables 3 and 4 list *all* of our observations over the entire course of the eruption, including those taken during or near eclipse, with Table 3 giving all of the IR to UV magnitudes and Table 4 showing the X-ray count rates.

[9] http://irsa.ipac.caltech.edu/cgi-bin/Gator/nph-dd?catalog=wise_allsky_4band_p1bs_psd

3. UNIVERSAL DECLINE LAW

Hachisu & Kato (2006) introduced a universal decline law for novae that can be used to predict the turn-on and turn-off of supersoft X-ray flux as well as estimate the mass of the WD in some cases. Their template light curve has a slope of $F \sim t^{-1.75}$ shortly after peak, where F is flux (measured in magnitudes) and t is time (in days from peak), and a slope of $F \sim t^{-3.5}$ in the later part of the eruption light curve. They note that it is best to look at the narrow Strömgren *y*-band light curve to test this law, because it is free of contamination from strong emission lines. We therefore arranged for as many Strömgren *y* observations of U Sco as possible. This is difficult because Strömgren *y* is no longer a common filter, but we were able to obtain coverage from Handler on the SAAO 0.5 m, Landolt on the KPNO 2.1 m, Clem on the CTIO 1.0 m, Kiyota using his personal 0.25 m Schmidt–Cassegrain telescope, and Maehara using the Kwasan Observatory 0.25 m. The full Strömgren *y* light curve can be seen in Figure 6. Figure 7 shows the best fit power laws for the Strömgren *y* data (using only the data from phases 0.1 to 0.9 to avoid the eclipses), with indices and 1σ errors of -1.68 ± 0.03 for the first power law and -3.18 ± 0.10 for the second. However, since the coverage is somewhat sparse, the break time is not well defined. To remedy this, we also fit the *V*-band

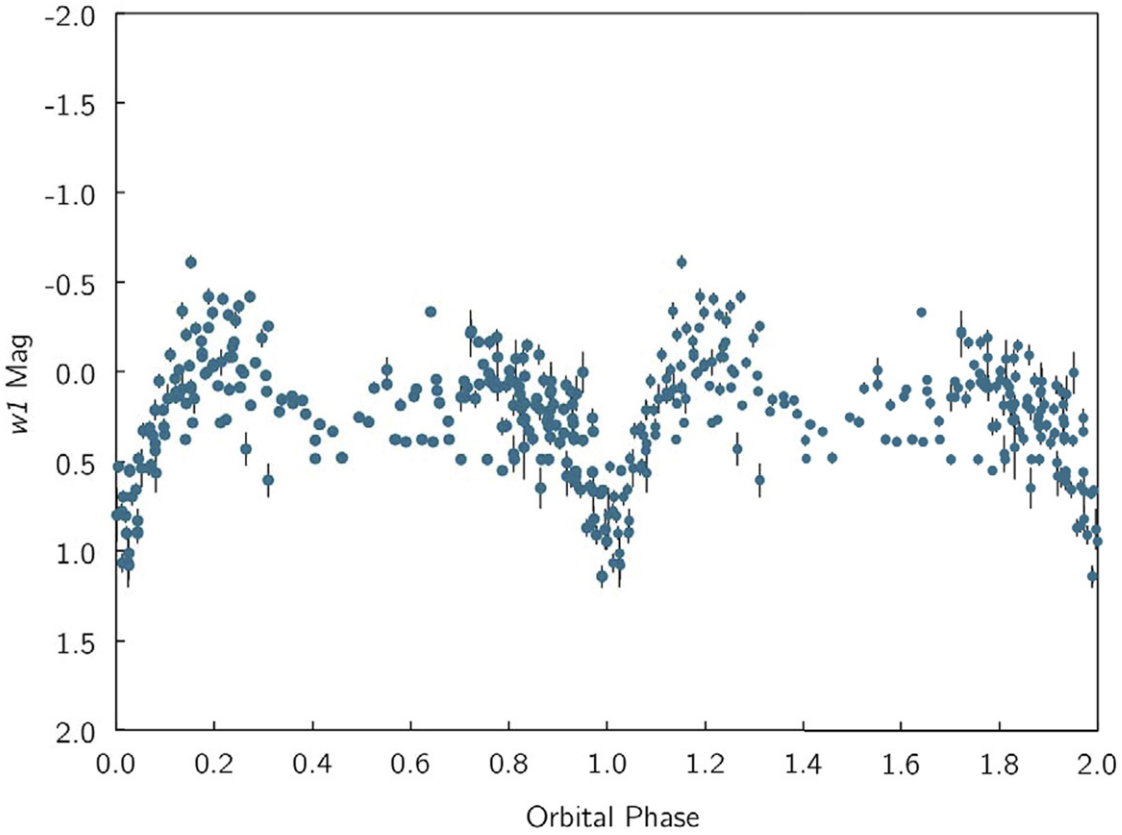

Figure 4. Phased UV light curve. The *Swift* *w*1 light curve is folded on the known orbital period of U Sco ($P_{\rm orb} = 1.23$ days, Schaefer 2010) and the phased light curve is plotted twice to make it easier to visually identify the primary eclipse, which occurs at phase 0. The error bars represent the 1σ error; when they are not visible it is because the error is smaller than the point size. The points in the figure come from all times after the reappearance of the eclipses on Day 14 except during the second plateau (Days 41–54), during which the aperiodic optical dips (see Section 2 and Schaefer et al. 2011) add noise to the phased light curve. The primary eclipse is clearly visible, and there appears to be an indication of the secondary eclipse as well, although there is too much scatter to say that it is definitively detected.

data, shown in Figure 8, which gives power law indices of -1.71 ± 0.02 and -3.36 ± 0.14 for the first and second power laws, respectively, and a break time of $\log(T - T_0) = 1.487 \pm 0.005$, which gives $T =$ HJD 2455255.38 ± 1.01 days. Despite the fact that *V* is a broad-band filter which includes some contaminating emission line fluxes, it is reasonable to fit the *V*-band data as well because *V* and Strömgren *y* track each other almost identically, as shown in Figure 9. We then used the break time found from the *V* band data to better determine the slopes of the Strömgren *y* fits, and from that we obtained the fit values quoted above. For both bands, our results are nearly consistent with the predictions of Hachisu & Kato (2006) within errors, with the small differences possibly due to the unusual features of the U Sco light curve such as the two plateaus.

For some novae, if they fit the model well, the break time can be used to determine the composition of the WD, whether it is carbon–oxygen or oxygen–neon–magnesium. Unfortunately for our case with U Sco, the models do not yet account for WDs very close to the Chandrasekhar limit, nor are they fully capable of dealing with RNe (I. Hachisu 2010, private communication), so we are unable to use this method to reliably determine the type of WD in the U Sco system. A crude extrapolation of Hachisu & Kato's (2006) Table 10 indicates that U Sco, with a $T - T_0 = 30.7$, should have a WD with a high neon content, but this is not a conclusive result.

4. SPECTRAL ENERGY DISTRIBUTION

With our comprehensive data set, we can construct daily SEDs for the entire eruption, allowing us to closely follow the multi-wavelength evolution of U Sco. The SEDs were constructed using predominantly the CTIO 1.3 m, SAAO 0.5 m, and *Swift* UVOT observations, so the average wavelength coverage is from 193 nm (*Swift* UVOT *w2*) to 2200 nm (*K*-band). Selected SEDs can be seen in Figure 10, which includes scientifically interesting days such as those just after peak (when most of the energy is released, in a wavelength range that unfortunately coincides with a gap in our coverage) and one of the days with *WISE* coverage, as well as more average days later in the eruption. Because of the scarcity of the *WISE* data and our lack of confidence in any extrapolation over the entire length of the eruption, the far-IR observations from *WISE* are only included on the actual days they were made. Since the amount of energy released in the far-IR is negligible compared to that released in shorter wavelengths, the inclusion of two days of *WISE* data does not introduce any measurable errors to the overall calculation. This is the first time any nova has had enough observations over a wide range of wavelengths and at such a fast time cadence that a plot such as this could be constructed.

Using a distance of 12 kpc (Schaefer 2010), the average luminosity of the system in erg s^{-1} can be calculated on a daily basis and then summed to obtain the total amount of radiated

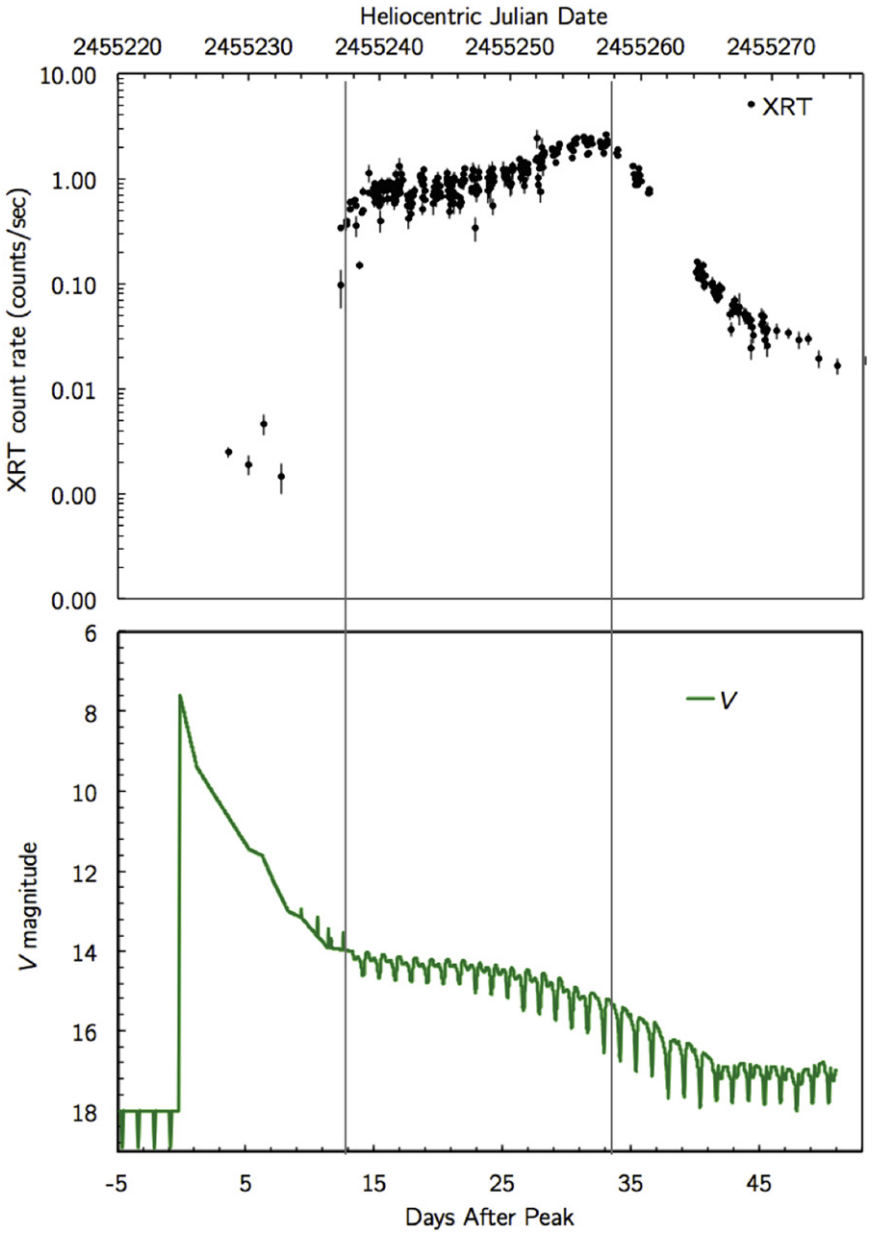

Figure 5. *Swift* XRT+*V*-Band Light Curve. The *Swift* XRT light curve is shown in the top figure, and compared to the idealized *V*-band light curve, shown in the bottom (Pagnotta et al. 2010). The X-rays brighten drastically around day 14. At the same time, the optical plateau begins and the eclipses reappear. These three effects are all observed at the same time, when the expanding nova shell becomes optically thin and we can once again see down to the underlying binary system. The X-ray turn-on and peak are marked on this figure with solid gray vertical lines.

energy, $E_{\rm rad}$. We start with the observed magnitudes available for each HJD and then bin each day's observations to get a daily average. On days where there was no observation in a given band, the average luminosity was linearly interpolated based on the values for that band on the days immediately preceding and following it, or linearly extrapolated based on its average difference from a neighboring band for which there was an observation. The latter extrapolation is reasonable since the colors during eruption are relatively constant, as discussed in Section 2. For bands with shorter wavelengths (*Swift w1* and *w2* and Johnson *U*-band), we extrapolated based on the average *B*-band magnitude for that day, because *B*-band observations were made frequently and come closest to representing the amount of energy emitted in the near- and far-UV. For longer wavelength filters (R_cI_cJHK), we extrapolated from the average *V*-band magnitude for the given day. The interpolated and extrapolated magnitudes are denoted in Table 2 with dagger (†) and double dagger (‡) symbols, respectively. We corrected most of the magnitudes for extinction using *A* values from the NASA/IPAC IRSA Galactic Dust Reddening and Extinction service; the *Swift w1* and *w2* bands were corrected using the relation from Cardelli et al. (1989), with $A_V = 0.74$, from an average $R_V = 3.1$ and $E(B-V) = 0.240$ (Webbink et al. 1987).

The majority of the energy of the eruption is released shortly after peak and is very blue, gaining in strength all the way through to the near-UV, seen by *Swift*. Our coverage of this regime is not as thorough as we would like it to be in either wavelength range or time; in an ideal world we would have observations at wavelengths shorter than the two *Swift* bands as

Table 2
Average Daily Magnitudes[a]

HJD	*Swift w2*	*Swift w1*	*U*	*B*	*V*	R_c	I_c	*J*	*H*	*K*	*WISE W1*	*WISE W2*
2455224.90	7.40‡	7.38‡	7.42‡	8.10‡	7.89	7.60‡	7.34‡	6.88‡	6.64‡	6.15‡	…	…
2455225.69	8.64‡	8.62‡	8.41	9.34	9.03	8.32	7.70	8.02‡	7.78‡	7.29‡	…	…
2455226.66	9.28‡	9.26‡	9.32	9.98	9.86	9.01	8.73	8.86‡	8.61‡	8.12‡	…	…
2455227.63	9.64‡	9.62‡	9.72†	10.34†	10.30†	9.53†	9.43†	9.29‡	9.05‡	8.56‡	…	…
2455228.59	10.00‡	9.98‡	10.13	10.70	10.74	10.06	10.14	9.73‡	9.49‡	8.99‡	…	…
2455229.69	10.40‡	10.38‡	10.60	11.09	11.26	10.62	10.67	10.12	9.83	9.37	…	…
2455230.68	10.72‡	10.70‡	10.82	11.42	11.61	11.07	11.06	10.60	10.30	9.66	…	…
2455231.83	11.30‡	11.27‡	11.35†	11.99	12.28	11.75	11.70	11.15	10.84	10.22	…	…
2455232.83	11.56‡	11.54‡	11.87†	12.26	12.87	12.42	12.23	11.52†	11.19†	10.56†	…	…
2455233.59	12.27‡	12.25‡	12.40	12.96	13.17	12.73	12.63	11.89†	11.55†	10.89†	…	…
2455234.60	12.40‡	12.38‡	12.42	13.10	13.28	12.90	12.80	12.26†	11.90†	11.23†	…	…
2455235.59	13.26‡	13.24‡	13.24	13.95	13.92	13.60	13.38	12.63†	12.26†	11.56†	…	…
2455236.84	13.38‡	13.36‡	13.43†	14.08	13.95	13.66	13.44	13.00	12.61	11.90	…	…
2455237.77	13.59	13.47	13.63†	14.02	13.90	13.68	13.42	13.06	12.74	12.08	…	…
2455238.43	13.66	13.73	13.83	14.47	14.30	13.95	13.73	13.20†	12.85†	12.19†	…	…
2455239.63	13.85	13.59	13.66	14.39	14.19	13.89	13.64	13.35	12.96	12.30	…	…
2455240.51	13.59	13.56	13.86	14.52	14.31	14.07	13.84	13.30	13.00	12.41	…	…
2455241.61	13.31	13.42	13.73	14.43	14.18	13.93	13.82	13.42	13.05	12.53	…	…
2455242.54	13.54	13.56	13.81	14.53	14.30	14.05	13.69	13.32	12.98	12.46	…	…
2455243.52	13.93	13.77	13.85†	14.53	14.35	14.11	13.84	13.49	13.13	12.67	…	…
2455244.45	13.87	13.71	13.88	14.60	14.39	14.14	13.86	13.50†	13.09†	12.63†	…	…
2455245.58	13.52	13.56	14.03	14.62	14.40	14.18	14.01	13.51	13.05	12.59	…	…
2455246.49	13.27	13.33	13.74	14.51	14.35	14.09	13.91	13.57†	13.18†	12.71†	…	…
2455247.52	13.41	13.48	13.87	14.60	14.41	14.15	13.94	13.64†	13.30†	12.84†	…	…
2455248.58	13.58	13.73	13.92†	14.60	14.39	14.23	13.95	13.70	13.43	12.97	…	…
2455249.58	13.65	13.76†	13.98	14.83	14.55	14.33	14.12	13.80†	13.51†	12.89†	…	…
2455250.54	13.46	13.80	14.25‡	14.94	14.72	14.49	14.21	13.90	13.60	12.82	…	…
2455251.66	13.75	13.89	14.17‡	14.86	14.72†	14.42	14.13	13.91	13.58	13.29	…	…
2455252.32	14.36	14.25	14.20‡	14.89†	14.71†	14.48†	14.20†	13.92†	13.55†	13.21	12.17	12.66
2455253.61	14.44	14.26	14.23‡	14.92	14.70	14.54	14.26	13.93	13.53	13.14	12.14	12.51
2455254.78	14.27	14.31	14.41‡	15.10†	14.87†	14.70†	14.41†	14.07†	13.71†	13.38	…	…
2455255.66	14.39	14.48	14.60‡	15.28†	15.04†	14.86†	14.56†	14.22†	13.88†	13.63	…	…
2455256.66	14.73	14.74	14.78‡	15.46	15.22	15.01	14.71	14.36	14.06	13.87	…	…
2455257.35	15.23	14.87†	14.94‡	15.62†	15.38†	15.17†	14.88†	14.54†	14.23†	14.06	…	…
2455258.50	14.90	15.01	15.10‡	15.78	15.54	15.34	15.05	14.72	14.41	14.26	…	…
2455259.75	15.39	15.21	15.29‡	15.98	15.72	15.57	15.29	14.97	14.73	13.98‡	…	…
2455260.47	15.75	15.63	15.54‡	16.22†	15.96†	15.76†	15.46†	15.08†	14.83†	14.21‡	…	…
2455261.85	15.89†	15.80†	15.78‡	16.46	16.19	15.96	15.63	15.19	14.94†	14.45‡	…	…
2455262.76	15.86†	15.76†	15.73‡	16.42	16.15	16.07	15.76	15.20	15.04†	14.41‡	…	…
2455263.69	15.87†	15.77†	15.95‡	16.63†	16.33†	16.19†	15.87†	15.37†	15.15†	14.58‡	…	…
2455264.63	16.34	16.33	16.16‡	16.85	16.50	16.30	15.98	15.55	15.25	14.76‡	…	…
2455265.63	16.65	16.72	16.49‡	17.18†	16.83†	16.62†	16.28†	15.79†	15.57†	15.09‡	…	…
2455266.56	17.06	16.93	16.82‡	17.50	17.16	16.93	16.57	16.03	15.90	15.41‡	…	…
2455267.64	16.82	16.76	16.39‡	17.07	16.72	16.55	16.23	15.81	15.55	14.97‡	…	…
2455268.58	16.72	16.76	16.48‡	17.17	16.88	16.73	16.47	15.89	15.77	15.14‡	…	…
2455269.55	16.78	16.89	17.02‡	17.70	17.30	17.06	16.74	15.95†	15.81†	15.56‡	…	…
2455270.39	16.55	16.68	16.92‡	17.60†	17.24†	17.01†	16.69†	16.02†	15.84†	15.49‡	…	…
2455271.72	16.21	16.41	16.81‡	17.50	17.17	16.96	16.64	16.08	15.88	15.42‡	…	…
2455272.75	16.93	16.90	16.72‡	17.41	17.01	16.80	16.47	15.98	15.76	15.27‡	…	…
2455273.77	16.62	16.50	16.61‡	17.30	17.00	16.83	16.53	16.10	15.91	15.26‡	…	…
2455274.86	16.86	16.56	16.33‡	17.02	16.71	16.55	16.28	15.88	15.55	14.97‡	…	…
2455275.62	16.87	16.61	16.74‡	17.43	17.12	16.92	16.54	16.00	15.86	15.37‡	…	…
2455276.47	16.82†	16.48†	16.65‡	17.34†	17.03†	16.85†	16.49†	15.99†	15.86†	15.29‡	…	…
2455277.33	16.78	16.35	16.68‡	17.36†	17.05†	16.87†	16.50†	15.99†	15.86†	15.31‡	…	…
2455278.52	16.95†	16.74†	16.67‡	17.36†	17.05†	16.86†	16.50†	15.99†	15.86†	15.30‡	…	…
2455279.72	17.12	17.13	16.39‡	17.07	16.79	16.64	16.33	15.97	15.88	15.04‡	…	…
2455280.67	17.16	16.97	16.47‡	17.15	16.84	16.66	16.38	15.96	15.70	15.10‡	…	…
2455281.73	17.40†	17.26†	16.81‡	17.50†	17.14†	16.95†	16.64†	16.13†	15.86†	15.40‡	…	…
2455282.79	17.64	17.56	17.16‡	17.84	17.44	17.25	16.90	16.30	16.02	15.70‡	…	…
2455283.72	17.57†	17.48†	17.20‡	17.89	17.47	17.32	16.99	16.31	16.24	15.73‡	…	…
2455284.70	17.50	17.40	17.20‡	17.88	17.55	17.30	16.97	16.32	16.16	15.80‡	…	…
2455285.73	17.71†	17.54†	17.11‡	17.79	17.51	17.33	16.96	15.95	15.91	15.76‡	…	…
2455286.61	17.91†	17.67†	17.41‡	18.09†	17.69†	17.47†	17.09†	16.18†	16.09†	15.94‡	…	…
2455287.50	18.12	17.81	17.71‡	18.39	17.87	17.60	17.21	16.41	16.26	16.13‡	…	…
2455288.75	17.48‡	17.46‡	17.49‡	18.18	17.72	17.47	17.14	16.49	16.30	15.98‡	…	…
2455289.75	17.68‡	17.65‡	17.69‡	18.37	17.71	17.51	17.21	16.59	16.35†	15.97‡	…	…
2455290.75	17.71‡	17.69‡	17.72‡	18.41†	17.85†	17.58†	17.28†	16.68†	16.39†	16.10‡	…	…
2455291.74	17.74‡	17.72‡	17.75‡	18.44†	17.98†	17.64†	17.35†	16.77†	16.43†	16.23‡	…	…
2455292.74	17.78‡	17.76‡	17.79‡	18.47	18.11	17.71	17.42	16.86	16.48†	16.37‡	…	…
2455293.74	17.87‡	17.85‡	17.88‡	18.56	17.99	17.77	17.34	16.65	16.52	16.25‡	…	…

Note.
[a] Interpolated values are denoted with a single dagger (†); extrapolated values are denoted with a double dagger (‡). See Section 4 for more details.

Table 3
U Sco 2010 Observations, Infrared to Ultraviolet Magnitudes

HJD	Phase	Observer	Telescope	Filter	Magnitude	Error
2455224.9352	0.795	Harris	0.4 m Schmidt–Cassegrain	V	7.89	0.01
2455225.2886	0.082	Maehara	Kwasan 0.25 m	Stromgren y	8.47	0.02
2455225.3382	0.122	Kiyota	0.25 m Schmidt–Cassegrain	Stromgren y	8.60	0.02
2455225.5749	0.314	Handler	SAAO 0.5 m	V	8.88	0.02
2455225.5749	0.314	Handler	SAAO 0.5 m	I_c	7.58	0.02
2455225.5749	0.314	Handler	SAAO 0.5 m	B	9.23	0.02
2455225.5907	0.327	Handler	SAAO 0.5 m	V	8.90	0.02
2455225.5907	0.327	Handler	SAAO 0.5 m	U	8.38	0.02
2455225.5907	0.327	Handler	SAAO 0.5 m	R_c	8.22	0.02
2455225.5907	0.327	Handler	SAAO 0.5 m	I_c	7.60	0.02
2455225.5907	0.327	Handler	SAAO 0.5 m	B	9.25	0.02
2455225.5916	0.328	Handler	SAAO 0.5 m	Stromgren y	9.05	0.02
2455225.5916	0.328	Handler	SAAO 0.5 m	Stromgren b	9.29	0.02
2455225.6140	0.346	Handler	SAAO 0.5 m	V	8.96	0.02
2455225.6140	0.346	Handler	SAAO 0.5 m	U	8.43	0.02
2455225.6140	0.346	Handler	SAAO 0.5 m	R_c	8.26	0.02
2455225.6140	0.346	Handler	SAAO 0.5 m	I_c	7.63	0.02
2455225.6140	0.346	Handler	SAAO 0.5 m	B	9.32	0.02
2455225.8271	0.519	Pagnotta	CTIO 1.3 m	B	9.47	0.04
2455225.8288	0.521	Pagnotta	CTIO 1.3 m	I	7.82	0.01
2455225.8305	0.522	Pagnotta	CTIO 1.3 m	R	8.39	0.01
2455225.8321	0.524	Pagnotta	CTIO 1.3 m	V	9.12	0.02
2455225.8652	0.550	Pagnotta	CTIO 1.3 m	B	9.41	0.02
2455225.8668	0.552	Pagnotta	CTIO 1.3 m	I	7.86	0.01
2455225.8685	0.553	Pagnotta	CTIO 1.3 m	R	8.42	0.01
2455225.8701	0.554	Pagnotta	CTIO 1.3 m	V	9.30	0.01
2455226.3438	0.939	Kiyota	0.25 m Schmidt–Cassegrain	Stromgren y	10.07	0.02
2455226.3708	0.961	Maehara	Kwasan 0.25 m	Stromgren y	10.04	0.02
2455226.5811	0.132	Handler	SAAO 0.5 m	Stromgren y	10.13	0.02
2455226.5811	0.132	Handler	SAAO 0.5 m	Stromgren b	10.05	0.02
2455226.5843	0.135	Handler	SAAO 0.5 m	V	9.81	0.02
2455226.5843	0.135	Handler	SAAO 0.5 m	U	9.30	0.02
2455226.5843	0.135	Handler	SAAO 0.5 m	R_c	8.99	0.02
2455226.5843	0.135	Handler	SAAO 0.5 m	I_c	8.64	0.02
2455226.5843	0.135	Handler	SAAO 0.5 m	B	9.98	0.02
2455226.5969	0.145	Handler	SAAO 0.5 m	Stromgren y	10.15	0.02
2455226.5969	0.145	Handler	SAAO 0.5 m	Stromgren b	10.06	0.02
2455226.6000	0.148	Handler	SAAO 0.5 m	V	9.85	0.02
2455226.6000	0.148	Handler	SAAO 0.5 m	U	9.33	0.02
2455226.6000	0.148	Handler	SAAO 0.5 m	R_c	9.00	0.02
2455226.6000	0.148	Handler	SAAO 0.5 m	I_c	8.67	0.02
2455226.6000	0.148	Handler	SAAO 0.5 m	B	9.99	0.02
2455226.6104	0.156	Handler	SAAO 0.5 m	Stromgren y	10.18	0.02
2455226.6104	0.156	Handler	SAAO 0.5 m	Stromgren b	10.09	0.02
2455226.6131	0.158	Handler	SAAO 0.5 m	V	9.86	0.02
2455226.6131	0.158	Handler	SAAO 0.5 m	U	9.34	0.02
2455226.6131	0.158	Handler	SAAO 0.5 m	R_c	9.03	0.02
2455226.6131	0.158	Handler	SAAO 0.5 m	I_c	8.70	0.02
2455226.6131	0.158	Handler	SAAO 0.5 m	B	10.03	0.02
2455226.8821	0.377	Pagnotta	CTIO 1.3 m	B	9.91	0.05
2455226.8840	0.378	Pagnotta	CTIO 1.3 m	I	8.90	0.02
2455226.8849	0.379	Pagnotta	CTIO 1.3 m	R	9.01	0.02
2455226.8857	0.380	Pagnotta	CTIO 1.3 m	V	9.93	0.03
2455227.5814	0.945	Handler	SAAO 0.5 m	V	10.19	0.02
2455227.5814	0.945	Handler	SAAO 0.5 m	U	9.62	0.02
2455227.5814	0.945	Handler	SAAO 0.5 m	R_c	9.45	0.02
2455227.5814	0.945	Handler	SAAO 0.5 m	I_c	9.36	0.02
2455227.5814	0.945	Handler	SAAO 0.5 m	B	10.25	0.02
2455227.5845	0.948	Handler	SAAO 0.5 m	Stromgren y	10.52	0.02
2455227.5845	0.948	Handler	SAAO 0.5 m	Stromgren b	10.27	0.02
2455227.5942	0.955	Handler	SAAO 0.5 m	V	10.20	0.02
2455227.5942	0.955	Handler	SAAO 0.5 m	U	9.65	0.02
2455227.5942	0.955	Handler	SAAO 0.5 m	R_c	9.48	0.02
2455227.5942	0.955	Handler	SAAO 0.5 m	I_c	9.37	0.02

Table 3
(Continued)

HJD	Phase	Observer	Telescope	Filter	Magnitude	Error
2455227.5942	0.955	Handler	SAAO 0.5 m	B	10.29	0.02
2455227.5975	0.958	Handler	SAAO 0.5 m	Stromgren y	10.58	0.02
2455227.5975	0.958	Handler	SAAO 0.5 m	Stromgren b	10.32	0.02
2455227.6075	0.966	Handler	SAAO 0.5 m	V	10.23	0.02
2455227.6075	0.966	Handler	SAAO 0.5 m	U	9.68	0.02
2455227.6075	0.966	Handler	SAAO 0.5 m	R_c	9.47	0.02
2455227.6075	0.966	Handler	SAAO 0.5 m	I_c	9.40	0.02
2455227.6075	0.966	Handler	SAAO 0.5 m	B	10.29	0.02
2455227.6106	0.969	Handler	SAAO 0.5 m	Stromgren y	10.57	0.02
2455227.6106	0.969	Handler	SAAO 0.5 m	Stromgren b	10.31	0.02
2455228.5775	0.755	Handler	SAAO 0.5 m	V	10.72	0.02
2455228.5775	0.755	Handler	SAAO 0.5 m	U	10.09	0.03
2455228.5775	0.755	Handler	SAAO 0.5 m	R_c	10.04	0.02
2455228.5775	0.755	Handler	SAAO 0.5 m	I_c	10.13	0.02
2455228.5775	0.755	Handler	SAAO 0.5 m	B	10.67	0.02
2455228.5809	0.757	Handler	SAAO 0.5 m	Stromgren y	11.14	0.02
2455228.5809	0.757	Handler	SAAO 0.5 m	Stromgren b	10.54	0.02
2455228.5910	0.766	Handler	SAAO 0.5 m	V	10.74	0.02
2455228.5910	0.766	Handler	SAAO 0.5 m	U	10.13	0.02
2455228.5910	0.766	Handler	SAAO 0.5 m	R_c	10.05	0.02
2455228.5910	0.766	Handler	SAAO 0.5 m	I_c	10.13	0.02
2455228.5910	0.766	Handler	SAAO 0.5 m	B	10.71	0.02
2455228.5945	0.768	Handler	SAAO 0.5 m	Stromgren y	11.15	0.02
2455228.5945	0.768	Handler	SAAO 0.5 m	Stromgren b	10.59	0.02
2455228.5983	0.771	Handler	SAAO 0.5 m	Stromgren y	11.16	0.02
2455228.5983	0.771	Handler	SAAO 0.5 m	Stromgren b	10.58	0.02
2455228.6093	0.780	Handler	SAAO 0.5 m	V	10.76	0.02
2455228.6093	0.780	Handler	SAAO 0.5 m	U	10.16	0.02
2455228.6093	0.780	Handler	SAAO 0.5 m	R_c	10.08	0.02
2455228.6093	0.780	Handler	SAAO 0.5 m	I_c	10.16	0.02
2455228.6093	0.780	Handler	SAAO 0.5 m	B	10.72	0.02
2455228.6125	0.783	Handler	SAAO 0.5 m	Stromgren y	11.19	0.02
2455228.6125	0.783	Handler	SAAO 0.5 m	Stromgren b	10.58	0.02
2455228.8623	0.986	Pagnotta	CTIO 1.3 m	J	9.81	0.01
2455228.8623	0.986	Pagnotta	CTIO 1.3 m	B	10.79	0.02
2455228.8633	0.987	Pagnotta	CTIO 1.3 m	K	8.93	0.09
2455228.8633	0.987	Pagnotta	CTIO 1.3 m	I	10.33	0.01
2455228.8642	0.988	Pagnotta	CTIO 1.3 m	K	8.95	0.08
2455228.8642	0.988	Pagnotta	CTIO 1.3 m	R	10.24	0.01
2455228.8650	0.988	Pagnotta	CTIO 1.3 m	H	9.56	0.04
2455228.8651	0.988	Pagnotta	CTIO 1.3 m	V	10.99	0.01
2455229.3451	0.378	Kiyota	0.25 m Schmidt–Cassegrain	Stromgren y	11.13	0.02
2455229.5734	0.564	Handler	SAAO 0.5 m	V	11.20	0.02
2455229.5734	0.564	Handler	SAAO 0.5 m	U	10.57	0.03
2455229.5734	0.564	Handler	SAAO 0.5 m	R_c	10.58	0.02
2455229.5734	0.564	Handler	SAAO 0.5 m	I_c	10.64	0.02
2455229.5734	0.564	Handler	SAAO 0.5 m	B	11.07	0.02
2455229.5776	0.567	Handler	SAAO 0.5 m	Stromgren y	11.54	0.02
2455229.5776	0.567	Handler	SAAO 0.5 m	Stromgren b	10.81	0.02
2455229.5892	0.577	Handler	SAAO 0.5 m	V	11.23	0.02
2455229.5892	0.577	Handler	SAAO 0.5 m	U	10.62	0.03
2455229.5892	0.577	Handler	SAAO 0.5 m	R_c	10.61	0.02
2455229.5892	0.577	Handler	SAAO 0.5 m	I_c	10.67	0.02
2455229.5892	0.577	Handler	SAAO 0.5 m	B	11.10	0.02
2455229.5931	0.580	Handler	SAAO 0.5 m	Stromgren y	11.58	0.02
2455229.5931	0.580	Handler	SAAO 0.5 m	Stromgren b	10.85	0.02
2455229.6047	0.589	Handler	SAAO 0.5 m	V	11.28	0.02
2455229.6047	0.589	Handler	SAAO 0.5 m	U	10.62	0.02
2455229.6047	0.589	Handler	SAAO 0.5 m	R_c	10.65	0.02
2455229.6047	0.589	Handler	SAAO 0.5 m	I_c	10.71	0.02
2455229.6047	0.589	Handler	SAAO 0.5 m	B	11.16	0.02
2455229.6084	0.592	Handler	SAAO 0.5 m	Stromgren y	11.63	0.02
2455229.6084	0.592	Handler	SAAO 0.5 m	Stromgren b	10.89	0.02
2455229.8809	0.814	Pagnotta	CTIO 1.3 m	J	10.12	0.01

Table 3
(Continued)

HJD	Phase	Observer	Telescope	Filter	Magnitude	Error
2455229.8810	0.814	Pagnotta	CTIO 1.3 m	*B*	11.05	0.03
2455229.8824	0.815	Pagnotta	CTIO 1.3 m	*K*	9.36	0.07
2455229.8824	0.815	Pagnotta	CTIO 1.3 m	*I*	10.66	0.01
2455229.8836	0.816	Pagnotta	CTIO 1.3 m	*K*	9.38	0.08
2455229.8836	0.816	Pagnotta	CTIO 1.3 m	*R*	10.64	0.02
2455229.8847	0.817	Pagnotta	CTIO 1.3 m	*H*	9.83	0.02
2455229.8848	0.817	Pagnotta	CTIO 1.3 m	*V*	11.33	0.02
2455230.5683	0.372	Handler	SAAO 0.5 m	*V*	11.48	0.02
2455230.5683	0.372	Handler	SAAO 0.5 m	*U*	10.81	0.03
2455230.5683	0.372	Handler	SAAO 0.5 m	R_c	11.01	0.02
2455230.5683	0.372	Handler	SAAO 0.5 m	I_c	11.00	0.02
2455230.5683	0.372	Handler	SAAO 0.5 m	*B*	11.35	0.02
2455230.5728	0.376	Handler	SAAO 0.5 m	Stromgren *y*	11.71	0.02
2455230.5728	0.376	Handler	SAAO 0.5 m	Stromgren *b*	11.06	0.02
2455230.5848	0.386	Handler	SAAO 0.5 m	*V*	11.51	0.02
2455230.5848	0.386	Handler	SAAO 0.5 m	*U*	10.79	0.03
2455230.5848	0.386	Handler	SAAO 0.5 m	R_c	11.00	0.02
2455230.5848	0.386	Handler	SAAO 0.5 m	I_c	10.99	0.02
2455230.5848	0.386	Handler	SAAO 0.5 m	*B*	11.35	0.02
2455230.5884	0.389	Handler	SAAO 0.5 m	Stromgreny	11.70	0.02
2455230.5884	0.389	Handler	SAAO 0.5 m	Stromgren *b*	11.04	0.02
2455230.6004	0.398	Handler	SAAO 0.5 m	*V*	11.54	0.02
2455230.6004	0.398	Handler	SAAO 0.5 m	*U*	10.87	0.03
2455230.6004	0.398	Handler	SAAO 0.5 m	R_c	11.05	0.02
2455230.6004	0.398	Handler	SAAO 0.5 m	I_c	11.03	0.02
2455230.6004	0.398	Handler	SAAO 0.5 m	*B*	11.38	0.02
2455230.6048	0.402	Handler	SAAO 0.5 m	Stromgren *y*	11.73	0.02
2455230.6048	0.402	Handler	SAAO 0.5 m	Stromgren *b*	11.04	0.02
2455230.8597	0.609	Pagnotta	CTIO 1.3 m	*J*	10.60	0.01
2455230.8597	0.609	Pagnotta	CTIO 1.3 m	*B*	11.59	0.02
2455230.8612	0.610	Pagnotta	CTIO 1.3 m	*K*	9.65	0.09
2455230.8612	0.610	Pagnotta	CTIO 1.3 m	*I*	11.20	0.01
2455230.8623	0.611	Pagnotta	CTIO 1.3 m	*K*	9.67	0.09
2455230.8624	0.611	Pagnotta	CTIO 1.3 m	*R*	11.25	0.01
2455230.8635	0.612	Pagnotta	CTIO 1.3 m	*H*	10.30	0.03
2455230.8635	0.612	Pagnotta	CTIO 1.3 m	*V*	11.89	0.01
2455231.3229	0.986	Maehara	Kwasan 0.25 m	Stromgren *y*	12.16	0.02
2455231.8280	0.396	Pagnotta	CTIO 1.3 m	*J*	11.15	0.01
2455231.8280	0.396	Pagnotta	CTIO 1.3 m	*B*	11.99	0.04
2455231.8294	0.397	Pagnotta	CTIO 1.3 m	*K*	10.24	0.11
2455231.8295	0.397	Pagnotta	CTIO 1.3 m	*I*	11.70	0.01
2455231.8306	0.398	Pagnotta	CTIO 1.3 m	*K*	10.20	0.12
2455231.8307	0.398	Pagnotta	CTIO 1.3 m	*R*	11.75	0.02
2455231.8318	0.399	Pagnotta	CTIO 1.3 m	*H*	10.84	0.03
2455231.8318	0.399	Pagnotta	CTIO 1.3 m	*V*	12.28	0.01
2455232.2618	0.749	Kiyota	0.25 m Schmidt–Cassegrain	Stromgren *y*	12.71	0.02
2455232.5665	0.996	Handler	SAAO 0.5 m	*V*	12.94	0.02
2455232.5665	0.996	Handler	SAAO 0.5 m	*U*	12.42	0.05
2455232.5665	0.996	Handler	SAAO 0.5 m	R_c	12.38	0.03
2455232.5665	0.996	Handler	SAAO 0.5 m	I_c	12.35	0.03
2455232.5665	0.996	Handler	SAAO 0.5 m	*B*	12.80	0.03
2455232.5714	0.000	Handler	SAAO 0.5 m	*V*	12.94	0.02
2455232.5714	0.000	Handler	SAAO 0.5 m	*U*	12.31	0.04
2455232.5714	0.000	Handler	SAAO 0.5 m	R_c	12.39	0.03
2455232.5714	0.000	Handler	SAAO 0.5 m	I_c	12.34	0.03
2455232.5714	0.000	Handler	SAAO 0.5 m	*B*	12.78	0.03
2455232.5756	0.004	Handler	SAAO 0.5 m	Stromgren *y*	13.08	0.02
2455232.5756	0.004	Handler	SAAO 0.5 m	Stromgren *b*	12.24	0.03
2455232.5913	0.016	Handler	SAAO 0.5 m	*V*	12.97	0.02
2455232.5913	0.016	Handler	SAAO 0.5 m	*U*	12.26	0.04
2455232.5913	0.016	Handler	SAAO 0.5 m	R_c	12.38	0.02
2455232.5913	0.016	Handler	SAAO 0.5 m	I_c	12.32	0.03
2455232.5913	0.016	Handler	SAAO 0.5 m	*B*	12.75	0.03
2455232.5968	0.021	Handler	SAAO 0.5 m	Stromgren *y*	13.14	0.02

Table 3
(Continued)

HJD	Phase	Observer	Telescope	Filter	Magnitude	Error
2455232.5968	0.021	Handler	SAAO 0.5 m	Stromgren *b*	12.27	0.03
2455232.8304	0.211	Pagnotta	CTIO 1.3 m	*B*	12.26	0.11
2455232.8328	0.213	Pagnotta	CTIO 1.3 m	*I*	12.23	0.07
2455232.8340	0.214	Pagnotta	CTIO 1.3 m	*R*	12.42	0.05
2455232.8351	0.214	Pagnotta	CTIO 1.3 m	*V*	12.87	0.13
2455233.2521	0.553	Kiyota	0.25 m Schmidt–Cassegrain	Stromgren *y*	13.39	0.02
2455233.5689	0.811	Handler	SAAO 0.5 m	Stromgren *y*	13.23	0.03
2455233.5689	0.811	Handler	SAAO 0.5 m	Stromgren *b*	12.35	0.03
2455233.5758	0.816	Handler	SAAO 0.5 m	*V*	13.10	0.02
2455233.5758	0.816	Handler	SAAO 0.5 m	*U*	12.27	0.04
2455233.5758	0.816	Handler	SAAO 0.5 m	R_c	12.67	0.03
2455233.5758	0.816	Handler	SAAO 0.5 m	I_c	12.60	0.03
2455233.5758	0.816	Handler	SAAO 0.5 m	*B*	12.85	0.03
2455233.5894	0.827	Handler	SAAO 0.5 m	Stromgren *y*	13.22	0.02
2455233.5894	0.827	Handler	SAAO 0.5 m	Stromgren *b*	12.39	0.03
2455233.5962	0.833	Handler	SAAO 0.5 m	*V*	13.24	0.02
2455233.5962	0.833	Handler	SAAO 0.5 m	*U*	12.53	0.04
2455233.5962	0.833	Handler	SAAO 0.5 m	R_c	12.79	0.03
2455233.5962	0.833	Handler	SAAO 0.5 m	I_c	12.67	0.03
2455233.5962	0.833	Handler	SAAO 0.5 m	*B*	13.08	0.03
2455233.8484	0.038	Pagnotta	CTIO 1.3 m	*J*	12.07	0.01
2455233.8485	0.038	Pagnotta	CTIO 1.3 m	*B*	12.87	0.03
2455233.8499	0.039	Pagnotta	CTIO 1.3 m	*K*	10.97	0.12
2455233.8499	0.039	Pagnotta	CTIO 1.3 m	*I*	12.51	0.01
2455233.8511	0.040	Pagnotta	CTIO 1.3 m	*K*	10.96	0.12
2455233.8511	0.040	Pagnotta	CTIO 1.3 m	*R*	12.70	0.02
2455233.8522	0.041	Pagnotta	CTIO 1.3 m	*H*	11.69	0.02
2455233.8523	0.041	Pagnotta	CTIO 1.3 m	*V*	13.14	0.02
2455234.3389	0.437	Kiyota	0.25 m Schmidt–Cassegrain	Stromgren *y*	13.10	0.02
2455234.5841	0.636	Handler	SAAO 0.5 m	Stromgren *y*	13.48	0.03
2455234.5841	0.636	Handler	SAAO 0.5 m	Stromgren *b*	12.77	0.03
2455234.6001	0.649	Handler	SAAO 0.5 m	*V*	13.28	0.02
2455234.6001	0.649	Handler	SAAO 0.5 m	*U*	12.42	0.04
2455234.6001	0.649	Handler	SAAO 0.5 m	R_c	12.90	0.03
2455234.6001	0.649	Handler	SAAO 0.5 m	I_c	12.80	0.03
2455234.6001	0.649	Handler	SAAO 0.5 m	*B*	13.10	0.03
2455234.6061	0.654	Handler	SAAO 0.5 m	Stromgren *y*	13.31	0.03
2455234.6061	0.654	Handler	SAAO 0.5 m	Stromgren *b*	12.48	0.03
2455235.2639	0.188	Kiyota	0.25 m Schmidt–Cassegrain	Stromgren *y*	13.56	0.02
2455235.5556	0.425	Handler	SAAO 0.5 m	Stromgren *y*	13.85	0.07
2455235.5556	0.425	Handler	SAAO 0.5 m	Stromgren *b*	13.59	0.10
2455235.5649	0.433	Handler	SAAO 0.5 m	Stromgren *y*	13.60	0.03
2455235.5649	0.433	Handler	SAAO 0.5 m	Stromgren *b*	13.47	0.04
2455235.5720	0.439	Handler	SAAO 0.5 m	*V*	13.99	0.03
2455235.5720	0.439	Handler	SAAO 0.5 m	*U*	13.26	0.06
2455235.5720	0.439	Handler	SAAO 0.5 m	R_c	13.64	0.05
2455235.5720	0.439	Handler	SAAO 0.5 m	I_c	13.47	0.06
2455235.5720	0.439	Handler	SAAO 0.5 m	*B*	13.99	0.05
2455235.5912	0.454	Handler	SAAO 0.5 m	Stromgren *y*	14.02	0.04
2455235.5912	0.454	Handler	SAAO 0.5 m	Stromgren *b*	13.63	0.05
2455235.5981	0.460	Handler	SAAO 0.5 m	*V*	13.85	0.03
2455235.5981	0.460	Handler	SAAO 0.5 m	*U*	13.21	0.05
2455235.5981	0.460	Handler	SAAO 0.5 m	R_c	13.55	0.04
2455235.5981	0.460	Handler	SAAO 0.5 m	I_c	13.29	0.04
2455235.5981	0.460	Handler	SAAO 0.5 m	*B*	13.92	0.04
2455235.8593	0.672	Clem	CTIO 1.0 m	Stromgren *y*	13.28	0.02
2455235.8702	0.681	Clem	CTIO 1.0 m	Stromgren *y*	13.30	0.01
2455236.3194	0.046	Kiyota	0.25 m Schmidt–Cassegrain	Stromgren *y*	14.20	0.02
2455236.8390	0.468	Pagnotta	CTIO 1.3 m	*J*	13.00	0.01
2455236.8391	0.468	Pagnotta	CTIO 1.3 m	*B*	14.08	0.02
2455236.8405	0.469	Pagnotta	CTIO 1.3 m	*K*	11.87	0.09
2455236.8406	0.469	Pagnotta	CTIO 1.3 m	*I*	13.44	0.01
2455236.8417	0.470	Pagnotta	CTIO 1.3 m	*K*	11.93	0.09
2455236.8417	0.470	Pagnotta	CTIO 1.3 m	*R*	13.66	0.01

Table 3
(Continued)

HJD	Phase	Observer	Telescope	Filter	Magnitude	Error
2455236.8428	0.471	Pagnotta	CTIO 1.3 m	*H*	12.61	0.03
2455236.8429	0.471	Pagnotta	CTIO 1.3 m	*V*	13.95	0.01
2455236.8595	0.485	Clem	CTIO 1.0 m	Stromgren *y*	13.95	0.01
2455236.8720	0.495	Clem	CTIO 1.0 m	Stromgren *y*	13.84	0.01
2455237.0499	0.640	*Swift*	UVOT	*w*1	13.48	0.02
2455237.4559	0.970	*Swift*	UVOT	*w*1	14.08	0.02
2455237.4669	0.978	*Swift*	UVOT	*w*2	14.34	0.03
2455237.7209	0.185	*Swift*	UVOT	*w*2	13.60	0.01
2455237.7229	0.187	*Swift*	UVOT	*w*1	13.46	0.02
2455237.7339	0.195	*Swift*	UVOT	*w*2	13.58	0.02
2455237.8561	0.295	Clem	CTIO 1.0 m	Stromgren *y*	13.94	0.01
2455237.8686	0.305	Clem	CTIO 1.0 m	Stromgren *y*	13.95	0.01
2455237.8794	0.314	Pagnotta	CTIO 1.3 m	*J*	13.06	0.01
2455237.8794	0.314	Pagnotta	CTIO 1.3 m	*B*	14.02	0.01
2455237.8809	0.315	Pagnotta	CTIO 1.3 m	*K*	12.06	0.08
2455237.8809	0.315	Pagnotta	CTIO 1.3 m	*I*	13.42	0.01
2455237.8820	0.316	Pagnotta	CTIO 1.3 m	*K*	12.11	0.08
2455237.8821	0.316	Pagnotta	CTIO 1.3 m	*R*	13.68	0.01
2455237.8832	0.317	Pagnotta	CTIO 1.3 m	*H*	12.74	0.01
2455237.8832	0.317	Pagnotta	CTIO 1.3 m	*V*	13.90	0.01
2455238.1130	0.504	*Swift*	UVOT	*w*2	13.77	0.01
2455238.2430	0.609	*Swift*	UVOT	*w*2	13.64	0.01
2455238.2440	0.610	*Swift*	UVOT	*w*1	13.73	0.02
2455238.2560	0.620	*Swift*	UVOT	*w*2	14.02	0.02
2455238.4570	0.783	*Swift*	UVOT	*w*2	13.20	0.01
2455238.5799	0.883	Handler	SAAO 0.5 m	Stromgren *y*	14.24	0.03
2455238.5799	0.883	Handler	SAAO 0.5 m	Stromgren *b*	14.25	0.05
2455238.5885	0.890	Handler	SAAO 0.5 m	*V*	14.30	0.03
2455238.5885	0.890	Handler	SAAO 0.5 m	*U*	13.83	0.05
2455238.5885	0.890	Handler	SAAO 0.5 m	R_c	13.95	0.04
2455238.5885	0.890	Handler	SAAO 0.5 m	I_c	13.73	0.04
2455238.5885	0.890	Handler	SAAO 0.5 m	*B*	14.47	0.04
2455238.7290	0.004	*Swift*	UVOT	*w*1	14.10	0.03
2455238.7390	0.012	*Swift*	UVOT	*w*2	14.49	0.03
2455238.8021	0.064	Pagnotta	CTIO 1.3 m	*B*	14.57	0.01
2455238.8036	0.065	Pagnotta	CTIO 1.3 m	*I*	13.81	0.01
2455238.8049	0.066	Pagnotta	CTIO 1.3 m	*R*	14.07	0.01
2455238.8063	0.067	Pagnotta	CTIO 1.3 m	*V*	14.37	0.01
2455238.8518	0.104	Clem	CTIO 1.0 m	Stromgren *y*	14.34	0.01
2455238.8643	0.114	Clem	CTIO 1.0 m	Stromgren *y*	14.31	0.01
2455239.1901	0.379	*Swift*	UVOT	*w*1	13.68	0.02
2455239.2011	0.388	*Swift*	UVOT	*w*2	13.97	0.03
2455239.5251	0.651	*Swift*	UVOT	*w*1	13.53	0.02
2455239.5261	0.652	*Swift*	UVOT	*w*1	13.59	0.02
2455239.5411	0.664	*Swift*	UVOT	*w*2	13.75	0.02
2455239.5418	0.665	Handler	SAAO 0.5 m	*V*	14.14	0.02
2455239.5418	0.665	Handler	SAAO 0.5 m	*U*	13.71	0.05
2455239.5418	0.665	Handler	SAAO 0.5 m	R_c	13.85	0.03
2455239.5418	0.665	Handler	SAAO 0.5 m	I_c	13.53	0.04
2455239.5418	0.665	Handler	SAAO 0.5 m	*B*	14.41	0.03
2455239.5490	0.670	Handler	SAAO 0.5 m	Stromgren *y*	14.10	0.03
2455239.5490	0.670	Handler	SAAO 0.5 m	Stromgren *b*	14.13	0.04
2455239.5658	0.684	Handler	SAAO 0.5 m	Stromgren *y*	14.13	0.03
2455239.5658	0.684	Handler	SAAO 0.5 m	Stromgren *b*	14.19	0.04
2455239.5746	0.691	Handler	SAAO 0.5 m	*V*	14.13	0.03
2455239.5746	0.691	Handler	SAAO 0.5 m	*U*	13.63	0.05
2455239.5746	0.691	Handler	SAAO 0.5 m	R_c	13.81	0.04
2455239.5746	0.691	Handler	SAAO 0.5 m	I_c	13.58	0.05
2455239.5746	0.691	Handler	SAAO 0.5 m	*B*	14.34	0.04
2455239.5926	0.706	Handler	SAAO 0.5 m	Stromgren *y*	14.19	0.03
2455239.5926	0.706	Handler	SAAO 0.5 m	Stromgren *b*	14.22	0.04
2455239.5951	0.708	*Swift*	UVOT	*w*1	13.53	0.01
2455239.5961	0.709	*Swift*	UVOT	*w*1	13.62	0.02
2455239.6005	0.712	Handler	SAAO 0.5 m	*V*	14.18	0.03

Table 3
(Continued)

HJD	Phase	Observer	Telescope	Filter	Magnitude	Error
2455239.6005	0.712	Handler	SAAO 0.5 m	U	13.65	0.05
2455239.6005	0.712	Handler	SAAO 0.5 m	R_c	13.88	0.04
2455239.6005	0.712	Handler	SAAO 0.5 m	I_c	13.70	0.05
2455239.6005	0.712	Handler	SAAO 0.5 m	B	14.33	0.04
2455239.6081	0.719	*Swift*	UVOT	$w2$	13.84	0.02
2455239.6571	0.758	*Swift*	UVOT	$w1$	13.48	0.01
2455239.6591	0.760	*Swift*	UVOT	$w1$	13.53	0.02
2455239.6751	0.773	*Swift*	UVOT	$w2$	13.85	0.02
2455239.7321	0.819	*Swift*	UVOT	$w1$	13.55	0.01
2455239.7341	0.821	*Swift*	UVOT	$w1$	13.59	0.02
2455239.7421	0.827	*Swift*	UVOT	$w2$	13.84	0.03
2455239.8028	0.877	Pagnotta	CTIO 1.3 m	J	13.35	0.01
2455239.8028	0.877	Pagnotta	CTIO 1.3 m	B	14.50	0.01
2455239.8042	0.878	Pagnotta	CTIO 1.3 m	K	12.29	0.10
2455239.8043	0.878	Pagnotta	CTIO 1.3 m	I	13.76	0.01
2455239.8056	0.879	Pagnotta	CTIO 1.3 m	K	12.30	0.10
2455239.8056	0.879	Pagnotta	CTIO 1.3 m	R	14.03	0.01
2455239.8062	0.879	*Swift*	UVOT	$w1$	13.71	0.01
2455239.8062	0.879	*Swift*	UVOT	$w1$	13.71	0.01
2455239.8069	0.880	Pagnotta	CTIO 1.3 m	H	12.96	0.03
2455239.8070	0.880	Pagnotta	CTIO 1.3 m	V	14.31	0.01
2455239.8645	0.927	Clem	CTIO 1.0 m	Stromgren y	14.48	0.01
2455239.8742	0.935	*Swift*	UVOT	$w1$	14.01	0.01
2455239.8742	0.935	*Swift*	UVOT	$w1$	14.01	0.01
2455239.8770	0.937	Clem	CTIO 1.0 m	Stromgren y	14.51	0.01
2455239.9172	0.970	*Swift*	UVOT	$w1$	14.01	0.01
2455239.9172	0.970	*Swift*	UVOT	$w1$	14.01	0.01
2455239.9422	0.990	*Swift*	UVOT	$w1$	14.11	0.02
2455239.9422	0.990	*Swift*	UVOT	$w1$	14.11	0.02
2455239.9872	0.027	*Swift*	UVOT	$w1$	14.00	0.01
2455239.9872	0.027	*Swift*	UVOT	$w1$	13.99	0.01
2455240.0502	0.078	*Swift*	UVOT	$w1$	13.88	0.02
2455240.0512	0.079	*Swift*	UVOT	$w1$	13.84	0.02
2455240.0632	0.088	*Swift*	UVOT	$w2$	14.00	0.03
2455240.1262	0.140	*Swift*	UVOT	$w1$	13.81	0.02
2455240.1282	0.141	*Swift*	UVOT	$w1$	13.61	0.02
2455240.1362	0.148	*Swift*	UVOT	$w2$	13.84	0.03
2455240.1952	0.196	*Swift*	UVOT	$w1$	13.40	0.02
2455240.1962	0.196	*Swift*	UVOT	$w1$	13.40	0.02
2455240.2632	0.251	*Swift*	UVOT	$w1$	13.51	0.02
2455240.2642	0.252	*Swift*	UVOT	$w1$	13.51	0.02
2455240.3292	0.305	*Swift*	UVOT	$w1$	13.44	0.02
2455240.3312	0.306	*Swift*	UVOT	$w1$	13.53	0.02
2455240.3952	0.358	*Swift*	UVOT	$w1$	13.55	0.01
2455240.3972	0.360	*Swift*	UVOT	$w1$	13.59	0.02
2455240.4622	0.413	*Swift*	UVOT	$w1$	13.70	0.02
2455240.4642	0.414	*Swift*	UVOT	$w1$	13.70	0.02
2455240.5554	0.488	Handler	SAAO 0.5 m	Stromgren y	14.37	0.03
2455240.5554	0.488	Handler	SAAO 0.5 m	Stromgren b	14.43	0.05
2455240.5636	0.495	Handler	SAAO 0.5 m	V	14.37	0.03
2455240.5636	0.495	Handler	SAAO 0.5 m	U	13.92	0.07
2455240.5636	0.495	Handler	SAAO 0.5 m	R_c	14.19	0.06
2455240.5636	0.495	Handler	SAAO 0.5 m	I_c	14.15	0.08
2455240.5636	0.495	Handler	SAAO 0.5 m	B	14.59	0.05
2455240.5793	0.508	Handler	SAAO 0.5 m	Stromgren y	14.40	0.03
2455240.5793	0.508	Handler	SAAO 0.5 m	Stromgren b	14.38	0.05
2455240.5872	0.514	Handler	SAAO 0.5 m	V	14.41	0.03
2455240.5872	0.514	Handler	SAAO 0.5 m	U	13.82	0.06
2455240.5872	0.514	Handler	SAAO 0.5 m	R_c	14.07	0.05
2455240.5872	0.514	Handler	SAAO 0.5 m	I_c	13.80	0.05
2455240.5872	0.514	Handler	SAAO 0.5 m	B	14.57	0.05
2455240.5992	0.524	*Swift*	UVOT	$w1$	13.49	0.03
2455240.6022	0.526	Handler	SAAO 0.5 m	Stromgren y	14.34	0.03
2455240.6022	0.526	Handler	SAAO 0.5 m	Stromgren b	14.36	0.05

Table 3
(Continued)

HJD	Phase	Observer	Telescope	Filter	Magnitude	Error
2455240.6082	0.531	Handler	SAAO 0.5 m	V	14.30	0.03
2455240.6082	0.531	Handler	SAAO 0.5 m	U	13.83	0.05
2455240.6082	0.531	Handler	SAAO 0.5 m	R_c	14.09	0.04
2455240.6082	0.531	Handler	SAAO 0.5 m	I_c	13.72	0.05
2455240.6082	0.531	Handler	SAAO 0.5 m	B	14.50	0.04
2455240.6112	0.534	*Swift*	UVOT	$w2$	13.34	0.03
2455240.6652	0.578	*Swift*	UVOT	$w1$	13.58	0.03
2455240.8069	0.693	Pagnotta	CTIO 1.3 m	J	13.30	0.01
2455240.8070	0.693	Pagnotta	CTIO 1.3 m	B	14.40	0.01
2455240.8084	0.694	Pagnotta	CTIO 1.3 m	I	13.68	0.01
2455240.8098	0.695	Pagnotta	CTIO 1.3 m	R	13.94	0.02
2455240.8111	0.696	Pagnotta	CTIO 1.3 m	V	14.15	0.03
2455241.0553	0.895	*Swift*	UVOT	$w1$	13.67	0.03
2455241.0663	0.903	*Swift*	UVOT	$w2$	13.59	0.03
2455241.1223	0.949	*Swift*	UVOT	$w1$	13.75	0.03
2455241.1373	0.961	*Swift*	UVOT	$w2$	13.79	0.03
2455241.2013	0.013	*Swift*	UVOT	$w1$	14.06	0.03
2455241.2683	0.068	*Swift*	UVOT	$w1$	13.67	0.03
2455241.3333	0.120	*Swift*	UVOT	$w1$	13.50	0.03
2455241.4003	0.175	*Swift*	UVOT	$w1$	13.27	0.03
2455241.4673	0.229	*Swift*	UVOT	$w1$	13.27	0.03
2455241.4813	0.241	*Swift*	UVOT	$w2$	13.26	0.03
2455241.5313	0.281	*Swift*	UVOT	$w2$	13.30	0.04
2455241.5323	0.282	*Swift*	UVOT	$w1$	13.30	0.03
2455241.5359	0.285	Handler	SAAO 0.5 m	Stromgren y	13.98	0.05
2455241.5359	0.285	Handler	SAAO 0.5 m	Stromgren b	14.23	0.08
2455241.5403	0.289	Handler	SAAO 0.5 m	Stromgren y	14.09	0.03
2455241.5403	0.289	Handler	SAAO 0.5 m	Stromgren b	14.24	0.05
2455241.5476	0.295	Handler	SAAO 0.5 m	V	14.14	0.03
2455241.5476	0.295	Handler	SAAO 0.5 m	U	13.77	0.06
2455241.5476	0.295	Handler	SAAO 0.5 m	R_c	13.86	0.04
2455241.5476	0.295	Handler	SAAO 0.5 m	I_c	13.66	0.05
2455241.5476	0.295	Handler	SAAO 0.5 m	B	14.45	0.04
2455241.5634	0.307	Handler	SAAO 0.5 m	Stromgren y	14.17	0.03
2455241.5634	0.307	Handler	SAAO 0.5 m	Stromgren b	14.23	0.05
2455241.5711	0.314	Handler	SAAO 0.5 m	V	14.11	0.03
2455241.5711	0.314	Handler	SAAO 0.5 m	U	13.69	0.05
2455241.5711	0.314	Handler	SAAO 0.5 m	R_c	13.87	0.04
2455241.5711	0.314	Handler	SAAO 0.5 m	I_c	14.00	0.05
2455241.5711	0.314	Handler	SAAO 0.5 m	B	14.38	0.04
2455241.5973	0.335	*Swift*	UVOT	$w2$	13.30	0.04
2455241.5983	0.336	*Swift*	UVOT	$w1$	13.50	0.03
2455241.6753	0.398	*Swift*	UVOT	$w2$	13.40	0.04
2455241.7413	0.452	*Swift*	UVOT	$w2$	13.30	0.03
2455241.8271	0.522	Pagnotta	CTIO 1.3 m	J	13.42	0.01
2455241.8271	0.522	Pagnotta	CTIO 1.3 m	B	14.48	0.01
2455241.8285	0.523	Pagnotta	CTIO 1.3 m	K	12.50	0.09
2455241.8286	0.523	Pagnotta	CTIO 1.3 m	I	13.80	0.01
2455241.8299	0.524	Pagnotta	CTIO 1.3 m	K	12.55	0.09
2455241.8299	0.524	Pagnotta	CTIO 1.3 m	R	14.05	0.01
2455241.8312	0.525	Pagnotta	CTIO 1.3 m	H	13.05	0.02
2455241.8312	0.525	Pagnotta	CTIO 1.3 m	V	14.28	0.01
2455241.8689	0.556	Clem	CTIO 1.0 m	Stromgren y	14.34	0.01
2455241.8814	0.566	Clem	CTIO 1.0 m	Stromgren y	14.35	0.01
2455242.1274	0.766	*Swift*	UVOT	$w2$	13.30	0.03
2455242.1294	0.767	*Swift*	UVOT	$w1$	13.40	0.03
2455242.1424	0.778	*Swift*	UVOT	$w2$	13.30	0.03
2455242.2044	0.828	*Swift*	UVOT	$w2$	13.40	0.03
2455242.2054	0.829	*Swift*	UVOT	$w1$	13.60	0.03
2455242.2174	0.839	*Swift*	UVOT	$w2$	13.70	0.03
2455242.2624	0.876	*Swift*	UVOT	$w2$	13.50	0.03
2455242.2644	0.877	*Swift*	UVOT	$w1$	13.60	0.03
2455242.2834	0.893	*Swift*	UVOT	$w2$	13.50	0.03
2455242.3294	0.930	*Swift*	UVOT	$w2$	13.60	0.03

Table 3
(Continued)

HJD	Phase	Observer	Telescope	Filter	Magnitude	Error
2455242.3314	0.932	*Swift*	UVOT	*w*1	13.70	0.03
2455242.3504	0.947	*Swift*	UVOT	*w*2	13.70	0.03
2455242.3964	0.984	*Swift*	UVOT	*w*2	13.80	0.03
2455242.3984	0.986	*Swift*	UVOT	*w*1	14.00	0.03
2455242.4164	0.001	*Swift*	UVOT	*w*2	13.90	0.03
2455242.4684	0.043	*Swift*	UVOT	*w*2	13.80	0.03
2455242.4704	0.045	*Swift*	UVOT	*w*1	13.80	0.03
2455242.4844	0.056	*Swift*	UVOT	*w*2	13.70	0.03
2455242.5374	0.099	Handler	SAAO 0.5 m	Stromgren *y*	14.40	0.03
2455242.5374	0.099	Handler	SAAO 0.5 m	Stromgren *b*	14.56	0.06
2455242.5459	0.106	Handler	SAAO 0.5 m	*V*	14.37	0.03
2455242.5459	0.106	Handler	SAAO 0.5 m	*U*	13.91	0.06
2455242.5459	0.106	Handler	SAAO 0.5 m	R_c	14.13	0.04
2455242.5459	0.106	Handler	SAAO 0.5 m	I_c	13.64	0.04
2455242.5459	0.106	Handler	SAAO 0.5 m	*B*	14.67	0.05
2455242.5635	0.120	Handler	SAAO 0.5 m	Stromgren *y*	14.35	0.03
2455242.5635	0.120	Handler	SAAO 0.5 m	Stromgren *b*	14.40	0.05
2455242.5716	0.127	Handler	SAAO 0.5 m	*V*	14.36	0.03
2455242.5716	0.127	Handler	SAAO 0.5 m	*U*	13.80	0.06
2455242.5716	0.127	Handler	SAAO 0.5 m	R_c	14.12	0.04
2455242.5716	0.127	Handler	SAAO 0.5 m	I_c	13.70	0.04
2455242.5716	0.127	Handler	SAAO 0.5 m	*B*	14.59	0.04
2455242.5873	0.140	Handler	SAAO 0.5 m	Stromgren *y*	14.26	0.03
2455242.5873	0.140	Handler	SAAO 0.5 m	Stromgren *b*	14.36	0.05
2455242.5947	0.146	Handler	SAAO 0.5 m	*V*	14.31	0.02
2455242.5947	0.146	Handler	SAAO 0.5 m	*U*	13.72	0.05
2455242.5947	0.146	Handler	SAAO 0.5 m	R_c	14.03	0.04
2455242.5947	0.146	Handler	SAAO 0.5 m	I_c	13.76	0.04
2455242.5947	0.146	Handler	SAAO 0.5 m	*B*	14.50	0.04
2455242.6064	0.155	*Swift*	UVOT	*w*1	13.60	0.02
2455242.6204	0.166	*Swift*	UVOT	*w*2	13.80	0.02
2455242.6764	0.212	*Swift*	UVOT	*w*1	13.60	0.02
2455242.6854	0.219	*Swift*	UVOT	*w*2	13.80	0.03
2455242.8169	0.326	Pagnotta	CTIO 1.3 m	*J*	13.32	0.01
2455242.8170	0.326	Pagnotta	CTIO 1.3 m	*B*	14.36	0.01
2455242.8184	0.327	Pagnotta	CTIO 1.3 m	*K*	12.46	0.08
2455242.8184	0.327	Pagnotta	CTIO 1.3 m	*I*	13.66	0.01
2455242.8197	0.328	Pagnotta	CTIO 1.3 m	*K*	12.46	0.08
2455242.8198	0.328	Pagnotta	CTIO 1.3 m	*R*	13.93	0.01
2455242.8211	0.330	Pagnotta	CTIO 1.3 m	*H*	12.98	0.02
2455242.8211	0.330	Pagnotta	CTIO 1.3 m	*V*	14.16	0.01
2455243.1415	0.590	*Swift*	UVOT	*w*1	13.70	0.03
2455243.1485	0.596	*Swift*	UVOT	*w*2	13.80	0.03
2455243.2085	0.644	*Swift*	UVOT	*w*1	13.70	0.02
2455243.2205	0.654	*Swift*	UVOT	*w*2	13.90	0.02
2455243.2785	0.701	*Swift*	UVOT	*w*1	13.80	0.02
2455243.2875	0.709	*Swift*	UVOT	*w*2	14.00	0.03
2455243.3455	0.756	*Swift*	UVOT	*w*1	13.80	0.02
2455243.3545	0.763	*Swift*	UVOT	*w*2	13.90	0.03
2455243.4125	0.810	*Swift*	UVOT	*w*1	13.80	0.02
2455243.4205	0.817	*Swift*	UVOT	*w*2	14.00	0.03
2455243.4795	0.865	*Swift*	UVOT	*w*1	13.80	0.02
2455243.4905	0.874	*Swift*	UVOT	*w*2	14.00	0.02
2455243.5426	0.916	Handler	SAAO 0.5 m	Stromgren *y*	14.75	0.04
2455243.5426	0.916	Handler	SAAO 0.5 m	Stromgren *b*	14.74	0.06
2455243.5506	0.922	Handler	SAAO 0.5 m	*V*	14.64	0.04
2455243.5506	0.922	Handler	SAAO 0.5 m	*U*	14.03	0.08
2455243.5506	0.922	Handler	SAAO 0.5 m	R_c	14.33	0.06
2455243.5506	0.922	Handler	SAAO 0.5 m	I_c	13.86	0.06
2455243.5506	0.922	Handler	SAAO 0.5 m	*B*	14.78	0.06
2455243.5678	0.936	Handler	SAAO 0.5 m	Stromgren *y*	15.02	0.05
2455243.5678	0.936	Handler	SAAO 0.5 m	Stromgren *b*	14.96	0.09
2455243.5763	0.943	Handler	SAAO 0.5 m	*V*	14.84	0.04
2455243.5763	0.943	Handler	SAAO 0.5 m	*U*	14.32	0.09

Table 3
(Continued)

HJD	Phase	Observer	Telescope	Filter	Magnitude	Error
2455243.5763	0.943	Handler	SAAO 0.5 m	R_c	14.59	0.07
2455243.5763	0.943	Handler	SAAO 0.5 m	I_c	14.42	0.08
2455243.5763	0.943	Handler	SAAO 0.5 m	B	15.02	0.07
2455243.5949	0.958	Handler	SAAO 0.5 m	Stromgren y	15.00	0.05
2455243.5949	0.958	Handler	SAAO 0.5 m	Stromgren b	14.98	0.07
2455243.6089	0.970	Handler	SAAO 0.5 m	V	14.86	0.03
2455243.6089	0.970	Handler	SAAO 0.5 m	U	14.29	0.07
2455243.6089	0.970	Handler	SAAO 0.5 m	R_c	14.42	0.05
2455243.6089	0.970	Handler	SAAO 0.5 m	I_c	14.24	0.06
2455243.6089	0.970	Handler	SAAO 0.5 m	B	15.07	0.06
2455243.8184	0.140	Pagnotta	CTIO 1.3 m	J	13.49	0.01
2455243.8185	0.140	Pagnotta	CTIO 1.3 m	B	14.53	0.01
2455243.8199	0.141	Pagnotta	CTIO 1.3 m	K	12.64	0.12
2455243.8199	0.141	Pagnotta	CTIO 1.3 m	I	13.84	0.01
2455243.8212	0.142	Pagnotta	CTIO 1.3 m	K	12.69	0.13
2455243.8213	0.142	Pagnotta	CTIO 1.3 m	R	14.11	0.01
2455243.8226	0.143	Pagnotta	CTIO 1.3 m	H	13.13	0.02
2455243.8226	0.143	Pagnotta	CTIO 1.3 m	V	14.35	0.01
2455244.1436	0.404	*Swift*	UVOT	$w1$	13.70	0.03
2455244.1446	0.405	*Swift*	UVOT	$w1$	13.80	0.02
2455244.1566	0.415	*Swift*	UVOT	$w2$	13.90	0.02
2455244.2106	0.459	*Swift*	UVOT	$w1$	13.80	0.03
2455244.2116	0.460	*Swift*	UVOT	$w1$	13.80	0.02
2455244.2236	0.469	*Swift*	UVOT	$w2$	13.90	0.02
2455244.2776	0.513	*Swift*	UVOT	$w1$	13.60	0.03
2455244.2786	0.514	*Swift*	UVOT	$w1$	13.60	0.02
2455244.2906	0.524	*Swift*	UVOT	$w2$	13.70	0.02
2455244.3446	0.568	*Swift*	UVOT	$w1$	13.70	0.03
2455244.3456	0.568	*Swift*	UVOT	$w1$	13.70	0.02
2455244.3576	0.578	*Swift*	UVOT	$w2$	13.80	0.02
2455244.4116	0.622	*Swift*	UVOT	$w1$	13.70	0.03
2455244.4126	0.623	*Swift*	UVOT	$w1$	13.70	0.02
2455244.4246	0.633	*Swift*	UVOT	$w2$	13.80	0.02
2455244.4786	0.677	*Swift*	UVOT	$w1$	13.60	0.03
2455244.4796	0.677	*Swift*	UVOT	$w1$	13.70	0.02
2455244.4906	0.686	*Swift*	UVOT	$w2$	13.90	0.02
2455244.5429	0.729	Handler	SAAO 0.5 m	Stromgren y	14.41	0.03
2455244.5429	0.729	Handler	SAAO 0.5 m	Stromgren b	14.42	0.05
2455244.5504	0.735	Handler	SAAO 0.5 m	V	14.31	0.03
2455244.5504	0.735	Handler	SAAO 0.5 m	U	13.84	0.06
2455244.5504	0.735	Handler	SAAO 0.5 m	R_c	14.11	0.04
2455244.5504	0.735	Handler	SAAO 0.5 m	I_c	13.86	0.05
2455244.5504	0.735	Handler	SAAO 0.5 m	B	14.52	0.04
2455244.5724	0.753	Handler	SAAO 0.5 m	Stromgren y	14.41	0.03
2455244.5724	0.753	Handler	SAAO 0.5 m	Stromgren b	14.39	0.05
2455244.5797	0.759	Handler	SAAO 0.5 m	V	14.45	0.03
2455244.5797	0.759	Handler	SAAO 0.5 m	U	13.88	0.06
2455244.5797	0.759	Handler	SAAO 0.5 m	R_c	14.13	0.04
2455244.5797	0.759	Handler	SAAO 0.5 m	I_c	13.78	0.05
2455244.5797	0.759	Handler	SAAO 0.5 m	B	14.66	0.04
2455244.5960	0.772	Handler	SAAO 0.5 m	Stromgren y	14.45	0.03
2455244.5960	0.772	Handler	SAAO 0.5 m	Stromgren b	14.43	0.05
2455244.6036	0.778	Handler	SAAO 0.5 m	V	14.43	0.03
2455244.6036	0.778	Handler	SAAO 0.5 m	U	13.93	0.05
2455244.6036	0.778	Handler	SAAO 0.5 m	R_c	14.19	0.04
2455244.6036	0.778	Handler	SAAO 0.5 m	I_c	13.94	0.05
2455244.6036	0.778	Handler	SAAO 0.5 m	B	14.62	0.04
2455244.6126	0.785	*Swift*	UVOT	$w1$	13.88	0.02
2455244.6246	0.795	*Swift*	UVOT	$w2$	14.10	0.03
2455244.8267	0.959	Pagnotta	CTIO 1.3 m	J	13.78	0.01
2455244.8267	0.959	Pagnotta	CTIO 1.3 m	B	14.94	0.01
2455244.8282	0.961	Pagnotta	CTIO 1.3 m	K	13.02	0.09
2455244.8282	0.961	Pagnotta	CTIO 1.3 m	I	14.21	0.01
2455244.8295	0.962	Pagnotta	CTIO 1.3 m	K	13.04	0.09

Table 3
(Continued)

HJD	Phase	Observer	Telescope	Filter	Magnitude	Error
2455244.8295	0.962	Pagnotta	CTIO 1.3 m	*R*	14.50	0.01
2455244.8308	0.963	Pagnotta	CTIO 1.3 m	*H*	13.43	0.02
2455244.8309	0.963	Pagnotta	CTIO 1.3 m	*V*	14.78	0.01
2455245.0455	0.137	Landolt	KPNO 2.1 m	Stromgren *y*	14.44	0.01
2455245.1517	0.223	*Swift*	UVOT	*w*1	13.61	0.02
2455245.1637	0.233	*Swift*	UVOT	*w*2	13.75	0.02
2455245.2137	0.274	*Swift*	UVOT	*w*1	13.54	0.02
2455245.2267	0.284	*Swift*	UVOT	*w*2	13.70	0.02
2455245.2847	0.332	*Swift*	UVOT	*w*1	13.57	0.02
2455245.2977	0.342	*Swift*	UVOT	*w*2	13.73	0.02
2455245.3517	0.386	*Swift*	UVOT	*w*1	13.59	0.02
2455245.3647	0.397	*Swift*	UVOT	*w*2	13.71	0.02
2455245.4187	0.440	*Swift*	UVOT	*w*1	13.69	0.02
2455245.4317	0.451	*Swift*	UVOT	*w*2	13.69	0.02
2455245.4857	0.495	*Swift*	UVOT	*w*1	13.62	0.02
2455245.4987	0.506	*Swift*	UVOT	*w*2	13.70	0.02
2455245.5325	0.533	Handler	SAAO 0.5 m	Stromgren *y*	14.48	0.06
2455245.5325	0.533	Handler	SAAO 0.5 m	Stromgren *b*	14.50	0.09
2455245.5409	0.540	Handler	SAAO 0.5 m	*V*	14.44	0.02
2455245.5409	0.540	Handler	SAAO 0.5 m	*U*	14.03	0.05
2455245.5409	0.540	Handler	SAAO 0.5 m	R_c	14.21	0.04
2455245.5409	0.540	Handler	SAAO 0.5 m	I_c	14.15	0.05
2455245.5409	0.540	Handler	SAAO 0.5 m	*B*	14.65	0.04
2455245.5537	0.550	*Swift*	UVOT	*w*2	13.24	0.03
2455245.5547	0.551	*Swift*	UVOT	*w*1	13.44	0.03
2455245.5657	0.560	*Swift*	UVOT	*w*2	13.29	0.03
2455245.6207	0.605	*Swift*	UVOT	*w*2	13.42	0.03
2455245.6217	0.605	*Swift*	UVOT	*w*1	13.50	0.03
2455245.6327	0.614	*Swift*	UVOT	*w*2	13.33	0.03
2455245.6857	0.657	*Swift*	UVOT	*w*2	13.36	0.04
2455245.6867	0.658	*Swift*	UVOT	*w*1	13.55	0.03
2455245.6977	0.667	*Swift*	UVOT	*w*2	13.61	0.03
2455245.7557	0.714	*Swift*	UVOT	*w*2	13.32	0.03
2455245.7567	0.715	*Swift*	UVOT	*w*1	13.46	0.03
2455245.7667	0.723	*Swift*	UVOT	*w*2	13.36	0.03
2455245.7972	0.748	Pagnotta	CTIO 1.3 m	*J*	13.51	0.01
2455245.7972	0.748	Pagnotta	CTIO 1.3 m	*B*	14.59	0.01
2455245.7987	0.749	Pagnotta	CTIO 1.3 m	*K*	12.60	0.12
2455245.7987	0.749	Pagnotta	CTIO 1.3 m	*I*	13.86	0.01
2455245.8000	0.750	Pagnotta	CTIO 1.3 m	*K*	12.58	0.11
2455245.8001	0.750	Pagnotta	CTIO 1.3 m	*R*	14.15	0.01
2455245.8014	0.751	Pagnotta	CTIO 1.3 m	*H*	13.05	0.03
2455245.8014	0.751	Pagnotta	CTIO 1.3 m	*V*	14.36	0.01
2455245.8298	0.775	*Swift*	UVOT	*w*2	13.59	0.02
2455245.8978	0.830	*Swift*	UVOT	*w*2	13.56	0.02
2455246.0323	0.939	Landolt	KPNO 2.1 m	Stromgren *y*	14.78	0.01
2455246.0357	0.942	Landolt	KPNO 2.1 m	Stromgren *y*	14.79	0.01
2455246.0413	0.946	Landolt	KPNO 2.1 m	Stromgren *y*	14.81	0.01
2455246.1558	0.039	*Swift*	UVOT	*w*2	13.97	0.04
2455246.1568	0.040	*Swift*	UVOT	*w*1	14.06	0.03
2455246.1668	0.048	*Swift*	UVOT	*w*2	13.87	0.04
2455246.2228	0.094	*Swift*	UVOT	*w*2	13.46	0.03
2455246.2238	0.095	*Swift*	UVOT	*w*1	13.61	0.03
2455246.2338	0.103	*Swift*	UVOT	*w*2	13.42	0.03
2455246.2898	0.148	*Swift*	UVOT	*w*2	13.27	0.03
2455246.2908	0.149	*Swift*	UVOT	*w*1	13.37	0.03
2455246.3008	0.157	*Swift*	UVOT	*w*2	13.26	0.03
2455246.3222	0.175	Maehara	Kwasan 0.25 m	Stromgren *y*	14.66	0.10
2455246.3264	0.178	Kiyota	0.25 m Schmidt–Cassegrain	Stromgren *y*	14.29	0.02
2455246.3478	0.196	*Swift*	UVOT	*w*2	13.31	0.03
2455246.3498	0.197	*Swift*	UVOT	*w*1	13.37	0.03
2455246.3598	0.205	*Swift*	UVOT	*w*2	13.34	0.03
2455246.4188	0.253	*Swift*	UVOT	*w*2	13.32	0.04
2455246.4198	0.254	*Swift*	UVOT	*w*1	13.40	0.03

Table 3
(Continued)

HJD	Phase	Observer	Telescope	Filter	Magnitude	Error
2455246.4318	0.264	*Swift*	UVOT	*w*2	13.26	0.03
2455246.4868	0.308	*Swift*	UVOT	*w*2	13.06	0.03
2455246.4878	0.309	*Swift*	UVOT	*w*1	13.16	0.03
2455246.4988	0.318	*Swift*	UVOT	*w*2	13.15	0.03
2455246.5282	0.342	Handler	SAAO 0.5 m	Stromgren *y*	14.23	0.03
2455246.5282	0.342	Handler	SAAO 0.5 m	Stromgren *b*	14.35	0.04
2455246.5364	0.349	Handler	SAAO 0.5 m	*V*	14.28	0.02
2455246.5364	0.349	Handler	SAAO 0.5 m	*U*	13.70	0.05
2455246.5364	0.349	Handler	SAAO 0.5 m	R_c	14.01	0.03
2455246.5364	0.349	Handler	SAAO 0.5 m	I_c	13.87	0.04
2455246.5364	0.349	Handler	SAAO 0.5 m	*B*	14.47	0.04
2455246.5563	0.365	Handler	SAAO 0.5 m	Stromgren *y*	14.26	0.03
2455246.5563	0.365	Handler	SAAO 0.5 m	Stromgren *b*	14.41	0.04
2455246.5642	0.371	Handler	SAAO 0.5 m	*V*	14.34	0.02
2455246.5642	0.371	Handler	SAAO 0.5 m	*U*	13.79	0.05
2455246.5642	0.371	Handler	SAAO 0.5 m	R_c	14.05	0.03
2455246.5642	0.371	Handler	SAAO 0.5 m	I_c	13.87	0.04
2455246.5642	0.371	Handler	SAAO 0.5 m	*B*	14.56	0.03
2455246.5911	0.393	Handler	SAAO 0.5 m	*V*	14.42	0.02
2455246.5911	0.393	Handler	SAAO 0.5 m	*U*	13.74	0.04
2455246.5911	0.393	Handler	SAAO 0.5 m	R_c	14.22	0.04
2455246.5911	0.393	Handler	SAAO 0.5 m	I_c	13.99	0.04
2455246.5911	0.393	Handler	SAAO 0.5 m	*B*	14.53	0.03
2455246.5977	0.399	Handler	SAAO 0.5 m	Stromgren *y*	14.37	0.06
2455246.5977	0.399	Handler	SAAO 0.5 m	Stromgren *b*	14.41	0.09
2455246.6041	0.404	Handler	SAAO 0.5 m	Stromgren *y*	14.38	0.03
2455246.6041	0.404	Handler	SAAO 0.5 m	Stromgren *b*	14.40	0.04
2455246.8782	0.627	Pagnotta	CTIO 1.3 m	*B*	14.50	0.00
2455247.0243	0.745	Landolt	KPNO 2.1 m	Stromgren *y*	14.38	0.01
2455247.0308	0.751	Landolt	KPNO 2.1 m	Stromgren *y*	14.37	0.01
2455247.0929	0.801	*Swift*	UVOT	*w*1	13.45	0.03
2455247.1049	0.811	*Swift*	UVOT	*w*2	13.40	0.03
2455247.1589	0.855	*Swift*	UVOT	*w*1	13.65	0.03
2455247.1719	0.865	*Swift*	UVOT	*w*2	13.54	0.03
2455247.2279	0.911	*Swift*	UVOT	*w*1	13.68	0.03
2455247.2389	0.920	*Swift*	UVOT	*w*2	13.66	0.03
2455247.2949	0.965	*Swift*	UVOT	*w*1	14.11	0.03
2455247.3059	0.974	*Swift*	UVOT	*w*2	14.14	0.04
2455247.3609	0.019	*Swift*	UVOT	*w*1	14.28	0.04
2455247.3729	0.029	*Swift*	UVOT	*w*2	14.22	0.04
2455247.4289	0.074	*Swift*	UVOT	*w*1	13.84	0.03
2455247.4389	0.082	*Swift*	UVOT	*w*2	13.66	0.03
2455247.4959	0.129	*Swift*	UVOT	*w*1	13.48	0.03
2455247.5069	0.137	*Swift*	UVOT	*w*2	13.33	0.03
2455247.5257	0.153	Handler	SAAO 0.5 m	Stromgren *y*	14.49	0.04
2455247.5257	0.153	Handler	SAAO 0.5 m	Stromgren *b*	14.49	0.05
2455247.5384	0.163	Handler	SAAO 0.5 m	*V*	14.56	0.03
2455247.5384	0.163	Handler	SAAO 0.5 m	*U*	13.96	0.06
2455247.5384	0.163	Handler	SAAO 0.5 m	R_c	14.28	0.04
2455247.5384	0.163	Handler	SAAO 0.5 m	I_c	14.20	0.05
2455247.5384	0.163	Handler	SAAO 0.5 m	*B*	14.71	0.04
2455247.5545	0.176	Handler	SAAO 0.5 m	Stromgren *y*	14.50	0.03
2455247.5545	0.176	Handler	SAAO 0.5 m	Stromgren *b*	14.66	0.05
2455247.5599	0.181	*Swift*	UVOT	*w*1	13.51	0.03
2455247.5630	0.183	Handler	SAAO 0.5 m	*V*	14.40	0.02
2455247.5630	0.183	Handler	SAAO 0.5 m	*U*	13.88	0.05
2455247.5630	0.183	Handler	SAAO 0.5 m	R_c	14.19	0.04
2455247.5630	0.183	Handler	SAAO 0.5 m	I_c	13.89	0.04
2455247.5630	0.183	Handler	SAAO 0.5 m	*B*	14.66	0.04
2455247.5729	0.191	*Swift*	UVOT	*w*2	13.39	0.04
2455247.5794	0.196	Handler	SAAO 0.5 m	Stromgren *y*	14.44	0.03
2455247.5794	0.196	Handler	SAAO 0.5 m	Stromgren *b*	14.49	0.05
2455247.5876	0.203	Handler	SAAO 0.5 m	*V*	14.43	0.02
2455247.5876	0.203	Handler	SAAO 0.5 m	*U*	13.96	0.05

Table 3
(Continued)

HJD	Phase	Observer	Telescope	Filter	Magnitude	Error
2455247.5876	0.203	Handler	SAAO 0.5 m	R_c	14.12	0.03
2455247.5876	0.203	Handler	SAAO 0.5 m	I_c	13.91	0.04
2455247.5876	0.203	Handler	SAAO 0.5 m	B	14.57	0.04
2455247.6027	0.215	Handler	SAAO 0.5 m	Stromgren y	14.29	0.03
2455247.6027	0.215	Handler	SAAO 0.5 m	Stromgren b	14.32	0.04
2455247.6113	0.222	Handler	SAAO 0.5 m	V	14.25	0.02
2455247.6113	0.222	Handler	SAAO 0.5 m	U	13.68	0.04
2455247.6113	0.222	Handler	SAAO 0.5 m	R_c	14.00	0.03
2455247.6113	0.222	Handler	SAAO 0.5 m	I_c	13.75	0.04
2455247.6113	0.222	Handler	SAAO 0.5 m	B	14.46	0.03
2455247.6279	0.236	*Swift*	UVOT	$w1$	13.37	0.03
2455247.6289	0.237	*Swift*	UVOT	$w1$	13.42	0.03
2455247.6409	0.246	*Swift*	UVOT	$w2$	13.38	0.03
2455248.2940	0.777	*Swift*	UVOT	$w1$	13.65	0.04
2455248.2950	0.778	*Swift*	UVOT	$w1$	13.65	0.03
2455248.3050	0.786	*Swift*	UVOT	$w2$	13.56	0.03
2455248.3069	0.788	Kiyota	0.25 m Schmidt–Cassegrain	Stromgren y	14.74	0.02
2455248.3610	0.832	*Swift*	UVOT	$w1$	13.74	0.04
2455248.3620	0.832	*Swift*	UVOT	$w1$	13.59	0.03
2455248.3720	0.840	*Swift*	UVOT	$w2$	13.54	0.03
2455248.4250	0.884	*Swift*	UVOT	$w1$	13.94	0.04
2455248.4260	0.884	*Swift*	UVOT	$w1$	13.79	0.03
2455248.4370	0.893	*Swift*	UVOT	$w2$	13.64	0.03
2455248.4830	0.931	*Swift*	UVOT	$w1$	13.94	0.05
2455248.4840	0.931	*Swift*	UVOT	$w1$	13.87	0.03
2455248.4990	0.944	*Swift*	UVOT	$w2$	13.90	0.03
2455248.5274	0.967	Handler	SAAO 0.5 m	Stromgren y	15.09	0.06
2455248.5274	0.967	Handler	SAAO 0.5 m	Stromgren b	15.22	0.09
2455248.5954	0.022	Handler	SAAO 0.5 m	V	15.10	0.03
2455248.5954	0.022	Handler	SAAO 0.5 m	U	14.77	0.08
2455248.5954	0.022	Handler	SAAO 0.5 m	R_c	14.83	0.05
2455248.5954	0.022	Handler	SAAO 0.5 m	I_c	14.48	0.06
2455248.5954	0.022	Handler	SAAO 0.5 m	B	15.39	0.06
2455248.6148	0.038	Handler	SAAO 0.5 m	Stromgren y	15.39	0.06
2455248.6148	0.038	Handler	SAAO 0.5 m	Stromgren b	15.44	0.09
2455248.8197	0.204	Pagnotta	CTIO 1.3 m	J	13.70	0.01
2455248.8198	0.204	Pagnotta	CTIO 1.3 m	B	14.60	0.01
2455248.8212	0.206	Pagnotta	CTIO 1.3 m	K	12.97	0.13
2455248.8213	0.206	Pagnotta	CTIO 1.3 m	I	13.95	0.01
2455248.8226	0.207	Pagnotta	CTIO 1.3 m	K	12.96	0.13
2455248.8226	0.207	Pagnotta	CTIO 1.3 m	R	14.23	0.01
2455248.8239	0.208	Pagnotta	CTIO 1.3 m	H	13.43	0.02
2455248.8239	0.208	Pagnotta	CTIO 1.3 m	V	14.39	0.01
2455249.4951	0.753	*Swift*	UVOT	$w2$	13.90	0.02
2455249.5570	0.803	Handler	SAAO 0.5 m	Stromgren y	14.55	0.03
2455249.5570	0.803	Handler	SAAO 0.5 m	Stromgren b	14.62	0.05
2455249.5611	0.807	*Swift*	UVOT	$w2$	13.62	0.05
2455249.5661	0.811	Handler	SAAO 0.5 m	V	14.52	0.02
2455249.5661	0.811	Handler	SAAO 0.5 m	U	14.00	0.05
2455249.5661	0.811	Handler	SAAO 0.5 m	R_c	14.34	0.04
2455249.5661	0.811	Handler	SAAO 0.5 m	I_c	14.25	0.05
2455249.5661	0.811	Handler	SAAO 0.5 m	B	14.84	0.04
2455249.5671	0.812	*Swift*	UVOT	$w2$	13.56	0.02
2455249.5859	0.827	Handler	SAAO 0.5 m	Stromgren y	14.48	0.03
2455249.5859	0.827	Handler	SAAO 0.5 m	Stromgren b	14.66	0.05
2455249.5945	0.834	Handler	SAAO 0.5 m	V	14.58	0.02
2455249.5945	0.834	Handler	SAAO 0.5 m	U	13.95	0.05
2455249.5945	0.834	Handler	SAAO 0.5 m	R_c	14.31	0.04
2455249.5945	0.834	Handler	SAAO 0.5 m	I_c	13.99	0.04
2455249.5945	0.834	Handler	SAAO 0.5 m	B	14.83	0.04
2455249.6152	0.851	Handler	SAAO 0.5 m	Stromgren y	14.73	0.03
2455249.6152	0.851	Handler	SAAO 0.5 m	Stromgren b	14.93	0.05
2455249.6311	0.864	*Swift*	UVOT	$w2$	13.54	0.04
2455249.6371	0.869	*Swift*	UVOT	$w2$	13.61	0.02

Table 3
(Continued)

HJD	Phase	Observer	Telescope	Filter	Magnitude	Error
2455249.7011	0.921	*Swift*	UVOT	*w*2	13.72	0.04
2455249.7071	0.925	*Swift*	UVOT	*w*2	13.85	0.02
2455249.7712	0.977	*Swift*	UVOT	*w*2	14.55	0.04
2455249.7772	0.982	*Swift*	UVOT	*w*2	14.53	0.02
2455249.8785	0.065	Pagnotta	CTIO 1.3 m	*J*	14.04	0.01
2455249.8786	0.065	Pagnotta	CTIO 1.3 m	*B*	15.11	0.01
2455249.8800	0.066	Pagnotta	CTIO 1.3 m	*K*	12.94	0.10
2455249.8800	0.066	Pagnotta	CTIO 1.3 m	*I*	14.41	0.01
2455249.8813	0.067	Pagnotta	CTIO 1.3 m	*K*	12.93	0.10
2455249.8814	0.067	Pagnotta	CTIO 1.3 m	*R*	14.67	0.01
2455249.8827	0.068	Pagnotta	CTIO 1.3 m	*H*	13.70	0.03
2455249.8827	0.068	Pagnotta	CTIO 1.3 m	*V*	14.89	0.01
2455250.0222	0.181	*Swift*	UVOT	*w*2	13.41	0.04
2455250.0282	0.186	*Swift*	UVOT	*w*2	13.40	0.02
2455250.0892	0.236	*Swift*	UVOT	*w*2	13.44	0.04
2455250.0952	0.241	*Swift*	UVOT	*w*2	13.41	0.02
2455250.1562	0.290	*Swift*	UVOT	*w*2	13.41	0.04
2455250.1622	0.295	*Swift*	UVOT	*w*2	13.37	0.02
2455250.2232	0.345	*Swift*	UVOT	*w*2	13.29	0.04
2455250.2292	0.350	*Swift*	UVOT	*w*2	13.34	0.02
2455250.7062	0.737	*Swift*	UVOT	*w*1	13.67	0.03
2455250.7182	0.747	*Swift*	UVOT	*w*2	13.64	0.03
2455250.7763	0.794	*Swift*	UVOT	*w*1	13.93	0.03
2455250.7863	0.802	*Swift*	UVOT	*w*2	13.92	0.04
2455250.8385	0.845	Pagnotta	CTIO 1.3 m	*J*	13.90	0.01
2455250.8386	0.845	Pagnotta	CTIO 1.3 m	*B*	14.94	0.01
2455250.8400	0.846	Pagnotta	CTIO 1.3 m	*K*	12.82	0.10
2455250.8400	0.846	Pagnotta	CTIO 1.3 m	*I*	14.21	0.01
2455250.8413	0.847	Pagnotta	CTIO 1.3 m	*K*	12.81	0.10
2455250.8414	0.847	Pagnotta	CTIO 1.3 m	*R*	14.49	0.01
2455250.8427	0.848	Pagnotta	CTIO 1.3 m	*H*	13.60	0.03
2455250.8427	0.848	Pagnotta	CTIO 1.3 m	*V*	14.72	0.02
2455251.0433	0.011	*Swift*	UVOT	*w*1	14.66	0.04
2455251.0533	0.019	*Swift*	UVOT	*w*2	14.52	0.04
2455251.1093	0.065	*Swift*	UVOT	*w*1	14.22	0.04
2455251.1203	0.074	*Swift*	UVOT	*w*2	14.08	0.04
2455251.1773	0.120	*Swift*	UVOT	*w*1	13.94	0.03
2455251.1873	0.128	*Swift*	UVOT	*w*2	13.75	0.04
2455251.2433	0.174	*Swift*	UVOT	*w*1	13.74	0.03
2455251.2543	0.183	*Swift*	UVOT	*w*2	13.51	0.03
2455251.3103	0.228	*Swift*	UVOT	*w*1	13.60	0.03
2455251.3213	0.237	*Swift*	UVOT	*w*2	13.50	0.03
2455251.9051	0.712	Pagnotta	CTIO 1.3 m	*J*	13.91	0.01
2455251.9051	0.712	Pagnotta	CTIO 1.3 m	*B*	14.86	0.02
2455251.9065	0.713	Pagnotta	CTIO 1.3 m	*K*	13.27	0.08
2455251.9066	0.713	Pagnotta	CTIO 1.3 m	*I*	14.13	0.01
2455251.9079	0.714	Pagnotta	CTIO 1.3 m	*K*	13.31	0.10
2455251.9079	0.714	Pagnotta	CTIO 1.3 m	*R*	14.42	0.01
2455251.9784	0.771	*Swift*	UVOT	*w*1	14.06	0.04
2455251.9794	0.772	*Swift*	UVOT	*w*1	14.10	0.03
2455251.9904	0.781	*Swift*	UVOT	*w*2	14.26	0.03
2455252.0454	0.826	*Swift*	UVOT	*w*1	14.22	0.04
2455252.0464	0.826	*Swift*	UVOT	*w*1	14.29	0.03
2455252.0574	0.835	*Swift*	UVOT	*w*2	14.42	0.03
2455252.1124	0.880	*Swift*	UVOT	*w*1	14.34	0.03
2455252.1134	0.881	*Swift*	UVOT	*w*1	14.52	0.03
2455252.1244	0.890	*Swift*	UVOT	*w*2	14.60	0.03
2455252.1794	0.935	*Swift*	UVOT	*w*1	14.65	0.05
2455252.1804	0.935	*Swift*	UVOT	*w*1	14.62	0.03
2455252.1914	0.944	*Swift*	UVOT	*w*2	15.00	0.04
2455252.2464	0.989	*Swift*	UVOT	*w*1	15.19	0.06
2455252.2474	0.990	*Swift*	UVOT	*w*1	15.19	0.04
2455252.2574	0.998	*Swift*	UVOT	*w*2	15.36	0.05
2455252.3134	0.043	*Swift*	UVOT	*w*1	14.96	0.06

Table 3
(Continued)

HJD	Phase	Observer	Telescope	Filter	Magnitude	Error
2455252.3144	0.044	*Swift*	UVOT	*w*1	14.95	0.04
2455252.3254	0.053	*Swift*	UVOT	*w*2	15.06	0.04
2455252.3804	0.098	*Swift*	UVOT	*w*1	14.38	0.04
2455252.3814	0.099	*Swift*	UVOT	*w*1	14.42	0.03
2455252.3914	0.107	*Swift*	UVOT	*w*2	14.39	0.03
2455252.4474	0.152	*Swift*	UVOT	*w*1	14.17	0.04
2455252.4474	0.152	*Swift*	UVOT	*w*1	14.17	0.03
2455252.4574	0.160	*Swift*	UVOT	*w*2	14.27	0.03
2455252.4852	0.183	*WISE*	⋯	*W*2	12.57	0.05
2455252.4852	0.183	*WISE*	⋯	*W*1	12.18	0.03
2455252.5154	0.208	*Swift*	UVOT	*w*1	14.17	0.03
2455252.5264	0.217	*Swift*	UVOT	*w*2	14.28	0.03
2455252.5784	0.259	*Swift*	UVOT	*w*1	14.11	0.03
2455252.5894	0.268	*Swift*	UVOT	*w*2	14.17	0.03
2455252.6175	0.291	*WISE*	⋯	*W*2	12.66	0.07
2455252.6175	0.291	*WISE*	⋯	*W*1	12.12	0.03
2455252.7498	0.398	*WISE*	⋯	*W*2	12.64	0.06
2455252.7498	0.398	*WISE*	⋯	*W*1	12.08	0.03
2455252.8161	0.452	*WISE*	⋯	*W*2	12.81	0.06
2455252.8161	0.452	*WISE*	⋯	*W*1	12.47	0.03
2455252.8821	0.506	*WISE*	⋯	*W*2	12.55	0.06
2455252.8821	0.506	*WISE*	⋯	*W*1	12.17	0.03
2455252.9484	0.559	*WISE*	⋯	*W*2	12.53	0.06
2455252.9484	0.559	*WISE*	⋯	*W*1	12.19	0.03
2455253.0145	0.613	*WISE*	⋯	*W*2	12.51	0.05
2455253.0145	0.613	*WISE*	⋯	*W*1	12.15	0.04
2455253.0807	0.667	*WISE*	⋯	*W*2	12.46	0.05
2455253.0807	0.667	*WISE*	⋯	*W*1	12.12	0.03
2455253.1805	0.748	*Swift*	UVOT	*w*1	14.15	0.02
2455253.1915	0.757	*Swift*	UVOT	*w*2	14.33	0.03
2455253.2130	0.774	*WISE*	⋯	*W*2	12.39	0.05
2455253.2130	0.774	*WISE*	⋯	*W*1	12.16	0.03
2455253.2475	0.803	*Swift*	UVOT	*w*1	14.24	0.03
2455253.2585	0.811	*Swift*	UVOT	*w*2	14.38	0.03
2455253.3145	0.857	*Swift*	UVOT	*w*1	14.36	0.03
2455253.3255	0.866	*Swift*	UVOT	*w*2	14.52	0.03
2455253.3453	0.882	*WISE*	⋯	*W*2	12.59	0.06
2455253.3453	0.882	*WISE*	⋯	*W*1	12.23	0.04
2455253.3825	0.912	*Swift*	UVOT	*w*1	14.57	0.03
2455253.3945	0.922	*Swift*	UVOT	*w*2	14.84	0.04
2455253.4475	0.965	*Swift*	UVOT	*w*1	15.09	0.04
2455253.4595	0.975	*Swift*	UVOT	*w*2	15.20	0.04
2455253.5175	0.022	*Swift*	UVOT	*w*1	15.14	0.04
2455253.5295	0.032	*Swift*	UVOT	*w*2	15.22	0.06
2455253.5775	0.071	*Swift*	UVOT	*w*1	14.77	0.03
2455253.5905	0.081	*Swift*	UVOT	*w*2	14.81	0.05
2455253.6475	0.128	*Swift*	UVOT	*w*1	14.40	0.03
2455253.6605	0.138	*Swift*	UVOT	*w*2	14.59	0.04
2455253.7176	0.185	*Swift*	UVOT	*w*1	14.28	0.02
2455253.7296	0.194	*Swift*	UVOT	*w*2	14.57	0.04
2455253.7787	0.234	Pagnotta	CTIO 1.3 m	*J*	13.93	0.03
2455253.7788	0.234	Pagnotta	CTIO 1.3 m	*B*	14.92	0.02
2455253.7802	0.235	Pagnotta	CTIO 1.3 m	*K*	13.07	0.24
2455253.7802	0.235	Pagnotta	CTIO 1.3 m	*I*	14.26	0.01
2455253.7815	0.237	Pagnotta	CTIO 1.3 m	*K*	13.21	0.27
2455253.7816	0.237	Pagnotta	CTIO 1.3 m	*R*	14.54	0.01
2455253.7829	0.238	Pagnotta	CTIO 1.3 m	*H*	13.53	0.09
2455253.7829	0.238	Pagnotta	CTIO 1.3 m	*V*	14.70	0.01
2455253.7866	0.241	*Swift*	UVOT	*w*1	14.12	0.03
2455253.7966	0.249	*Swift*	UVOT	*w*2	14.22	0.03
2455254.5206	0.837	*Swift*	UVOT	*w*1	14.26	0.03
2455254.5326	0.847	*Swift*	UVOT	*w*2	14.30	0.04
2455254.5866	0.891	*Swift*	UVOT	*w*1	14.60	0.04
2455254.5996	0.901	*Swift*	UVOT	*w*2	14.80	0.04

Table 3
(Continued)

HJD	Phase	Observer	Telescope	Filter	Magnitude	Error
2455254.6546	0.946	*Swift*	UVOT	*w*1	15.09	0.04
2455254.6666	0.956	*Swift*	UVOT	*w*2	15.10	0.05
2455254.7207	1.000	*Swift*	UVOT	*w*1	15.39	0.05
2455254.7337	0.010	*Swift*	UVOT	*w*2	15.62	0.08
2455254.7695	0.039	Pagnotta	CTIO 1.3 m	*J*	14.77	0.03
2455254.7696	0.039	Pagnotta	CTIO 1.3 m	*B*	16.04	0.02
2455254.7710	0.041	Pagnotta	CTIO 1.3 m	*I*	15.24	0.01
2455254.7724	0.042	Pagnotta	CTIO 1.3 m	*R*	15.52	0.01
2455254.7737	0.043	Pagnotta	CTIO 1.3 m	*H*	14.40	0.09
2455254.7737	0.043	Pagnotta	CTIO 1.3 m	*V*	15.73	0.01
2455254.7897	0.056	*Swift*	UVOT	*w*1	14.78	0.04
2455254.8007	0.065	*Swift*	UVOT	*w*2	14.66	0.04
2455254.8577	0.111	*Swift*	UVOT	*w*1	14.37	0.04
2455254.8677	0.119	*Swift*	UVOT	*w*2	14.27	0.04
2455254.9207	0.162	*Swift*	UVOT	*w*1	14.23	0.03
2455254.9337	0.173	*Swift*	UVOT	*w*2	14.23	0.04
2455254.9887	0.217	*Swift*	UVOT	*w*1	14.08	0.03
2455255.0007	0.227	*Swift*	UVOT	*w*2	14.04	0.04
2455255.0557	0.272	*Swift*	UVOT	*w*1	14.08	0.03
2455255.0687	0.283	*Swift*	UVOT	*w*2	14.07	0.04
2455255.6577	0.761	*Swift*	UVOT	*w*1	14.44	0.04
2455255.6707	0.772	*Swift*	UVOT	*w*2	14.43	0.05
2455255.7228	0.814	*Swift*	UVOT	*w*1	14.54	0.11
2455255.7238	0.815	*Swift*	UVOT	*w*1	14.68	0.04
2455255.7368	0.825	*Swift*	UVOT	*w*2	14.70	0.04
2455255.7938	0.872	*Swift*	UVOT	*w*1	14.67	0.04
2455255.8048	0.881	*Swift*	UVOT	*w*2	14.72	0.06
2455255.8209	0.894	Pagnotta	CTIO 1.3 m	*J*	14.57	0.02
2455255.8209	0.894	Pagnotta	CTIO 1.3 m	*B*	15.67	0.02
2455255.8223	0.895	Pagnotta	CTIO 1.3 m	*K*	13.97	0.20
2455255.8224	0.895	Pagnotta	CTIO 1.3 m	*I*	14.94	0.01
2455255.8237	0.896	Pagnotta	CTIO 1.3 m	*K*	13.93	0.20
2455255.8237	0.896	Pagnotta	CTIO 1.3 m	*R*	15.25	0.01
2455255.8250	0.897	Pagnotta	CTIO 1.3 m	*H*	14.24	0.04
2455255.8251	0.897	Pagnotta	CTIO 1.3 m	*V*	15.44	0.01
2455255.8608	0.926	*Swift*	UVOT	*w*1	15.23	0.05
2455255.8618	0.927	*Swift*	UVOT	*w*1	14.75	0.04
2455255.8718	0.935	*Swift*	UVOT	*w*2	14.82	0.05
2455255.9258	0.979	*Swift*	UVOT	*w*1	15.56	0.05
2455255.9928	0.033	*Swift*	UVOT	*w*1	15.36	0.05
2455256.0058	0.044	*Swift*	UVOT	*w*2	15.26	0.07
2455256.0598	0.088	*Swift*	UVOT	*w*1	14.72	0.04
2455256.0728	0.098	*Swift*	UVOT	*w*2	14.57	0.06
2455256.1268	0.142	*Swift*	UVOT	*w*1	14.48	0.04
2455256.1398	0.153	*Swift*	UVOT	*w*2	14.33	0.05
2455256.1938	0.197	*Swift*	UVOT	*w*1	14.37	0.03
2455256.2068	0.207	*Swift*	UVOT	*w*2	14.44	0.05
2455256.2598	0.250	*Swift*	UVOT	*w*1	14.34	0.03
2455256.2728	0.261	*Swift*	UVOT	*w*2	14.49	0.05
2455256.8285	0.713	Pagnotta	CTIO 1.3 m	*J*	14.36	0.02
2455256.8285	0.713	Pagnotta	CTIO 1.3 m	*B*	15.46	0.02
2455256.8300	0.714	Pagnotta	CTIO 1.3 m	*K*	13.90	0.19
2455256.8300	0.714	Pagnotta	CTIO 1.3 m	*I*	14.71	0.01
2455256.8313	0.715	Pagnotta	CTIO 1.3 m	*K*	13.84	0.19
2455256.8313	0.715	Pagnotta	CTIO 1.3 m	*R*	15.01	0.01
2455256.8326	0.716	Pagnotta	CTIO 1.3 m	*H*	14.06	0.03
2455256.8327	0.716	Pagnotta	CTIO 1.3 m	*V*	15.22	0.01
2455256.8629	0.741	*Swift*	UVOT	*w*1	14.89	0.03
2455256.8759	0.751	*Swift*	UVOT	*w*2	15.05	0.04
2455256.9299	0.795	*Swift*	UVOT	*w*1	15.13	0.03
2455256.9429	0.806	*Swift*	UVOT	*w*2	15.32	0.06
2455256.9969	0.849	*Swift*	UVOT	*w*1	15.21	0.04
2455257.0099	0.860	*Swift*	UVOT	*w*2	15.43	0.06
2455257.0639	0.904	*Swift*	UVOT	*w*1	15.25	0.04

Table 3
(Continued)

HJD	Phase	Observer	Telescope	Filter	Magnitude	Error
2455257.0769	0.914	*Swift*	UVOT	*w2*	15.58	0.07
2455257.1309	0.958	*Swift*	UVOT	*w1*	15.73	0.05
2455257.1439	0.969	*Swift*	UVOT	*w2*	16.14	0.08
2455257.1979	0.013	*Swift*	UVOT	*w1*	15.94	0.05
2455257.2109	0.023	*Swift*	UVOT	*w2*	16.32	0.10
2455257.2649	0.067	*Swift*	UVOT	*w1*	15.42	0.04
2455257.2769	0.077	*Swift*	UVOT	*w2*	15.72	0.07
2455257.3319	0.122	*Swift*	UVOT	*w1*	15.01	0.03
2455257.3449	0.132	*Swift*	UVOT	*w2*	15.19	0.06
2455257.3989	0.176	*Swift*	UVOT	*w1*	14.81	0.03
2455257.4109	0.186	*Swift*	UVOT	*w2*	14.96	0.05
2455257.4659	0.231	*Swift*	UVOT	*w1*	15.02	0.03
2455257.4789	0.241	*Swift*	UVOT	*w2*	15.35	0.06
2455258.1360	0.775	*Swift*	UVOT	*w2*	14.76	0.08
2455258.1370	0.776	*Swift*	UVOT	*w1*	14.86	0.04
2455258.1470	0.784	*Swift*	UVOT	*w2*	14.90	0.05
2455258.2020	0.829	*Swift*	UVOT	*w2*	14.81	0.09
2455258.2030	0.830	*Swift*	UVOT	*w1*	14.98	0.04
2455258.2150	0.839	*Swift*	UVOT	*w2*	15.00	0.05
2455258.2690	0.883	*Swift*	UVOT	*w2*	14.93	0.09
2455258.2700	0.884	*Swift*	UVOT	*w1*	15.19	0.05
2455258.2810	0.893	*Swift*	UVOT	*w2*	14.98	0.05
2455258.8339	0.342	Pagnotta	CTIO 1.3 m	*J*	14.72	0.02
2455258.8340	0.342	Pagnotta	CTIO 1.3 m	*B*	15.78	0.02
2455258.8354	0.344	Pagnotta	CTIO 1.3 m	*K*	14.17	0.23
2455258.8355	0.344	Pagnotta	CTIO 1.3 m	*I*	15.05	0.01
2455258.8368	0.345	Pagnotta	CTIO 1.3 m	*K*	14.35	0.26
2455258.8368	0.345	Pagnotta	CTIO 1.3 m	*R*	15.34	0.01
2455258.8381	0.346	Pagnotta	CTIO 1.3 m	*H*	14.41	0.05
2455258.8381	0.346	Pagnotta	CTIO 1.3 m	*V*	15.54	0.01
2455259.4091	0.810	*Swift*	UVOT	*w1*	15.47	0.06
2455259.4191	0.818	*Swift*	UVOT	*w2*	16.11	0.25
2455259.4761	0.864	*Swift*	UVOT	*w1*	15.50	0.06
2455259.4861	0.872	*Swift*	UVOT	*w2*	15.56	0.07
2455259.5421	0.918	*Swift*	UVOT	*w1*	15.81	0.06
2455259.5531	0.927	*Swift*	UVOT	*w2*	15.81	0.09
2455259.6101	0.973	*Swift*	UVOT	*w1*	16.14	0.08
2455259.6201	0.981	*Swift*	UVOT	*w2*	16.08	0.13
2455259.6762	0.027	*Swift*	UVOT	*w1*	16.41	0.08
2455259.6872	0.036	*Swift*	UVOT	*w2*	16.36	0.13
2455259.7422	0.080	*Swift*	UVOT	*w1*	15.56	0.05
2455259.7542	0.090	*Swift*	UVOT	*w2*	15.49	0.08
2455259.8092	0.135	*Swift*	UVOT	*w1*	15.02	0.04
2455259.8131	0.138	Pagnotta	CTIO 1.3 m	*J*	14.97	0.02
2455259.8131	0.138	Pagnotta	CTIO 1.3 m	*B*	15.98	0.02
2455259.8146	0.139	Pagnotta	CTIO 1.3 m	*I*	15.29	0.01
2455259.8160	0.140	Pagnotta	CTIO 1.3 m	*R*	15.57	0.01
2455259.8174	0.142	Pagnotta	CTIO 1.3 m	*H*	14.73	0.06
2455259.8175	0.142	Pagnotta	CTIO 1.3 m	*V*	15.72	0.01
2455259.8202	0.144	*Swift*	UVOT	*w2*	14.92	0.06
2455259.8762	0.189	*Swift*	UVOT	*w1*	14.95	0.04
2455259.8882	0.199	*Swift*	UVOT	*w2*	15.17	0.07
2455259.9432	0.244	*Swift*	UVOT	*w1*	15.10	0.05
2455259.9542	0.253	*Swift*	UVOT	*w2*	15.20	0.07
2455260.0092	0.297	*Swift*	UVOT	*w1*	15.21	0.05
2455260.0212	0.307	*Swift*	UVOT	*w2*	15.12	0.07
2455260.5442	0.732	*Swift*	UVOT	*w1*	15.65	0.05
2455260.5562	0.742	*Swift*	UVOT	*w2*	15.91	0.05
2455260.6112	0.787	*Swift*	UVOT	*w1*	15.81	0.05
2455260.6232	0.796	*Swift*	UVOT	*w2*	15.97	0.06
2455260.6783	0.841	*Swift*	UVOT	*w1*	15.85	0.05
2455260.6903	0.851	*Swift*	UVOT	*w2*	15.98	0.06
2455260.8155	0.953	Pagnotta	CTIO 1.3 m	*J*	15.75	0.05
2455260.8155	0.953	Pagnotta	CTIO 1.3 m	*B*	16.98	0.02

Table 3
(Continued)

HJD	Phase	Observer	Telescope	Filter	Magnitude	Error
2455260.8170	0.954	Pagnotta	CTIO 1.3 m	*I*	16.26	0.02
2455260.8191	0.956	Pagnotta	CTIO 1.3 m	*R*	16.56	0.01
2455260.8207	0.957	Pagnotta	CTIO 1.3 m	*H*	15.66	0.17
2455260.8207	0.957	Pagnotta	CTIO 1.3 m	*V*	16.77	0.02
2455261.8497	0.793	Pagnotta	CTIO 1.3 m	*J*	15.19	0.03
2455261.8498	0.793	Pagnotta	CTIO 1.3 m	*B*	16.46	0.02
2455261.8512	0.794	Pagnotta	CTIO 1.3 m	*I*	15.63	0.02
2455261.8533	0.796	Pagnotta	CTIO 1.3 m	*R*	15.96	0.01
2455261.8549	0.797	Pagnotta	CTIO 1.3 m	*V*	16.19	0.02
2455262.7558	0.529	Pagnotta	CTIO 1.3 m	*J*	15.20	0.09
2455262.7558	0.529	Pagnotta	CTIO 1.3 m	*B*	16.42	0.03
2455262.7573	0.531	Pagnotta	CTIO 1.3 m	*I*	15.76	0.06
2455262.7602	0.533	Pagnotta	CTIO 1.3 m	*V*	16.15	0.02
2455264.8196	0.207	Pagnotta	CTIO 1.3 m	*J*	15.55	0.02
2455264.8197	0.207	Pagnotta	CTIO 1.3 m	*B*	16.85	0.01
2455264.8213	0.208	Pagnotta	CTIO 1.3 m	*H*	15.25	0.05
2455264.8214	0.208	Pagnotta	CTIO 1.3 m	*I*	15.98	0.01
2455264.8230	0.209	Pagnotta	CTIO 1.3 m	*H*	15.25	0.05
2455264.8231	0.209	Pagnotta	CTIO 1.3 m	*R*	16.30	0.01
2455264.8247	0.211	Pagnotta	CTIO 1.3 m	*H*	15.26	0.05
2455264.8247	0.211	Pagnotta	CTIO 1.3 m	*V*	16.50	0.01
2455265.8041	0.007	Pagnotta	CTIO 1.3 m	*B*	18.26	0.02
2455265.8058	0.008	Pagnotta	CTIO 1.3 m	*I*	17.32	0.02
2455265.8075	0.009	Pagnotta	CTIO 1.3 m	*R*	17.64	0.02
2455265.8091	0.011	Pagnotta	CTIO 1.3 m	*V*	17.90	0.02
2455266.7923	0.810	Pagnotta	CTIO 1.3 m	*J*	16.03	0.04
2455266.7923	0.810	Pagnotta	CTIO 1.3 m	*B*	17.50	0.01
2455266.7940	0.811	Pagnotta	CTIO 1.3 m	*H*	15.91	0.14
2455266.7940	0.811	Pagnotta	CTIO 1.3 m	*I*	16.57	0.01
2455266.7957	0.812	Pagnotta	CTIO 1.3 m	*H*	15.90	0.14
2455266.7957	0.812	Pagnotta	CTIO 1.3 m	*R*	16.93	0.01
2455266.7973	0.814	Pagnotta	CTIO 1.3 m	*H*	15.90	0.14
2455266.7974	0.814	Pagnotta	CTIO 1.3 m	*V*	17.16	0.01
2455267.8325	0.655	Pagnotta	CTIO 1.3 m	*J*	15.81	0.03
2455267.8326	0.655	Pagnotta	CTIO 1.3 m	*B*	17.07	0.01
2455267.8342	0.656	Pagnotta	CTIO 1.3 m	*H*	15.57	0.07
2455267.8342	0.656	Pagnotta	CTIO 1.3 m	*I*	16.23	0.01
2455267.8359	0.658	Pagnotta	CTIO 1.3 m	*H*	15.54	0.07
2455267.8359	0.658	Pagnotta	CTIO 1.3 m	*R*	16.55	0.01
2455267.8376	0.659	Pagnotta	CTIO 1.3 m	*H*	15.55	0.06
2455267.8376	0.659	Pagnotta	CTIO 1.3 m	*V*	16.72	0.01
2455268.7834	0.428	Pagnotta	CTIO 1.3 m	*J*	15.89	0.03
2455268.7834	0.428	Pagnotta	CTIO 1.3 m	*B*	17.17	0.01
2455268.7851	0.429	Pagnotta	CTIO 1.3 m	*H*	15.78	0.12
2455268.7851	0.429	Pagnotta	CTIO 1.3 m	*I*	16.47	0.01
2455268.7868	0.430	Pagnotta	CTIO 1.3 m	*H*	15.78	0.10
2455268.7868	0.431	Pagnotta	CTIO 1.3 m	*R*	16.73	0.01
2455268.7884	0.432	Pagnotta	CTIO 1.3 m	*H*	15.75	0.11
2455268.7885	0.432	Pagnotta	CTIO 1.3 m	*V*	16.88	0.01
2455269.0037	0.607	Landolt	KPNO 2.1 m	Stromgren *y*	16.96	0.01
2455269.0126	0.614	Landolt	KPNO 2.1 m	Stromgren *y*	17.02	0.01
2455269.8119	0.264	Pagnotta	CTIO 1.3 m	*B*	17.70	0.01
2455269.8136	0.265	Pagnotta	CTIO 1.3 m	*I*	16.74	0.01
2455269.8153	0.266	Pagnotta	CTIO 1.3 m	*R*	17.06	0.01
2455269.8169	0.268	Pagnotta	CTIO 1.3 m	*V*	17.30	0.01
2455270.7772	0.048	Pagnotta	CTIO 1.3 m	*J*	16.52	0.05
2455270.7773	0.048	Pagnotta	CTIO 1.3 m	*B*	18.02	0.02
2455270.7789	0.049	Pagnotta	CTIO 1.3 m	*H*	16.17	0.14
2455270.7790	0.049	Pagnotta	CTIO 1.3 m	*I*	17.15	0.02
2455270.7806	0.051	Pagnotta	CTIO 1.3 m	*H*	16.17	0.14
2455270.7807	0.051	Pagnotta	CTIO 1.3 m	*R*	17.45	0.01
2455270.7823	0.052	Pagnotta	CTIO 1.3 m	*H*	16.17	0.13
2455270.7823	0.052	Pagnotta	CTIO 1.3 m	*V*	17.62	0.01

Table 3
(Continued)

HJD	Phase	Observer	Telescope	Filter	Magnitude	Error
2455271.0147	0.241	Landolt	KPNO 2.1 m	Stromgren *y*	17.42	0.01
2455271.8151	0.891	Pagnotta	CTIO 1.3 m	*J*	16.08	0.04
2455271.8152	0.891	Pagnotta	CTIO 1.3 m	*B*	17.50	0.01
2455271.8168	0.893	Pagnotta	CTIO 1.3 m	*H*	15.88	0.11
2455271.8169	0.893	Pagnotta	CTIO 1.3 m	*I*	16.64	0.01
2455271.8185	0.894	Pagnotta	CTIO 1.3 m	*H*	15.86	0.10
2455271.8186	0.894	Pagnotta	CTIO 1.3 m	*R*	16.96	0.01
2455271.8202	0.896	Pagnotta	CTIO 1.3 m	*H*	15.90	0.11
2455271.8202	0.896	Pagnotta	CTIO 1.3 m	*V*	17.17	0.01
2455272.0176	0.056	Landolt	KPNO 2.1 m	Stromgren *y*	17.97	0.02
2455272.7882	0.682	Pagnotta	CTIO 1.3 m	*J*	15.98	0.03
2455272.7882	0.682	Pagnotta	CTIO 1.3 m	*B*	17.41	0.01
2455272.7899	0.684	Pagnotta	CTIO 1.3 m	*H*	15.80	0.10
2455272.7899	0.684	Pagnotta	CTIO 1.3 m	*I*	16.47	0.01
2455272.7916	0.685	Pagnotta	CTIO 1.3 m	*H*	15.72	0.09
2455272.7916	0.685	Pagnotta	CTIO 1.3 m	*R*	16.80	0.01
2455272.7932	0.686	Pagnotta	CTIO 1.3 m	*H*	15.76	0.10
2455272.7933	0.686	Pagnotta	CTIO 1.3 m	*V*	17.01	0.01
2455273.0160	0.867	Landolt	KPNO 2.1 m	Stromgren *y*	17.39	0.01
2455273.0266	0.876	Landolt	KPNO 2.1 m	Stromgren *y*	17.36	0.02
2455273.8381	0.535	Pagnotta	CTIO 1.3 m	*J*	16.10	0.03
2455273.8381	0.535	Pagnotta	CTIO 1.3 m	*B*	17.30	0.01
2455273.8398	0.537	Pagnotta	CTIO 1.3 m	*H*	15.90	0.09
2455273.8398	0.537	Pagnotta	CTIO 1.3 m	*I*	16.53	0.01
2455273.8415	0.538	Pagnotta	CTIO 1.3 m	*H*	15.93	0.10
2455273.8415	0.538	Pagnotta	CTIO 1.3 m	*R*	16.83	0.01
2455273.8431	0.540	Pagnotta	CTIO 1.3 m	*H*	15.89	0.09
2455273.8432	0.540	Pagnotta	CTIO 1.3 m	*V*	17.00	0.01
2455273.9968	0.664	Landolt	KPNO 2.1 m	Stromgren *y*	17.36	0.01
2455274.0090	0.674	Landolt	KPNO 2.1 m	Stromgren *y*	17.34	0.01
2455274.8451	0.354	Pagnotta	CTIO 1.3 m	*J*	15.88	0.03
2455274.8451	0.354	Pagnotta	CTIO 1.3 m	*B*	17.02	0.01
2455274.8468	0.355	Pagnotta	CTIO 1.3 m	*H*	15.54	0.08
2455274.8468	0.355	Pagnotta	CTIO 1.3 m	*I*	16.28	0.01
2455274.8485	0.357	Pagnotta	CTIO 1.3 m	*H*	15.57	0.09
2455274.8485	0.357	Pagnotta	CTIO 1.3 m	*R*	16.55	0.01
2455274.8502	0.358	Pagnotta	CTIO 1.3 m	*H*	15.55	0.09
2455274.8502	0.358	Pagnotta	CTIO 1.3 m	*V*	16.71	0.01
2455274.9992	0.479	Landolt	KPNO 2.1 m	Stromgren *y*	17.00	0.01
2455275.0099	0.488	Landolt	KPNO 2.1 m	Stromgren *y*	17.00	0.01
2455275.0203	0.496	Landolt	KPNO 2.1 m	Stromgren *y*	17.02	0.01
2455275.8388	0.161	Pagnotta	CTIO 1.3 m	*J*	16.00	0.04
2455275.8388	0.161	Pagnotta	CTIO 1.3 m	*B*	17.43	0.01
2455275.8405	0.163	Pagnotta	CTIO 1.3 m	*H*	15.84	0.16
2455275.8405	0.163	Pagnotta	CTIO 1.3 m	*I*	16.54	0.01
2455275.8422	0.164	Pagnotta	CTIO 1.3 m	*H*	15.92	0.17
2455275.8422	0.164	Pagnotta	CTIO 1.3 m	*R*	16.92	0.01
2455275.8438	0.165	Pagnotta	CTIO 1.3 m	*H*	15.82	0.15
2455275.8438	0.165	Pagnotta	CTIO 1.3 m	*V*	17.12	0.01
2455276.8625	0.993	Pagnotta	CTIO 1.3 m	*J*	16.81	0.06
2455276.8626	0.993	Pagnotta	CTIO 1.3 m	*B*	18.40	0.02
2455276.8642	0.995	Pagnotta	CTIO 1.3 m	*H*	16.57	0.17
2455276.8642	0.995	Pagnotta	CTIO 1.3 m	*I*	17.52	0.03
2455276.8659	0.996	Pagnotta	CTIO 1.3 m	*H*	16.56	0.18
2455276.8659	0.996	Pagnotta	CTIO 1.3 m	*R*	17.81	0.02
2455276.8676	0.997	Pagnotta	CTIO 1.3 m	*H*	16.52	0.17
2455276.8676	0.997	Pagnotta	CTIO 1.3 m	*V*	18.04	0.02
2455279.8534	0.424	Pagnotta	CTIO 1.3 m	*J*	15.97	0.04
2455279.8535	0.424	Pagnotta	CTIO 1.3 m	*B*	17.07	0.01
2455279.8551	0.425	Pagnotta	CTIO 1.3 m	*H*	15.85	0.12
2455279.8552	0.425	Pagnotta	CTIO 1.3 m	*I*	16.33	0.01
2455279.8568	0.427	Pagnotta	CTIO 1.3 m	*H*	15.91	0.13
2455279.8569	0.427	Pagnotta	CTIO 1.3 m	*R*	16.64	0.01

Table 3
(Continued)

HJD	Phase	Observer	Telescope	Filter	Magnitude	Error
2455279.8585	0.428	Pagnotta	CTIO 1.3 m	*H*	15.87	0.12
2455279.8585	0.428	Pagnotta	CTIO 1.3 m	*V*	16.79	0.01
2455280.8951	0.270	Pagnotta	CTIO 1.3 m	*J*	15.96	0.05
2455280.8951	0.270	Pagnotta	CTIO 1.3 m	*B*	17.15	0.01
2455280.8968	0.272	Pagnotta	CTIO 1.3 m	*H*	15.71	0.09
2455280.8968	0.272	Pagnotta	CTIO 1.3 m	*I*	16.38	0.01
2455280.8985	0.273	Pagnotta	CTIO 1.3 m	*H*	15.71	0.09
2455280.8985	0.273	Pagnotta	CTIO 1.3 m	*R*	16.66	0.01
2455280.9001	0.274	Pagnotta	CTIO 1.3 m	*H*	15.68	0.09
2455280.9002	0.274	Pagnotta	CTIO 1.3 m	*V*	16.84	0.01
2455281.7943	0.001	Pagnotta	CTIO 1.3 m	*J*	16.98	0.07
2455281.7943	0.001	Pagnotta	CTIO 1.3 m	*B*	18.69	0.02
2455281.7960	0.002	Pagnotta	CTIO 1.3 m	*H*	16.78	0.19
2455281.7960	0.002	Pagnotta	CTIO 1.3 m	*I*	17.81	0.03
2455281.7977	0.004	Pagnotta	CTIO 1.3 m	*H*	16.76	0.18
2455281.7977	0.004	Pagnotta	CTIO 1.3 m	*R*	18.10	0.02
2455281.7993	0.005	Pagnotta	CTIO 1.3 m	*H*	16.75	0.17
2455281.7994	0.005	Pagnotta	CTIO 1.3 m	*V*	18.23	0.02
2455282.8262	0.840	Pagnotta	CTIO 1.3 m	*J*	16.30	0.05
2455282.8262	0.840	Pagnotta	CTIO 1.3 m	*B*	17.84	0.02
2455282.8279	0.841	Pagnotta	CTIO 1.3 m	*H*	16.00	0.13
2455282.8279	0.841	Pagnotta	CTIO 1.3 m	*I*	16.90	0.02
2455282.8296	0.842	Pagnotta	CTIO 1.3 m	*H*	16.11	0.14
2455282.8296	0.842	Pagnotta	CTIO 1.3 m	*R*	17.25	0.01
2455282.8313	0.844	Pagnotta	CTIO 1.3 m	*H*	15.96	0.13
2455282.8313	0.844	Pagnotta	CTIO 1.3 m	*V*	17.44	0.01
2455283.7153	0.562	Pagnotta	CTIO 1.3 m	*J*	16.31	0.05
2455283.7153	0.562	Pagnotta	CTIO 1.3 m	*B*	17.89	0.03
2455283.7170	0.563	Pagnotta	CTIO 1.3 m	*H*	16.21	0.22
2455283.7170	0.563	Pagnotta	CTIO 1.3 m	*I*	16.99	0.02
2455283.7187	0.565	Pagnotta	CTIO 1.3 m	*H*	16.27	0.23
2455283.7187	0.565	Pagnotta	CTIO 1.3 m	*R*	17.32	0.02
2455283.7203	0.566	Pagnotta	CTIO 1.3 m	*H*	16.25	0.23
2455283.7204	0.566	Pagnotta	CTIO 1.3 m	*V*	17.47	0.02
2455284.7789	0.426	Pagnotta	CTIO 1.3 m	*J*	16.32	0.06
2455284.7789	0.426	Pagnotta	CTIO 1.3 m	*B*	17.88	0.03
2455284.7806	0.428	Pagnotta	CTIO 1.3 m	*H*	16.16	0.22
2455284.7806	0.428	Pagnotta	CTIO 1.3 m	*I*	16.97	0.02
2455284.7823	0.429	Pagnotta	CTIO 1.3 m	*H*	16.21	0.23
2455284.7823	0.429	Pagnotta	CTIO 1.3 m	*R*	17.30	0.02
2455284.7840	0.431	Pagnotta	CTIO 1.3 m	*H*	16.12	0.22
2455284.7840	0.431	Pagnotta	CTIO 1.3 m	*V*	17.55	0.02
2455285.7232	0.194	Pagnotta	CTIO 1.3 m	*J*	15.95	0.08
2455285.7232	0.194	Pagnotta	CTIO 1.3 m	*B*	17.79	0.08
2455285.7249	0.195	Pagnotta	CTIO 1.3 m	*H*	15.89	0.21
2455285.7249	0.195	Pagnotta	CTIO 1.3 m	*I*	16.96	0.06
2455285.7266	0.197	Pagnotta	CTIO 1.3 m	*H*	15.91	0.21
2455285.7266	0.197	Pagnotta	CTIO 1.3 m	*R*	17.33	0.05
2455285.7282	0.198	Pagnotta	CTIO 1.3 m	*H*	15.93	0.21
2455285.7283	0.198	Pagnotta	CTIO 1.3 m	*V*	17.51	0.06
2455286.7191	0.003	Pagnotta	CTIO 1.3 m	*J*	16.84	0.12
2455286.7191	0.003	Pagnotta	CTIO 1.3 m	*B*	18.73	0.08
2455286.7208	0.005	Pagnotta	CTIO 1.3 m	*I*	17.88	0.09
2455286.7225	0.006	Pagnotta	CTIO 1.3 m	*R*	18.23	0.08
2455287.7166	0.814	Pagnotta	CTIO 1.3 m	*J*	16.41	0.08
2455287.7166	0.814	Pagnotta	CTIO 1.3 m	*B*	18.39	0.06
2455287.7182	0.815	Pagnotta	CTIO 1.3 m	*H*	16.34	0.26
2455287.7183	0.815	Pagnotta	CTIO 1.3 m	*I*	17.21	0.05
2455287.7199	0.816	Pagnotta	CTIO 1.3 m	*H*	16.24	0.23
2455287.7200	0.816	Pagnotta	CTIO 1.3 m	*R*	17.60	0.04
2455287.7216	0.818	Pagnotta	CTIO 1.3 m	*H*	16.20	0.22
2455287.7216	0.818	Pagnotta	CTIO 1.3 m	*V*	17.87	0.05
2455288.7453	0.650	Pagnotta	CTIO 1.3 m	*J*	16.49	0.07

Table 3
(Continued)

HJD	Phase	Observer	Telescope	Filter	Magnitude	Error
2455288.7454	0.650	Pagnotta	CTIO 1.3 m	*B*	18.18	0.04
2455288.7470	0.651	Pagnotta	CTIO 1.3 m	*H*	16.32	0.14
2455288.7471	0.651	Pagnotta	CTIO 1.3 m	*I*	17.14	0.04
2455288.7487	0.652	Pagnotta	CTIO 1.3 m	*H*	16.25	0.13
2455288.7488	0.653	Pagnotta	CTIO 1.3 m	*R*	17.47	0.04
2455288.7504	0.654	Pagnotta	CTIO 1.3 m	*H*	16.34	0.14
2455288.7504	0.654	Pagnotta	CTIO 1.3 m	*V*	17.72	0.04
2455289.7516	0.467	Pagnotta	CTIO 1.3 m	*J*	16.59	0.13
2455289.7516	0.467	Pagnotta	CTIO 1.3 m	*B*	18.37	0.06
2455289.7533	0.469	Pagnotta	CTIO 1.3 m	*I*	17.21	0.06
2455289.7550	0.470	Pagnotta	CTIO 1.3 m	*R*	17.51	0.05
2455289.7567	0.472	Pagnotta	CTIO 1.3 m	*V*	17.71	0.05
2455291.7310	0.076	Pagnotta	CTIO 1.3 m	*J*	16.65	0.08
2455291.7311	0.076	Pagnotta	CTIO 1.3 m	*B*	18.76	0.04
2455291.7328	0.077	Pagnotta	CTIO 1.3 m	*I*	17.54	0.04
2455291.7345	0.079	Pagnotta	CTIO 1.3 m	*R*	17.92	0.03
2455291.7361	0.080	Pagnotta	CTIO 1.3 m	*V*	18.14	0.03
2455292.7340	0.891	Pagnotta	CTIO 1.3 m	*J*	16.86	0.12
2455292.7340	0.891	Pagnotta	CTIO 1.3 m	*B*	18.47	0.04
2455292.7357	0.892	Pagnotta	CTIO 1.3 m	*I*	17.42	0.06
2455292.7374	0.894	Pagnotta	CTIO 1.3 m	*R*	17.71	0.05
2455292.7391	0.895	Pagnotta	CTIO 1.3 m	*V*	18.11	0.07
2455293.7421	0.710	Pagnotta	CTIO 1.3 m	*J*	16.65	0.07
2455293.7422	0.710	Pagnotta	CTIO 1.3 m	*B*	18.56	0.03
2455293.7438	0.712	Pagnotta	CTIO 1.3 m	*H*	16.51	0.21
2455293.7439	0.712	Pagnotta	CTIO 1.3 m	*I*	17.34	0.03
2455293.7456	0.713	Pagnotta	CTIO 1.3 m	*H*	16.49	0.21
2455293.7456	0.713	Pagnotta	CTIO 1.3 m	*R*	17.77	0.02
2455293.7472	0.715	Pagnotta	CTIO 1.3 m	*H*	16.57	0.22
2455293.7473	0.715	Pagnotta	CTIO 1.3 m	*V*	17.99	0.02
2455294.7657	0.542	Pagnotta	CTIO 1.3 m	*J*	16.96	0.07
2455294.7657	0.542	Pagnotta	CTIO 1.3 m	*B*	18.56	0.02
2455294.7674	0.544	Pagnotta	CTIO 1.3 m	*H*	16.63	0.14
2455294.7674	0.544	Pagnotta	CTIO 1.3 m	*I*	17.40	0.02
2455294.7691	0.545	Pagnotta	CTIO 1.3 m	*H*	16.51	0.12
2455294.7691	0.545	Pagnotta	CTIO 1.3 m	*R*	17.76	0.02
2455294.7707	0.546	Pagnotta	CTIO 1.3 m	*H*	16.54	0.12
2455294.7708	0.546	Pagnotta	CTIO 1.3 m	*V*	17.96	0.02
2455295.7298	0.326	Pagnotta	CTIO 1.3 m	*J*	16.58	0.05
2455295.7299	0.326	Pagnotta	CTIO 1.3 m	*B*	18.51	0.02
2455295.7315	0.327	Pagnotta	CTIO 1.3 m	*H*	16.27	0.17
2455295.7316	0.327	Pagnotta	CTIO 1.3 m	*I*	17.35	0.02
2455295.7332	0.328	Pagnotta	CTIO 1.3 m	*H*	16.39	0.19
2455295.7333	0.328	Pagnotta	CTIO 1.3 m	*R*	17.74	0.02
2455295.7349	0.330	Pagnotta	CTIO 1.3 m	*H*	16.32	0.17
2455295.7349	0.330	Pagnotta	CTIO 1.3 m	*V*	17.98	0.02
2455296.7466	0.152	Pagnotta	CTIO 1.3 m	*J*	16.65	0.06
2455296.7466	0.152	Pagnotta	CTIO 1.3 m	*B*	18.71	0.02
2455296.7483	0.153	Pagnotta	CTIO 1.3 m	*H*	16.41	0.18
2455296.7483	0.153	Pagnotta	CTIO 1.3 m	*I*	17.45	0.02
2455296.7500	0.155	Pagnotta	CTIO 1.3 m	*H*	16.45	0.17
2455296.7500	0.155	Pagnotta	CTIO 1.3 m	*R*	17.86	0.02
2455296.7516	0.156	Pagnotta	CTIO 1.3 m	*H*	16.35	0.15
2455296.7517	0.156	Pagnotta	CTIO 1.3 m	*V*	18.10	0.02
2455296.9359	0.306	Landolt	KPNO 2.1 m	Stromgren *y*	18.06	0.02
2455296.9477	0.315	Landolt	KPNO 2.1 m	Stromgren *y*	18.08	0.02
2455296.9583	0.324	Landolt	KPNO 2.1 m	Stromgren *y*	18.04	0.02
2455297.7253	0.947	Pagnotta	CTIO 1.3 m	*J*	16.81	0.07
2455297.7253	0.947	Pagnotta	CTIO 1.3 m	*B*	18.90	0.03
2455297.7270	0.949	Pagnotta	CTIO 1.3 m	*H*	16.62	0.22
2455297.7270	0.949	Pagnotta	CTIO 1.3 m	*I*	17.80	0.03
2455297.7287	0.950	Pagnotta	CTIO 1.3 m	*H*	16.63	0.22
2455297.7287	0.950	Pagnotta	CTIO 1.3 m	*R*	18.08	0.02

Table 3
(Continued)

HJD	Phase	Observer	Telescope	Filter	Magnitude	Error
2455297.7303	0.951	Pagnotta	CTIO 1.3 m	*H*	16.63	0.22
2455297.7304	0.951	Pagnotta	CTIO 1.3 m	*V*	18.28	0.02
2455297.9668	0.143	Landolt	KPNO 2.1 m	Stromgren *y*	17.61	0.01
2455297.9777	0.152	Landolt	KPNO 2.1 m	Stromgren *y*	17.99	0.02
2455298.7527	0.782	Pagnotta	CTIO 1.3 m	*J*	16.57	0.05
2455298.7527	0.782	Pagnotta	CTIO 1.3 m	*B*	18.50	0.02
2455298.7545	0.784	Pagnotta	CTIO 1.3 m	*I*	17.32	0.02
2455298.7562	0.785	Pagnotta	CTIO 1.3 m	*R*	17.70	0.02
2455298.7579	0.786	Pagnotta	CTIO 1.3 m	*V*	17.89	0.02
2455298.9307	0.927	Landolt	KPNO 2.1 m	Stromgren *y*	18.14	0.02
2455298.9431	0.937	Landolt	KPNO 2.1 m	Stromgren *y*	18.36	0.02
2455299.6321	0.497	Pagnotta	CTIO 1.3 m	*J*	16.47	0.09
2455299.6321	0.497	Pagnotta	CTIO 1.3 m	*B*	18.58	0.03
2455299.6338	0.498	Pagnotta	CTIO 1.3 m	*I*	17.45	0.03
2455299.6355	0.500	Pagnotta	CTIO 1.3 m	*R*	17.81	0.02
2455299.6372	0.501	Pagnotta	CTIO 1.3 m	*V*	18.00	0.02
2455300.6848	0.352	Pagnotta	CTIO 1.3 m	*J*	16.46	0.07
2455300.6848	0.352	Pagnotta	CTIO 1.3 m	*B*	18.34	0.02
2455300.6865	0.354	Pagnotta	CTIO 1.3 m	*I*	17.23	0.02
2455300.6882	0.355	Pagnotta	CTIO 1.3 m	*R*	17.59	0.02
2455300.6899	0.356	Pagnotta	CTIO 1.3 m	*V*	17.82	0.02
2455300.9358	0.556	Landolt	KPNO 2.1 m	Stromgren *y*	17.87	0.01
2455300.9469	0.565	Landolt	KPNO 2.1 m	Stromgren *y*	17.91	0.02
2455301.6407	0.129	Pagnotta	CTIO 1.3 m	*J*	16.44	0.11
2455301.6408	0.129	Pagnotta	CTIO 1.3 m	*B*	18.66	0.03
2455301.6425	0.131	Pagnotta	CTIO 1.3 m	*I*	17.35	0.03
2455301.6442	0.132	Pagnotta	CTIO 1.3 m	*R*	17.78	0.02
2455301.6459	0.133	Pagnotta	CTIO 1.3 m	*V*	18.01	0.02
2455302.6487	0.948	Pagnotta	CTIO 1.3 m	*B*	18.78	0.08
2455302.6504	0.950	Pagnotta	CTIO 1.3 m	*I*	17.61	0.15
2455302.6521	0.951	Pagnotta	CTIO 1.3 m	*R*	18.30	0.12
2455302.6538	0.952	Pagnotta	CTIO 1.3 m	*V*	18.51	0.10
2455304.6716	0.592	Pagnotta	CTIO 1.3 m	*J*	16.45	0.13
2455304.6716	0.592	Pagnotta	CTIO 1.3 m	*B*	18.24	0.02
2455304.6733	0.594	Pagnotta	CTIO 1.3 m	*I*	17.07	0.02
2455304.6750	0.595	Pagnotta	CTIO 1.3 m	*R*	17.45	0.02
2455304.6767	0.596	Pagnotta	CTIO 1.3 m	*V*	17.70	0.02
2455305.6687	0.402	Pagnotta	CTIO 1.3 m	*J*	16.22	0.06
2455305.6688	0.403	Pagnotta	CTIO 1.3 m	*B*	17.72	0.01
2455305.6704	0.404	Pagnotta	CTIO 1.3 m	*H*	16.14	0.22
2455305.6705	0.404	Pagnotta	CTIO 1.3 m	*I*	16.74	0.02
2455305.6721	0.405	Pagnotta	CTIO 1.3 m	*R*	17.09	0.01
2455305.6738	0.407	Pagnotta	CTIO 1.3 m	*H*	16.25	0.24
2455305.6738	0.407	Pagnotta	CTIO 1.3 m	*V*	17.30	0.01
2455306.6092	0.167	Pagnotta	CTIO 1.3 m	*B*	18.14	0.02
2455306.6108	0.168	Pagnotta	CTIO 1.3 m	*I*	17.05	0.03
2455306.6125	0.169	Pagnotta	CTIO 1.3 m	*R*	17.44	0.02
2455306.6142	0.171	Pagnotta	CTIO 1.3 m	*V*	17.66	0.02
2455307.6631	0.023	Pagnotta	CTIO 1.3 m	*J*	17.18	0.17
2455307.6632	0.023	Pagnotta	CTIO 1.3 m	*B*	19.50	0.05
2455307.6649	0.025	Pagnotta	CTIO 1.3 m	*I*	18.03	0.05
2455307.6666	0.026	Pagnotta	CTIO 1.3 m	*R*	18.45	0.03
2455307.6682	0.027	Pagnotta	CTIO 1.3 m	*V*	18.80	0.04
2455308.8012	0.948	Pagnotta	CTIO 1.3 m	*J*	16.95	0.08
2455308.8012	0.948	Pagnotta	CTIO 1.3 m	*B*	18.62	0.02
2455308.8028	0.949	Pagnotta	CTIO 1.3 m	*H*	16.49	0.16
2455308.8029	0.949	Pagnotta	CTIO 1.3 m	*I*	17.52	0.03
2455308.8045	0.951	Pagnotta	CTIO 1.3 m	*H*	16.52	0.16
2455308.8046	0.951	Pagnotta	CTIO 1.3 m	*R*	17.85	0.02
2455308.8062	0.952	Pagnotta	CTIO 1.3 m	*H*	16.60	0.17
2455308.8062	0.952	Pagnotta	CTIO 1.3 m	*V*	18.13	0.02
2455309.5895	0.589	Pagnotta	CTIO 1.3 m	*J*	16.25	0.10
2455309.5895	0.589	Pagnotta	CTIO 1.3 m	*B*	18.32	0.04

Table 3
(Continued)

HJD	Phase	Observer	Telescope	Filter	Magnitude	Error
2455309.5911	0.590	Pagnotta	CTIO 1.3 m	*J*	16.27	0.10
2455309.5911	0.590	Pagnotta	CTIO 1.3 m	*I*	17.15	0.03
2455309.5928	0.591	Pagnotta	CTIO 1.3 m	*J*	16.24	0.09
2455309.5928	0.591	Pagnotta	CTIO 1.3 m	*R*	17.52	0.02
2455309.5944	0.593	Pagnotta	CTIO 1.3 m	*J*	16.20	0.09
2455309.5945	0.593	Pagnotta	CTIO 1.3 m	*V*	17.77	0.03
2455310.6308	0.435	Pagnotta	CTIO 1.3 m	*J*	16.24	0.07
2455310.6308	0.435	Pagnotta	CTIO 1.3 m	*B*	17.95	0.03
2455310.6325	0.436	Pagnotta	CTIO 1.3 m	*J*	16.26	0.07
2455310.6325	0.436	Pagnotta	CTIO 1.3 m	*I*	16.91	0.02
2455310.6341	0.438	Pagnotta	CTIO 1.3 m	*J*	16.25	0.07
2455310.6342	0.438	Pagnotta	CTIO 1.3 m	*R*	17.32	0.02
2455310.6358	0.439	Pagnotta	CTIO 1.3 m	*J*	16.31	0.07
2455310.6358	0.439	Pagnotta	CTIO 1.3 m	*V*	17.53	0.02
2455315.6321	0.499	Pagnotta	CTIO 1.3 m	*B*	18.48	0.10
2455315.6338	0.501	Pagnotta	CTIO 1.3 m	*I*	17.29	0.08
2455315.6355	0.502	Pagnotta	CTIO 1.3 m	*R*	17.80	0.08
2455315.6371	0.503	Pagnotta	CTIO 1.3 m	*V*	17.84	0.07
2455317.7483	0.219	Pagnotta	CTIO 1.3 m	*J*	16.78	0.17
2455317.7484	0.219	Pagnotta	CTIO 1.3 m	*B*	18.60	0.08
2455317.7500	0.220	Pagnotta	CTIO 1.3 m	*J*	16.81	0.18
2455317.7500	0.220	Pagnotta	CTIO 1.3 m	*I*	17.20	0.07
2455317.7517	0.222	Pagnotta	CTIO 1.3 m	*J*	16.80	0.19
2455317.7517	0.222	Pagnotta	CTIO 1.3 m	*R*	17.70	0.07
2455317.7533	0.223	Pagnotta	CTIO 1.3 m	*J*	16.84	0.19
2455317.7534	0.223	Pagnotta	CTIO 1.3 m	*V*	18.04	0.07
2455319.6613	0.774	Pagnotta	CTIO 1.3 m	*B*	18.73	0.05
2455319.6630	0.775	Pagnotta	CTIO 1.3 m	*I*	17.34	0.03
2455319.6647	0.776	Pagnotta	CTIO 1.3 m	*R*	17.80	0.03
2455319.6664	0.778	Pagnotta	CTIO 1.3 m	*V*	18.05	0.03
2455320.6661	0.590	Pagnotta	CTIO 1.3 m	*J*	16.57	0.10
2455320.6661	0.590	Pagnotta	CTIO 1.3 m	*B*	18.55	0.03
2455320.6678	0.591	Pagnotta	CTIO 1.3 m	*J*	16.58	0.10
2455320.6678	0.591	Pagnotta	CTIO 1.3 m	*I*	17.23	0.03
2455320.6695	0.593	Pagnotta	CTIO 1.3 m	*J*	16.64	0.11
2455320.6695	0.593	Pagnotta	CTIO 1.3 m	*R*	17.62	0.02
2455320.6711	0.594	Pagnotta	CTIO 1.3 m	*J*	16.52	0.10
2455320.6712	0.594	Pagnotta	CTIO 1.3 m	*V*	17.94	0.02
2455321.6527	0.392	Pagnotta	CTIO 1.3 m	*J*	16.66	0.16
2455321.6528	0.392	Pagnotta	CTIO 1.3 m	*B*	18.60	0.03
2455321.6544	0.393	Pagnotta	CTIO 1.3 m	*J*	16.65	0.14
2455321.6545	0.393	Pagnotta	CTIO 1.3 m	*I*	17.30	0.03
2455321.6561	0.395	Pagnotta	CTIO 1.3 m	*J*	16.43	0.11
2455321.6561	0.395	Pagnotta	CTIO 1.3 m	*R*	17.69	0.02
2455321.6578	0.396	Pagnotta	CTIO 1.3 m	*J*	16.55	0.12
2455321.6578	0.396	Pagnotta	CTIO 1.3 m	*V*	18.02	0.02
2455323.5975	0.972	Pagnotta	CTIO 1.3 m	*B*	19.09	0.03
2455323.5992	0.974	Pagnotta	CTIO 1.3 m	*I*	17.81	0.05
2455323.6009	0.975	Pagnotta	CTIO 1.3 m	*R*	18.24	0.03
2455323.6026	0.976	Pagnotta	CTIO 1.3 m	*V*	18.59	0.03
2455324.5965	0.784	Pagnotta	CTIO 1.3 m	*B*	18.55	0.02
2455324.5982	0.785	Pagnotta	CTIO 1.3 m	*I*	17.28	0.03
2455324.5999	0.787	Pagnotta	CTIO 1.3 m	*R*	17.62	0.02
2455324.6016	0.788	Pagnotta	CTIO 1.3 m	*V*	17.96	0.02
2455325.7090	0.688	Pagnotta	CTIO 1.3 m	*B*	18.35	0.02
2455325.7107	0.690	Pagnotta	CTIO 1.3 m	*I*	17.09	0.02
2455325.7124	0.691	Pagnotta	CTIO 1.3 m	*R*	17.53	0.02
2455325.7141	0.692	Pagnotta	CTIO 1.3 m	*V*	17.86	0.02
2455326.6976	0.492	Pagnotta	CTIO 1.3 m	*B*	18.32	0.02
2455326.6993	0.493	Pagnotta	CTIO 1.3 m	*I*	17.28	0.02
2455326.7010	0.494	Pagnotta	CTIO 1.3 m	*R*	17.63	0.02
2455326.7027	0.496	Pagnotta	CTIO 1.3 m	*V*	17.87	0.02
2455327.6331	0.252	Pagnotta	CTIO 1.3 m	*B*	18.55	0.02

Table 3
(Continued)

HJD	Phase	Observer	Telescope	Filter	Magnitude	Error
2455327.6348	0.253	Pagnotta	CTIO 1.3 m	*I*	17.22	0.02
2455327.6365	0.254	Pagnotta	CTIO 1.3 m	*R*	17.59	0.02
2455327.6381	0.256	Pagnotta	CTIO 1.3 m	*V*	17.95	0.02
2455328.6055	0.042	Pagnotta	CTIO 1.3 m	*B*	19.25	0.09
2455328.6072	0.043	Pagnotta	CTIO 1.3 m	*I*	17.85	0.14
2455328.6089	0.045	Pagnotta	CTIO 1.3 m	*R*	18.40	0.11
2455328.6106	0.046	Pagnotta	CTIO 1.3 m	*V*	18.56	0.08
2455334.5924	0.907	Pagnotta	CTIO 1.3 m	*B*	18.45	0.02
2455334.5941	0.909	Pagnotta	CTIO 1.3 m	*I*	17.24	0.03
2455334.5958	0.910	Pagnotta	CTIO 1.3 m	*R*	15.91	0.02
2455334.5974	0.911	Pagnotta	CTIO 1.3 m	*V*	17.95	0.02
2455335.6387	0.757	Pagnotta	CTIO 1.3 m	*B*	18.36	0.02
2455335.6403	0.759	Pagnotta	CTIO 1.3 m	*I*	17.05	0.02
2455335.6420	0.760	Pagnotta	CTIO 1.3 m	*R*	17.50	0.01
2455335.6437	0.762	Pagnotta	CTIO 1.3 m	*V*	17.83	0.02
2455338.6302	0.188	Pagnotta	CTIO 1.3 m	*B*	17.55	0.03
2455338.6319	0.190	Pagnotta	CTIO 1.3 m	*I*	16.61	0.03
2455338.6336	0.191	Pagnotta	CTIO 1.3 m	*R*	16.94	0.03
2455338.6352	0.193	Pagnotta	CTIO 1.3 m	*V*	17.09	0.04
2455339.6837	0.045	Pagnotta	CTIO 1.3 m	*B*	19.15	0.05
2455339.6854	0.046	Pagnotta	CTIO 1.3 m	*I*	17.66	0.04
2455339.6870	0.047	Pagnotta	CTIO 1.3 m	*R*	18.07	0.03
2455339.6887	0.049	Pagnotta	CTIO 1.3 m	*V*	18.45	0.04
2455340.6322	0.815	Pagnotta	CTIO 1.3 m	*B*	18.08	0.03
2455340.6339	0.817	Pagnotta	CTIO 1.3 m	*I*	16.89	0.02
2455340.6356	0.818	Pagnotta	CTIO 1.3 m	*R*	17.30	0.02
2455340.6373	0.820	Pagnotta	CTIO 1.3 m	*V*	17.58	0.02
2455341.6516	0.644	Pagnotta	CTIO 1.3 m	*B*	18.33	0.04
2455341.6532	0.645	Pagnotta	CTIO 1.3 m	*I*	17.08	0.03
2455341.6549	0.647	Pagnotta	CTIO 1.3 m	*R*	17.51	0.03
2455341.6566	0.648	Pagnotta	CTIO 1.3 m	*V*	17.82	0.03
2455342.6908	0.488	Pagnotta	CTIO 1.3 m	*B*	18.37	0.05
2455342.6925	0.490	Pagnotta	CTIO 1.3 m	*I*	17.34	0.04
2455342.6942	0.491	Pagnotta	CTIO 1.3 m	*R*	17.67	0.03
2455342.6959	0.492	Pagnotta	CTIO 1.3 m	*V*	17.90	0.03
2455343.6045	0.231	Pagnotta	CTIO 1.3 m	*B*	18.07	0.06
2455343.6062	0.232	Pagnotta	CTIO 1.3 m	*I*	17.12	0.06
2455343.6079	0.234	Pagnotta	CTIO 1.3 m	*R*	17.38	0.05
2455343.6096	0.235	Pagnotta	CTIO 1.3 m	*V*	17.71	0.05
2455346.7432	0.782	Pagnotta	CTIO 1.3 m	*B*	18.54	0.05
2455346.7449	0.783	Pagnotta	CTIO 1.3 m	*I*	17.23	0.04
2455346.7466	0.784	Pagnotta	CTIO 1.3 m	*R*	17.67	0.04
2455346.7483	0.786	Pagnotta	CTIO 1.3 m	*V*	18.01	0.04
2455347.6779	0.541	Pagnotta	CTIO 1.3 m	*B*	18.75	0.04
2455347.6796	0.542	Pagnotta	CTIO 1.3 m	*I*	17.47	0.03
2455347.6813	0.544	Pagnotta	CTIO 1.3 m	*R*	17.90	0.03
2455347.6829	0.545	Pagnotta	CTIO 1.3 m	*V*	18.16	0.03
2455348.6602	0.339	Pagnotta	CTIO 1.3 m	*B*	18.87	0.04
2455348.6619	0.341	Pagnotta	CTIO 1.3 m	*I*	17.41	0.03
2455348.6636	0.342	Pagnotta	CTIO 1.3 m	*R*	17.86	0.02
2455348.6652	0.343	Pagnotta	CTIO 1.3 m	*V*	18.06	0.03
2455349.6300	0.127	Pagnotta	CTIO 1.3 m	*B*	18.71	0.07
2455349.6317	0.129	Pagnotta	CTIO 1.3 m	*I*	17.43	0.06
2455349.6334	0.130	Pagnotta	CTIO 1.3 m	*R*	17.70	0.04
2455349.6351	0.132	Pagnotta	CTIO 1.3 m	*V*	18.04	0.04
2455351.6893	0.801	Pagnotta	CTIO 1.3 m	*B*	18.35	0.02
2455351.6910	0.802	Pagnotta	CTIO 1.3 m	*I*	17.16	0.02
2455351.6927	0.804	Pagnotta	CTIO 1.3 m	*R*	17.51	0.01
2455351.6944	0.805	Pagnotta	CTIO 1.3 m	*V*	17.84	0.02
2455352.6576	0.588	Pagnotta	CTIO 1.3 m	*B*	18.73	0.02
2455352.6593	0.589	Pagnotta	CTIO 1.3 m	*I*	17.37	0.02
2455352.6610	0.591	Pagnotta	CTIO 1.3 m	*R*	17.81	0.02
2455352.6627	0.592	Pagnotta	CTIO 1.3 m	*V*	18.16	0.02

Table 3
(Continued)

HJD	Phase	Observer	Telescope	Filter	Magnitude	Error
2455353.6277	0.376	Pagnotta	CTIO 1.3 m	*B*	18.74	0.02
2455353.6294	0.378	Pagnotta	CTIO 1.3 m	*I*	17.36	0.02
2455353.6311	0.379	Pagnotta	CTIO 1.3 m	*R*	17.82	0.02
2455353.6328	0.380	Pagnotta	CTIO 1.3 m	*V*	18.19	0.02
2455355.6453	0.016	Pagnotta	CTIO 1.3 m	*B*	19.99	0.06
2455355.6469	0.017	Pagnotta	CTIO 1.3 m	*I*	18.29	0.05
2455355.6486	0.018	Pagnotta	CTIO 1.3 m	*R*	18.68	0.03
2455355.6503	0.020	Pagnotta	CTIO 1.3 m	*V*	19.15	0.04
2455356.6519	0.834	Pagnotta	CTIO 1.3 m	*B*	19.04	0.04
2455356.6536	0.835	Pagnotta	CTIO 1.3 m	*I*	17.50	0.03
2455356.6553	0.837	Pagnotta	CTIO 1.3 m	*R*	17.93	0.02
2455356.6570	0.838	Pagnotta	CTIO 1.3 m	*V*	18.35	0.02
2455359.7666	0.365	Pagnotta	CTIO 1.3 m	*B*	18.38	0.02
2455359.7683	0.366	Pagnotta	CTIO 1.3 m	*I*	17.18	0.02
2455359.7700	0.368	Pagnotta	CTIO 1.3 m	*R*	17.60	0.02
2455359.7717	0.369	Pagnotta	CTIO 1.3 m	*V*	17.91	0.02
2455360.5792	0.025	Pagnotta	CTIO 1.3 m	*B*	19.83	0.07
2455360.5809	0.027	Pagnotta	CTIO 1.3 m	*I*	18.10	0.07
2455360.5826	0.028	Pagnotta	CTIO 1.3 m	*R*	18.73	0.07
2455360.5842	0.029	Pagnotta	CTIO 1.3 m	*V*	19.11	0.13
2455368.5877	0.533	Pagnotta	CTIO 1.3 m	*B*	18.46	0.04
2455368.5893	0.535	Pagnotta	CTIO 1.3 m	*I*	17.28	0.03
2455368.5910	0.536	Pagnotta	CTIO 1.3 m	*R*	17.70	0.03
2455368.5927	0.537	Pagnotta	CTIO 1.3 m	*V*	18.03	0.03
2455369.6174	0.370	Pagnotta	CTIO 1.3 m	*B*	17.82	0.02
2455369.6191	0.372	Pagnotta	CTIO 1.3 m	*I*	16.86	0.02
2455369.6208	0.373	Pagnotta	CTIO 1.3 m	*R*	17.17	0.02
2455369.6225	0.374	Pagnotta	CTIO 1.3 m	*V*	17.46	0.03
2455372.6995	0.875	Pagnotta	CTIO 1.3 m	*B*	18.37	0.06
2455372.7012	0.876	Pagnotta	CTIO 1.3 m	*I*	17.15	0.06
2455372.7029	0.878	Pagnotta	CTIO 1.3 m	*R*	17.46	0.05
2455372.7046	0.879	Pagnotta	CTIO 1.3 m	*V*	17.75	0.05
2455373.6423	0.641	Pagnotta	CTIO 1.3 m	*B*	18.69	0.08
2455373.6440	0.642	Pagnotta	CTIO 1.3 m	*I*	17.12	0.05
2455373.6457	0.644	Pagnotta	CTIO 1.3 m	*R*	17.54	0.05
2455373.6473	0.645	Pagnotta	CTIO 1.3 m	*V*	17.87	0.06
2455374.6681	0.475	Pagnotta	CTIO 1.3 m	*B*	18.69	0.07
2455374.6697	0.476	Pagnotta	CTIO 1.3 m	*I*	17.52	0.06
2455374.6715	0.477	Pagnotta	CTIO 1.3 m	*R*	17.92	0.06
2455374.6731	0.479	Pagnotta	CTIO 1.3 m	*V*	18.05	0.06
2455375.5448	0.187	Pagnotta	CTIO 1.3 m	*B*	18.30	0.04
2455375.5465	0.188	Pagnotta	CTIO 1.3 m	*I*	17.14	0.03
2455375.5482	0.190	Pagnotta	CTIO 1.3 m	*R*	17.54	0.02
2455375.5498	0.191	Pagnotta	CTIO 1.3 m	*V*	17.94	0.03
2455377.6278	0.880	Pagnotta	CTIO 1.3 m	*B*	18.95	0.04
2455377.6295	0.881	Pagnotta	CTIO 1.3 m	*I*	17.61	0.03
2455377.6312	0.883	Pagnotta	CTIO 1.3 m	*R*	18.03	0.03
2455377.6329	0.884	Pagnotta	CTIO 1.3 m	*V*	18.41	0.03
2455378.6280	0.693	Pagnotta	CTIO 1.3 m	*B*	19.23	0.05
2455378.6297	0.694	Pagnotta	CTIO 1.3 m	*I*	17.56	0.03
2455378.6314	0.695	Pagnotta	CTIO 1.3 m	*R*	18.11	0.03
2455378.6330	0.697	Pagnotta	CTIO 1.3 m	*V*	18.50	0.03
2455379.6147	0.494	Pagnotta	CTIO 1.3 m	*B*	19.15	0.03
2455379.6163	0.496	Pagnotta	CTIO 1.3 m	*I*	17.74	0.03
2455379.6180	0.497	Pagnotta	CTIO 1.3 m	*R*	18.15	0.02
2455379.6197	0.498	Pagnotta	CTIO 1.3 m	*V*	18.52	0.03
2455380.5447	0.250	Pagnotta	CTIO 1.3 m	*B*	18.97	0.03
2455380.5464	0.252	Pagnotta	CTIO 1.3 m	*I*	17.52	0.03
2455380.5481	0.253	Pagnotta	CTIO 1.3 m	*R*	18.00	0.02
2455380.5498	0.254	Pagnotta	CTIO 1.3 m	*V*	18.40	0.02
2455381.5576	0.073	Pagnotta	CTIO 1.3 m	*B*	19.38	0.04
2455381.5593	0.075	Pagnotta	CTIO 1.3 m	*I*	17.87	0.04
2455381.5610	0.076	Pagnotta	CTIO 1.3 m	*R*	18.31	0.03

Table 3
(Continued)

HJD	Phase	Observer	Telescope	Filter	Magnitude	Error
2455381.5627	0.077	Pagnotta	CTIO 1.3 m	*V*	18.68	0.03
2455382.5505	0.880	Pagnotta	CTIO 1.3 m	*B*	18.88	0.03
2455382.5521	0.882	Pagnotta	CTIO 1.3 m	*I*	17.48	0.03
2455382.5538	0.883	Pagnotta	CTIO 1.3 m	*R*	17.95	0.02
2455382.5555	0.884	Pagnotta	CTIO 1.3 m	*V*	18.31	0.03
2455385.7049	0.444	Pagnotta	CTIO 1.3 m	*B*	19.03	0.03
2455385.7065	0.445	Pagnotta	CTIO 1.3 m	*I*	17.69	0.03
2455385.7082	0.446	Pagnotta	CTIO 1.3 m	*R*	18.09	0.02
2455385.7099	0.448	Pagnotta	CTIO 1.3 m	*V*	18.28	0.02
2455387.6231	0.002	Pagnotta	CTIO 1.3 m	*B*	19.90	0.06
2455387.6248	0.004	Pagnotta	CTIO 1.3 m	*I*	18.23	0.04
2455387.6265	0.005	Pagnotta	CTIO 1.3 m	*R*	18.63	0.03
2455387.6281	0.007	Pagnotta	CTIO 1.3 m	*V*	19.22	0.04
2455388.5325	0.741	Pagnotta	CTIO 1.3 m	*B*	18.96	0.03
2455388.5342	0.743	Pagnotta	CTIO 1.3 m	*I*	17.47	0.03
2455388.5359	0.744	Pagnotta	CTIO 1.3 m	*R*	17.94	0.02
2455388.5375	0.746	Pagnotta	CTIO 1.3 m	*V*	18.36	0.02
2455390.6123	0.432	Pagnotta	CTIO 1.3 m	*B*	18.69	0.02
2455390.6140	0.433	Pagnotta	CTIO 1.3 m	*I*	17.39	0.02
2455390.6157	0.434	Pagnotta	CTIO 1.3 m	*R*	17.79	0.02
2455390.6174	0.436	Pagnotta	CTIO 1.3 m	*V*	18.14	0.02
2455392.6360	0.076	Pagnotta	CTIO 1.3 m	*B*	19.27	0.04
2455392.6376	0.077	Pagnotta	CTIO 1.3 m	*I*	17.78	0.03
2455392.6393	0.079	Pagnotta	CTIO 1.3 m	*R*	18.26	0.03
2455392.6410	0.080	Pagnotta	CTIO 1.3 m	*V*	18.64	0.03
2455393.5613	0.828	Pagnotta	CTIO 1.3 m	*B*	18.86	0.04
2455393.5630	0.829	Pagnotta	CTIO 1.3 m	*I*	17.45	0.03
2455393.5647	0.831	Pagnotta	CTIO 1.3 m	*R*	17.88	0.02
2455393.5664	0.832	Pagnotta	CTIO 1.3 m	*V*	18.26	0.03
2455400.6402	0.581	Pagnotta	CTIO 1.3 m	*B*	18.74	0.08
2455400.6419	0.582	Pagnotta	CTIO 1.3 m	*I*	17.59	0.08
2455400.6436	0.583	Pagnotta	CTIO 1.3 m	*R*	17.97	0.06
2455400.6452	0.585	Pagnotta	CTIO 1.3 m	*V*	18.24	0.07
2455403.5813	0.971	Pagnotta	CTIO 1.3 m	*B*	19.31	0.11
2455403.5830	0.972	Pagnotta	CTIO 1.3 m	*I*	17.82	0.05
2455403.5847	0.974	Pagnotta	CTIO 1.3 m	*R*	18.21	0.05
2455403.5864	0.975	Pagnotta	CTIO 1.3 m	*V*	18.60	0.07
2455404.5254	0.738	Pagnotta	CTIO 1.3 m	*B*	18.44	0.04
2455404.5271	0.739	Pagnotta	CTIO 1.3 m	*I*	17.23	0.03
2455404.5288	0.741	Pagnotta	CTIO 1.3 m	*R*	17.62	0.02
2455404.5304	0.742	Pagnotta	CTIO 1.3 m	*V*	17.94	0.03
2455406.5743	0.403	Pagnotta	CTIO 1.3 m	*B*	18.64	0.03
2455406.5760	0.404	Pagnotta	CTIO 1.3 m	*I*	17.37	0.03
2455406.5777	0.406	Pagnotta	CTIO 1.3 m	*R*	17.79	0.02
2455406.5794	0.407	Pagnotta	CTIO 1.3 m	*V*	18.14	0.03
2455409.6233	0.881	Pagnotta	CTIO 1.3 m	*B*	18.74	0.04
2455409.6249	0.882	Pagnotta	CTIO 1.3 m	*I*	17.41	0.03
2455409.6266	0.883	Pagnotta	CTIO 1.3 m	*R*	17.85	0.03
2455409.6283	0.885	Pagnotta	CTIO 1.3 m	*V*	18.21	0.03

(This table is available in its entirety in machine-readable form.)

well as UV observations starting immediately after eruption. Although *Swift* did observe U Sco at very early times, UVOT photometry is unavailable from those times due to coincidence loss from the bright source. Although there is a possibility that a new analysis method may be able to be used to extract some information from these observations (Page et al. 2013), that is not currently an option. Instead we extrapolate to obtain sensible values for early UV magnitudes and acknowledge that we may be missing some of the energy being released in the nova, which introduces an unknown amount of systematic error. Overall, though, the extrapolation to near-UV from the early *B*-band magnitudes is reasonable.

The daily magnitude averages were then converted to Janskys and the quiescent flux level in each band, based on pre-2010-eruption photometry, was subtracted out of each daily average to isolate the flux due to the eruption. Each day was then summed across all bandpasses to give the average total eruption luminosity, $L_{\rm tot}$, for each day. The $L_{\rm tot}$ values were multiplied by the duration (in seconds) of the time from whence those data came (where some of the "days" are longer or

Table 4
U Sco 2010 Observations, X-Ray Count Rates

HJD	Phase	Count Rate	Error
2455232.5034	0.9449	0.0015	0.0005
2455229.9981	0.9090	0.0019	0.0004
2455228.4198	0.6264	0.0025	0.0003
2455282.7612	0.7867	0.0045	0.0012
2455231.1363	0.8340	0.0046	0.0010
2455287.9803	0.0280	0.0068	0.0016
2455287.2818	0.4604	0.0071	0.0014
2455284.6330	0.3079	0.0072	0.0015
2455279.2933	0.9686	0.0095	0.0015
2455280.6267	0.0522	0.0107	0.0019
2455280.2467	0.7433	0.0128	0.0038
2455277.9670	0.8907	0.0146	0.0072
2455275.0320	0.5056	0.0166	0.0030
2455277.2110	0.2764	0.0187	0.0019
2455273.6379	0.3727	0.0194	0.0037
2455268.4489	0.1559	0.0241	0.0055
2455269.6544	0.1355	0.0253	0.0053
2455272.0862	0.1117	0.0292	0.0054
2455269.4536	0.9724	0.0293	0.0058
2455272.8307	0.7167	0.0299	0.0040
2455268.5807	0.2630	0.0326	0.0058
2455271.3161	0.4859	0.0337	0.0042
2455269.5880	0.0816	0.0344	0.0065
2455270.3884	0.7320	0.0353	0.0059
2455269.5115	0.0194	0.0354	0.0049
2455266.9076	0.9034	0.0368	0.0057
2455269.7096	0.1804	0.0369	0.0053
2455268.5136	0.2085	0.0381	0.0065
2455269.1852	0.7542	0.0405	0.0065
2455269.3223	0.8657	0.0422	0.0096
2455268.2426	0.9882	0.0434	0.0066
2455268.3824	0.1019	0.0447	0.0072
2455268.3110	0.0438	0.0464	0.0066
2455269.3865	0.9178	0.0484	0.0071
2455267.9815	0.7761	0.0487	0.0079
2455269.2508	0.8076	0.0504	0.0069
2455268.0471	0.8294	0.0509	0.0078
2455267.9148	0.7219	0.0514	0.0082
2455266.8402	0.8486	0.0515	0.0066
2455267.0409	0.0117	0.0535	0.0068
2455267.4422	0.3378	0.0539	0.0068
2455267.3757	0.2838	0.0565	0.0069
2455267.5588	0.4326	0.0600	0.0200
2455267.2416	0.1748	0.0605	0.0072
2455266.9743	0.9576	0.0624	0.0073
2455267.1083	0.0665	0.0645	0.0074
2455267.1750	0.1207	0.0694	0.0077
2455265.8324	0.0296	0.0717	0.0081
2455265.9681	0.1399	0.0746	0.0090
2455265.6340	0.8684	0.0782	0.0091
2455265.7672	0.9766	0.0800	0.0091
2455265.5666	0.8136	0.0825	0.0094
2455265.7006	0.9225	0.0875	0.0097
2455265.9007	0.0851	0.0878	0.0098
2455266.1694	0.3035	0.0888	0.0097
2455266.1014	0.2482	0.0891	0.0098
2455266.0347	0.1940	0.0942	0.0100
2455265.4353	0.7069	0.0949	0.0090
2455264.8342	0.2184	0.0950	0.0100
2455237.0405	0.6320	0.0966	0.0390
2455264.9540	0.3158	0.0997	0.0094
2455265.4966	0.7567	0.1027	0.0139
2455264.6344	0.0561	0.1109	0.0115
2455264.4313	0.8910	0.1141	0.0101

Table 4
(Continued)

HJD	Phase	Count Rate	Error
2455264.8968	0.2693	0.1197	0.0109
2455264.7003	0.1096	0.1272	0.0113
2455264.2306	0.7279	0.1293	0.0107
2455264.5661	0.0005	0.1333	0.0114
2455264.3647	0.8369	0.1383	0.0110
2455264.7670	0.1638	0.1483	0.0122
2455238.4585	0.7843	0.1490	0.0124
2455264.4855	0.9350	0.1502	0.0114
2455264.2980	0.7827	0.1602	0.0118
2455237.0465	0.6368	0.3370	0.0191
2455247.3608	0.0187	0.3404	0.0900
2455238.2445	0.6104	0.3560	0.0785
2455237.4560	0.9696	0.3683	0.0513
2455237.4629	0.9752	0.3960	0.0202
2455240.0513	0.0787	0.3991	0.0958
2455242.2052	0.8290	0.4147	0.0869
2455242.3972	0.9851	0.4650	0.0648
2455238.6615	0.9492	0.4745	0.0222
2455245.3515	0.3859	0.4900	0.0738
2455238.7355	0.0094	0.4948	0.0234
2455243.2785	0.7012	0.5123	0.0679
2455237.7295	0.1919	0.5150	0.0228
2455242.4084	0.9942	0.5377	0.0175
2455238.2515	0.6161	0.5470	0.0224
2455239.9888	0.0279	0.5474	0.0260
2455239.9888	0.0279	0.5474	0.0260
2455248.6976	0.1051	0.5475	0.0998
2455246.1565	0.0400	0.5486	0.0918
2455242.1287	0.7669	0.5577	0.0893
2455245.4182	0.4401	0.5707	0.0788
2455245.6865	0.6581	0.5747	0.1198
2455242.4782	0.0509	0.5755	0.0208
2455241.1223	0.9490	0.5817	0.0786
2455244.1449	0.4053	0.5837	0.1350
2455237.7225	0.1862	0.5890	0.0554
2455239.5963	0.7089	0.5905	0.0608
2455246.2293	0.0992	0.5964	0.0256
2455246.2232	0.0943	0.6020	0.0948
2455241.2063	0.0173	0.6043	0.0301
2455241.0623	0.9003	0.6248	0.0253
2455240.1279	0.1409	0.6278	0.0835
2455242.2752	0.8859	0.6278	0.0190
2455239.9187	0.9709	0.6294	0.0422
2455239.9187	0.9709	0.6294	0.0422
2455243.4862	0.8700	0.6301	0.0251
2455238.1145	0.5047	0.6310	0.0254
2455242.2123	0.8348	0.6321	0.0241
2455240.2640	0.2515	0.6322	0.0833
2455242.2639	0.8767	0.6370	0.0754
2455244.4192	0.6282	0.6397	0.0242
2455242.3418	0.9400	0.6415	0.0192
2455240.5987	0.5235	0.6422	0.0822
2455245.4261	0.4465	0.6440	0.0240
2455244.4861	0.6826	0.6532	0.0253
2455241.0557	0.8949	0.6533	0.0833
2455239.6588	0.7597	0.6536	0.0639
2455246.1626	0.0450	0.6624	0.0270
2455241.1314	0.9564	0.6634	0.0219
2455243.3452	0.7555	0.6639	0.0793
2455244.3456	0.5684	0.6673	0.1369
2455239.9433	0.9909	0.6678	0.0734
2455239.9433	0.9909	0.6678	0.0734
2455242.4694	0.0437	0.6711	0.0777
2455244.7535	0.8999	0.6767	0.0443

Table 4
(Continued)

HJD	Phase	Count Rate	Error
2455239.8757	0.9360	0.6789	0.0385
2455239.8757	0.9360	0.6789	0.0385
2455245.7622	0.7196	0.6791	0.0287
2455245.2921	0.3376	0.6800	0.0238
2455241.2730	0.0715	0.6874	0.0316
2455244.1518	0.4109	0.6887	0.0251
2455245.8983	0.8302	0.6899	0.0498
2455239.5265	0.6522	0.6903	0.0866
2455245.6932	0.6635	0.6952	0.0259
2455242.6066	0.1552	0.6967	0.1126
2455242.1366	0.7733	0.7007	0.0241
2455241.4677	0.2297	0.7084	0.1096
2455241.2015	0.0134	0.7110	0.0879
2455242.3305	0.9309	0.7144	0.0801
2455247.4282	0.0735	0.7171	0.1235
2455244.6195	0.7910	0.7225	0.0256
2455239.1965	0.3840	0.7265	0.0272
2455244.6875	0.8463	0.7278	0.0280
2455241.6044	0.3408	0.7289	0.0281
2455260.5494	0.7364	0.7303	0.0251
2455239.8071	0.8802	0.7356	0.0322
2455239.8071	0.8802	0.7356	0.0322
2455260.6830	0.8450	0.7362	0.0259
2455241.4754	0.2360	0.7367	0.0248
2455247.5018	0.1333	0.7406	0.0275
2455252.3137	0.0437	0.7427	0.1557
2455245.6279	0.6105	0.7446	0.0272
2455247.0211	0.7427	0.7446	0.0446
2455238.7285	0.0037	0.7541	0.0683
2455244.2115	0.4594	0.7543	0.1244
2455242.6147	0.1618	0.7576	0.0244
2455247.6354	0.2419	0.7609	0.0273
2455241.3334	0.1206	0.7633	0.0896
2455240.2692	0.2558	0.7636	0.0321
2455248.2943	0.7773	0.7637	0.1887
2455242.6817	0.2163	0.7645	0.0298
2455245.3591	0.3920	0.7649	0.0259
2455240.5443	0.4793	0.7685	0.0360
2455242.6757	0.2114	0.7690	0.0874
2455247.3674	0.0241	0.7725	0.0281
2455243.4790	0.8642	0.7730	0.0918
2455247.3007	0.9699	0.7740	0.0278
2455245.2841	0.3311	0.7749	0.0909
2455240.3965	0.3592	0.7788	0.0713
2455240.4695	0.4185	0.7841	0.0315
2455244.2852	0.5193	0.7859	0.0267
2455245.4848	0.4942	0.7907	0.0934
2455240.1331	0.1452	0.7947	0.0326
2455240.9237	0.7876	0.7949	0.0419
2455244.3526	0.5741	0.7961	0.0271
2455241.4059	0.1795	0.7964	0.0307
2455260.6164	0.7908	0.7977	0.0269
2455240.0584	0.0844	0.7993	0.0277
2455247.0993	0.8062	0.8064	0.0266
2455240.3306	0.3056	0.8066	0.1023
2455239.7335	0.8204	0.8090	0.0725
2455239.7392	0.8250	0.8108	0.0334
2455247.4954	0.1281	0.8111	0.1150
2455239.5352	0.6593	0.8168	0.0247
2455240.6064	0.5298	0.8168	0.0266
2455241.5379	0.2868	0.8174	0.0310
2455248.4839	0.9314	0.8182	0.2384
2455248.3616	0.8320	0.8226	0.1767
2455245.4927	0.5006	0.8262	0.0262

Table 4
(Continued)

HJD	Phase	Count Rate	Error
2455244.2185	0.4651	0.8380	0.0277
2455240.7426	0.6405	0.8409	0.0302
2455250.0220	0.1813	0.8422	0.1678
2455251.1087	0.0644	0.8441	0.1279
2455247.4345	0.0786	0.8461	0.0294
2455245.5544	0.5508	0.8495	0.1095
2455241.3391	0.1252	0.8558	0.0321
2455244.6125	0.7853	0.8583	0.0927
2455240.4635	0.4137	0.8589	0.0808
2455246.2963	0.1537	0.8644	0.0317
2455248.3675	0.8368	0.8669	0.0308
2455241.5984	0.3359	0.8677	0.1646
2455243.2841	0.7058	0.8690	0.0329
2455259.7472	0.0845	0.8739	0.0294
2455252.1796	0.9347	0.8745	0.1713
2455248.5637	0.9963	0.8755	0.0300
2455240.3359	0.3100	0.8771	0.0344
2455240.1962	0.1964	0.8795	0.1255
2455259.6142	0.9764	0.8808	0.0314
2455243.3508	0.7600	0.8840	0.0332
2455240.6702	0.5816	0.8851	0.0335
2455240.9925	0.8435	0.8859	0.0343
2455250.0894	0.2361	0.8892	0.1899
2455240.4027	0.3642	0.8904	0.0337
2455239.6036	0.7149	0.8904	0.0291
2455245.1507	0.2227	0.8979	0.1086
2455239.6685	0.7676	0.8994	0.0248
2455246.3553	0.2016	0.9011	0.0303
2455245.5609	0.5560	0.9037	0.0304
2455259.6809	0.0306	0.9047	0.0299
2455246.2905	0.1489	0.9057	0.1125
2455240.2017	0.2009	0.9115	0.0328
2455244.4122	0.6225	0.9171	0.1397
2455240.6648	0.5772	0.9205	0.1044
2455246.4198	0.2540	0.9211	0.1439
2455240.8078	0.6934	0.9255	0.0855
2455248.4317	0.8890	0.9291	0.0307
2455248.4920	0.9380	0.9326	0.0266
2455241.4003	0.1749	0.9338	0.1233
2455243.2077	0.6437	0.9375	0.0963
2455244.2781	0.5136	0.9426	0.1416
2455248.7736	0.1668	0.9486	0.0323
2455260.0144	0.3016	0.9510	0.0301
2455241.7427	0.4532	0.9559	0.0730
2455251.0420	0.0102	0.9584	0.1359
2455246.3490	0.1965	0.9590	0.1365
2455245.2210	0.2798	0.9738	0.0276
2455246.4878	0.3093	0.9755	0.1448
2455245.8307	0.7753	0.9783	0.0381
2455247.1660	0.8604	0.9827	0.0299
2455243.4175	0.8142	0.9832	0.0350
2455259.5469	0.9217	0.9841	0.0312
2455245.6211	0.6050	0.9855	0.1232
2455249.7010	0.9205	0.9862	0.1410
2455247.2337	0.9154	0.9902	0.0324
2455248.5574	0.9911	0.9925	0.1760
2455247.2941	0.9645	1.0006	0.1510
2455249.7710	0.9774	1.0031	0.1588
2455248.6345	0.0538	1.0058	0.0319
2455247.5670	0.1863	1.0125	0.0301
2455249.6316	0.8641	1.0131	0.1558
2455245.7566	0.7151	1.0164	0.1336
2455252.1127	0.8803	1.0165	0.1156
2455244.4795	0.6772	1.0184	0.1529

Table 4
(Continued)

HJD	Phase	Count Rate	Error
2455250.7753	0.7935	1.0229	0.1339
2455245.1583	0.2289	1.0231	0.0303
2455248.3002	0.7821	1.0245	0.0334
2455247.0919	0.8002	1.0379	0.1294
2455243.1459	0.5935	1.0411	0.0389
2455248.7677	0.1620	1.0476	0.1306
2455249.5616	0.8072	1.0525	0.2297
2455243.1408	0.5893	1.0606	0.0896
2455249.7771	0.9823	1.0718	0.0343
2455259.9479	0.2476	1.0737	0.0317
2455248.7040	0.1103	1.0789	0.0332
2455243.2151	0.6497	1.0809	0.0315
2455241.6766	0.3995	1.0864	0.2059
2455246.4265	0.2595	1.0874	0.0324
2455259.4805	0.8678	1.0880	0.0360
2455241.2682	0.0676	1.1044	0.1078
2455259.8811	0.1933	1.1121	0.0329
2455249.5678	0.8122	1.1141	0.0337
2455251.0484	0.0154	1.1255	0.0339
2455245.2126	0.2730	1.1271	0.1092
2455251.3767	0.2822	1.1316	0.1587
2455239.1905	0.3792	1.1365	0.2220
2455248.4255	0.8839	1.1499	0.1898
2455247.6288	0.2365	1.1577	0.1894
2455247.2274	0.9103	1.1832	0.1601
2455250.0282	0.1864	1.1937	0.0348
2455250.1623	0.2953	1.1951	0.0348
2455249.6380	0.8693	1.2024	0.0349
2455249.4894	0.7485	1.2033	0.2645
2455249.7074	0.9257	1.2097	0.0350
2455249.4956	0.7536	1.2101	0.0351
2455250.2233	0.3449	1.2125	0.2465
2455247.1588	0.8546	1.2132	0.2224
2455243.4118	0.8096	1.2147	0.1074
2455251.3094	0.2275	1.2211	0.1495
2455250.1560	0.2902	1.2325	0.1968
2455251.2427	0.1733	1.2434	0.1579
2455250.7052	0.7365	1.2489	0.1443
2455259.8142	0.1389	1.2491	0.0352
2455250.0957	0.2412	1.2500	0.0358
2455246.4942	0.3145	1.2534	0.0361
2455252.2525	0.9939	1.2543	0.0357
2455248.6282	0.0487	1.2619	0.1776
2455252.5144	0.2068	1.2792	0.2265
2455259.4135	0.8133	1.3130	0.0390
2455252.3199	0.0487	1.3167	0.0366
2455250.2295	0.3500	1.3205	0.0370
2455241.5324	0.2823	1.3266	0.2368
2455250.7814	0.7985	1.3559	0.0383
2455251.1760	0.1191	1.3658	0.1551
2455251.1824	0.1243	1.3888	0.0377
2455251.2490	0.1785	1.3895	0.0378
2455251.3156	0.2326	1.3925	0.0380
2455253.4535	0.9699	1.4223	0.0370
2455251.1150	0.0696	1.4373	0.0382
2455252.1858	0.9397	1.4585	0.0389
2455252.2463	0.9889	1.4677	0.2426
2455252.1192	0.8856	1.4685	0.0386
2455252.3865	0.1028	1.4710	0.0389
2455251.9853	0.7768	1.4855	0.0395
2455250.7126	0.7425	1.5466	0.0365
2455252.0518	0.8308	1.5624	0.0398
2455254.7265	0.0044	1.5829	0.0368
2455252.5206	0.2118	1.5979	0.0402

Table 4
(Continued)

HJD	Phase	Count Rate	Error
2455253.3196	0.8611	1.6573	0.0399
2455258.2750	0.8881	1.6645	0.0403
2455252.4528	0.1567	1.6683	0.0427
2455252.5775	0.2581	1.6841	0.3232
2455252.3803	0.0978	1.6842	0.2308
2455255.9319	0.9840	1.7178	0.0383
2455253.5234	0.0267	1.7225	0.0395
2455257.2038	0.0176	1.7352	0.0394
2455257.1368	0.9632	1.7397	0.0384
2455255.9987	0.0383	1.7459	0.0386
2455258.1414	0.7795	1.7501	0.0422
2455253.5837	0.0757	1.7620	0.0398
2455252.5837	0.2631	1.7714	0.0427
2455253.3883	0.9169	1.7860	0.0415
2455254.7951	0.0602	1.8175	0.0421
2455253.1856	0.7522	1.8576	0.0423
2455258.2084	0.8340	1.8616	0.0423
2455253.6538	0.1327	1.9056	0.0411
2455253.2529	0.8069	1.9492	0.0434
2455254.6605	0.9508	1.9526	0.0409
2455257.0028	0.8543	1.9729	0.0409
2455252.4469	0.1519	1.9918	0.4266
2455254.5269	0.8422	2.0146	0.0427
2455254.5932	0.8961	2.0328	0.0418
2455257.2705	0.0718	2.0522	0.0428
2455255.8664	0.9308	2.0580	0.0464
2455257.0698	0.9087	2.0837	0.0431
2455253.7233	0.1892	2.0989	0.0435
2455257.4714	0.2351	2.1115	0.0427
2455254.9946	0.2223	2.1199	0.0427
2455256.2661	0.2556	2.1240	0.0432
2455256.0660	0.0930	2.1416	0.0426
2455254.8626	0.1150	2.1446	0.0484
2455253.7913	0.2444	2.1569	0.0476
2455256.8685	0.7451	2.1827	0.0429
2455255.7296	0.8196	2.2516	0.0430
2455256.9361	0.8001	2.2700	0.0444
2455254.9273	0.1676	2.2799	0.0445
2455256.1995	0.2015	2.2922	0.0446
2455257.4045	0.1807	2.3029	0.0454
2455255.7987	0.8757	2.3257	0.0473
2455256.1327	0.1472	2.4130	0.0453
2455252.0457	0.8259	2.4242	0.4868
2455255.0621	0.2772	2.4558	0.0468
2455255.6639	0.7662	2.4959	0.0461
2455257.3380	0.1267	2.6107	0.0488

(This table is available in its entirety in machine-readable form.)

shorter than 24 hr, since the timestamp given to each daily luminosity value is calculated as the average of the times of the observations that went into that day's average magnitudes) to give a daily total of radiated energy, and then finally each of those daily energies were summed to obtain the total amount of energy radiated during the eruption, $E_{\rm rad}$. For U Sco, $E_{\rm rad} = 6.99 \times 10^{44}$ erg. Table 5 gives the average daily luminosities for each band as well as the summed total for each day.

We then use the method of Shara et al. (2010) to estimate the total amount of mass ejected during the eruption. This mass measurement is difficult to make; many previously published

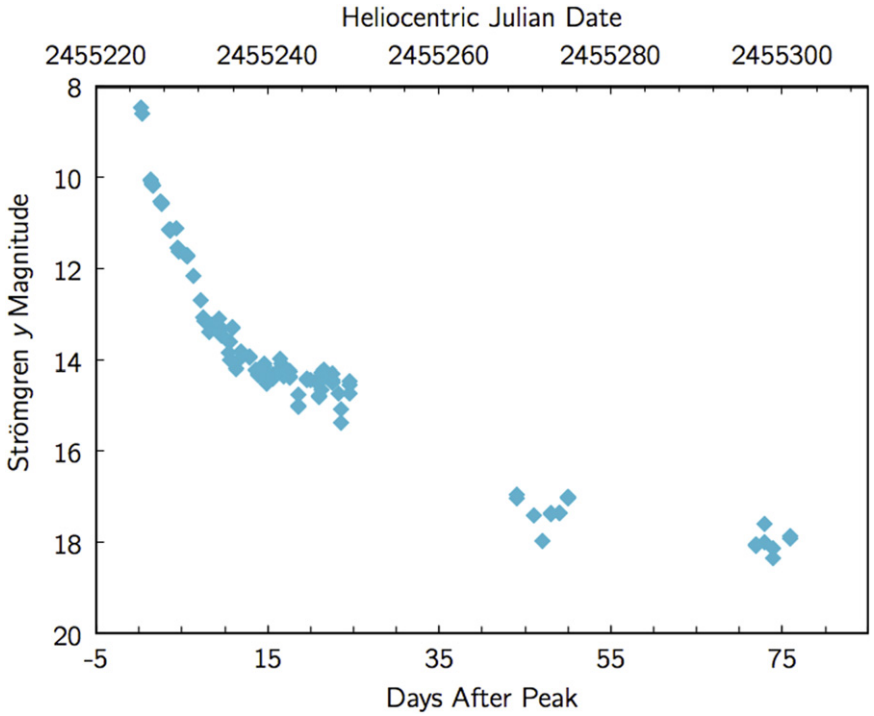

Figure 6. Strömgren *y* Light Curve, including all phases and therefore showing some eclipses. Strömgren *y*-band observations of U Sco during the 2010 eruption are from Handler on the SAAO 0.5 m, Landolt on the KPNO 2.1 m, Clem on the CTIO 1.0 m, Kiyota using his personal 0.25 m Schmidt–Cassegrain telescope, and Maehara using the Kwasan Observatory 0.25 m. This filter is no longer available at many telescopes, so we were unable to get complete coverage throughout the eruption, but we were able to get some epochs. Strömgren *y* is a narrow bandpass which is free from contamination by bright emission lines and is therefore ideal for testing Hachisu & Kato's (2006) universal decline law (Figure 7).

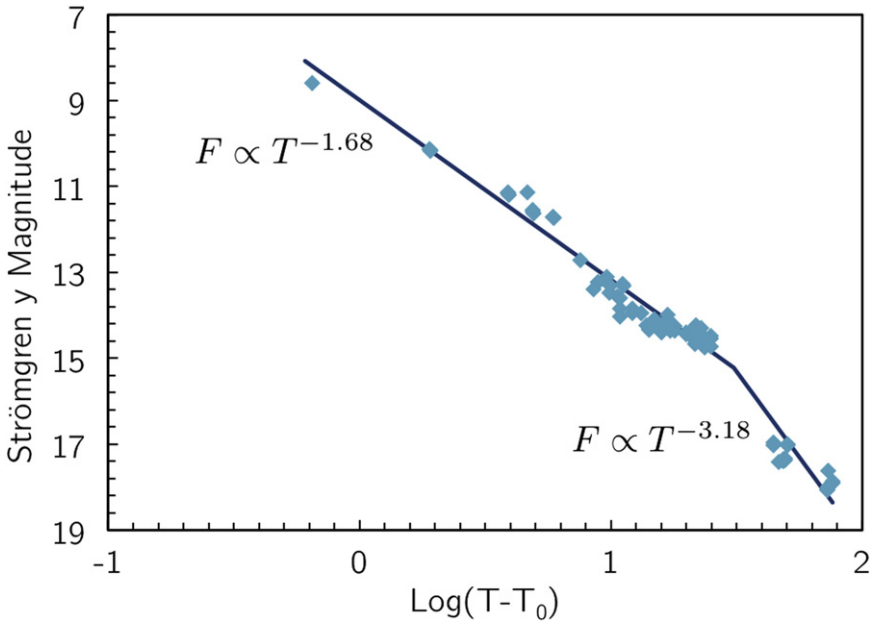

Figure 7. Strömgren *y* universal Decline Law. Strömgren *y* light curve (phases 0.1–0.9) of the U Sco 2010 eruption, plotted against the log of days after peak (Log $(T - T_0)$), and the best fit power laws to the data. The first power law has a best fit index of -1.68 ± 0.03, and the second has a best fit power law index of -3.18 ± 0.10. These are close to the predictions of Hachisu & Kato (2006), who give template fits of -1.75 and -3.5 for the first and second power laws, respectively.

methods rely on a number of assumptions and are uncertain to orders of magnitude (see below for further discussion of these methods). The Shara et al. (2010) method was developed by searching their extensive grid of nova models for characteristics that correlate with ejected mass, m_{ej}, under the important assumption that there is not equipartition between kinetic and radiated energy. They found a direct correlation between m_{ej} and E_{rad}. Obtaining E_{rad} requires comprehensive coverage of the eruption in multiple wavelengths and, for the first time, we have exactly what is needed. Although theory predicts that

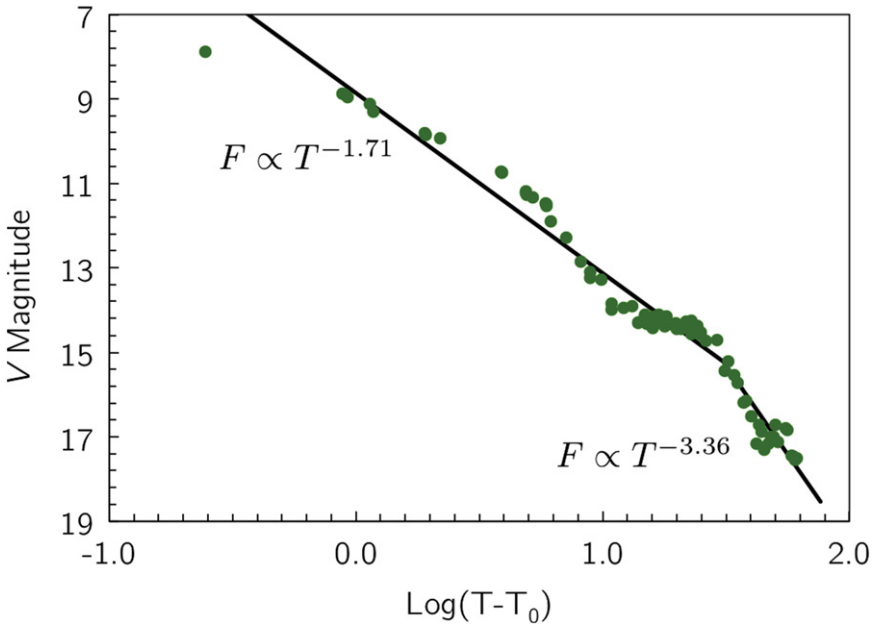

Figure 8. *V*-Band universal Decline Law. We also fit power laws to the *V*-band light curve, again plotted against the log of days after peak (Log($T - T_0$)), which give best fit indices of -1.71 ± 0.02 and -3.36 ± 0.14 for the first and second parts of the light curve, respectively. This is nearly consistent, within 1σ errors, with the predictions of Hachisu & Kato (2006). Although *V*-band does have potential emission line contamination, Figure 9 shows that it tracks well with Strömgren *y* and therefore the power law fits are still useful. The advantage of using *V*-band is that we have more comprehensive coverage, which allows us to better constrain the break time.

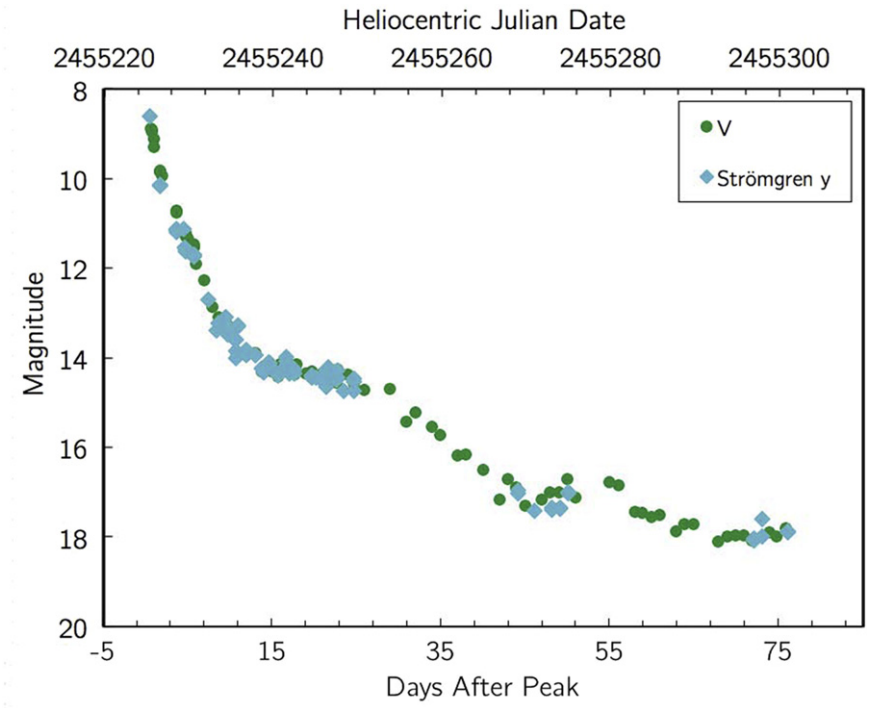

Figure 9. Strömgren *y* vs. *V*-Band. This comparison of the Strömgren *y* and *V*-band light curves shows that they are nearly identical, despite the extra emission line flux in the *V*-band. For this reason, we are confident that it is reasonable to fit the *V*-band light curve with a broken power law (Figure 8) to test the predictions of Hachisu & Kato's (2006) universal decline law.

most RNe should see a net WD mass gain over their eruption cycles (Yaron et al. 2005), we seek observational proof, and the Shara et al. (2010) method provides a new and independent way to evaluate this.

Following Shara et al. (2010), we can use $E_{\rm rad}$ to obtain the total $m_{\rm ej}$ as

$$m_{\rm ej} = 6 \times 10^{-18}\, E_{\rm rad} \quad (1)$$

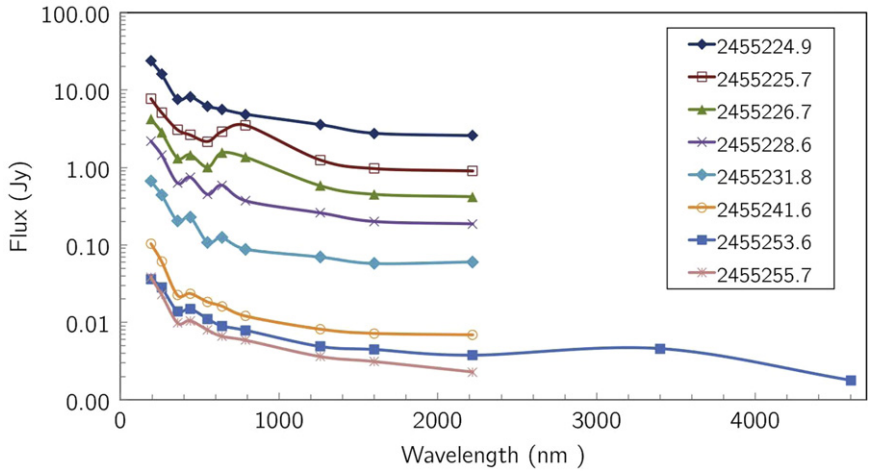

Figure 10. Spectral Energy Distributions (SEDs) for selected days (HJD listed in the legend) during the 2010 eruption of U Sco. The wavelength range extends from the *Swift* UVOT *w*2 filter (192.8 nm) to *K*-band (2200 nm) for most of the SEDs; on HJD 2455253.6 (Day +29) we also had serendipitous *WISE W*1 and *W*2 observations, so those are included for that day. (The SED for 2455252.3, which also had *WISE* observations, is essentially identical to that of day 2455253.6, so we only include one.) The legend in the figure gives the mean HJD of the observations that went into constructing that particular distribution. The majority of the energy is released early in the eruption near the short end of the spectrum, so the UVOT *w*1 and *w*2 coverage is particularly valuable. There were essentially zero usable UVOT observations just after the peak on JD 2455224.7, so the shortest wavelength points on days 2455224.9–2455236.8 were extrapolated from the *B* magnitudes on those dates as described in Section 4. The daily SEDs are used to calculate the total radiated energy, $E_{\rm rad} = 6.99^{+0.83}_{-0.57} \times 10^{44}$ erg, which is then used to estimate the total amount of mass ejected during the eruption, $m_{\rm ej} = 2.10^{+0.24}_{-0.17} \times 10^{-6}\,M_{\odot}$.

where $m_{\rm ej}$ is measured in g and $E_{\rm rad}$ in erg. With this, our estimate of the total mass ejected during the 2010 eruption is $m_{\rm ej} = 4.20 \times 10^{27}\,{\rm g} = 2.10 \times 10^{-6}\,M_{\odot}$.

It is difficult to place error bars on these values, as the uncertainties are not well defined, but we can make a good estimate. The majority of the radiated energy comes out right at the peak of the eruption in the UV regime. As noted previously, the early *Swift* observations are not usable, so the UVOT *w*1 and *w*2 values just after peak are extrapolated from the *B*-band measurement and model predictions. To estimate the error on the $m_{\rm ej}$ measurement, we vary the first extrapolated *w*2 value (which represents the majority of the energy released in the eruption) by one standard deviation of the $\langle B - w2\rangle$ values for times at which both were measured. This gives 1σ error bars on the $E_{\rm rad}$ of $+0.83 \times 10^{44}$ erg and -0.57×10^{44} erg, for a final $E_{\rm rad} = 6.99^{+0.83}_{-0.57} \times 10^{44}$ erg. For the ejected mass, the 1σ errors are $+0.24 \times 10^{-6}\,M_{\odot}$ and $-0.17 \times 10^{-6}\,M_{\odot}$. We thus conclude that $m_{\rm ej} = 2.10^{+0.24}_{-0.17} \times 10^{-6}\,M_{\odot}$.

Our new value of $m_{\rm ej} = 2.10^{+0.24}_{-0.17} \times 10^{-6}\,M_{\odot}$ is consistent with one of the (highly uncertain) measurements from previous eruptions, $\sim 3 \times 10^{-6}\,M_{\odot}$ from Hachisu et al. (2000), but an order of magnitude larger than the $\sim 10^{-7}\,M_{\odot}$ calculated by Anupama & Dewangan (2000). Hachisu et al. (2000) obtain their value of $m_{\rm ej}$ from light curve modeling, while Anupama & Dewangan (2000) consider the flux in the Balmer lines 11–12 days after peak. Both methods rely on a number of assumptions, detailed extensively in Appendix A of Schaefer (2011), which add significant uncertainties and model-dependencies to the results. Although the uncertainties on our $m_{\rm ej}$ value are not as well understood as we would like, the lack of dependence on any particular model gives us more confidence in our value than in these previous estimates.

Because U Sco is an eclipsing binary, the orbital period change across each eruption (ΔP) can be precisely calculated by measuring the change in eclipse times. The orbital period change across a given eruption and the amount of mass ejected during that eruption are related by $m_{\rm ej} = (M_{\rm WD}/A)(\Delta P/P)$, where A is a parameter that depends on the fraction of ejected matter captured by the companion and the specific angular momentum of the ejecta (Schaefer & Patterson 1983). Schaefer (2011) carefully measured ΔP across the 1999 eruption and, using the aforementioned relationship, derived $m_{\rm ej} = (4.3 \pm 6.7) \times 10^{-6}\,M_{\odot}$, which is consistent with our result. Using the same method for the 2010 eruption, however, results from Schaefer (2013) indicate that U Sco ejected $2.5 \times 10^{-5}\,M_{\odot}$ in its most recent eruption, which does not agree with our conclusions in this manuscript by an order of magnitude.

5. NET MASS CHANGE OF THE U SCO WHITE DWARF

The $m_{\rm ej}$ value is crucial for determining whether U Sco and similar RNe can become SNe Ia. For the WD to reach the Chandrasekhar limit and explode, it must have a net mass gain over its lifetime. We can compare the $m_{\rm ej}$ measurement with the total amount of mass accreted during the time preceding the eruption, $m_{\rm acc}$, to determine the overall mass change of the WD. Although in principle it is straightforward to measure the accreted mass by considering the *B*-band flux, in reality there are a number of uncertainties. The following values have been proposed for the yearly accretion rate of U Sco, all in units of $M_{\odot}\ {\rm yr}^{-1}$: $<3 \times 10^{-7}$ (Shen & Bildsten 2007), 4×10^{-7} (Duschl et al. 1990), 2.5×10^{-7} (Hachisu et al. 2000), 4.4×10^{-7} (Starrfield et al. 1988), and 1×10^{-7} (Kato 1990). $\dot{M}$ is therefore likely in the range of $1–4.4 \times 10^{-7}\,M_{\odot}\ {\rm yr}^{-1}$. For an average recurrence time of 10 years, this means that the total $m_{\rm acc}$ is therefore in the range $1–4.4 \times 10^{-6}\,M_{\odot}$ with an average value and 1σ error of $(2.9 \pm 1.3) \times 10^{-6}\,M_{\odot}$. Unfortunately, the values of $m_{\rm ej}$ and $m_{\rm acc}$ are too close, and the error bars too large, to make a conclusive statement about the net mass change of U Sco. An increase, decrease, or no change at all in the mass of the U Sco WD would all be consistent with this result.

Table 5
Average Daily U Sco Luminosities in erg s^{-1}

HJD	*Swift w2*	*Swift w1*	*U*	*B*	*V*	R_c	I_c	*J*	*H*	*K*	*WISE W1*	*WISE W2*	$L_{\rm total}$
2455224.90	2.60E+39	1.02E+39	3.10E+38	2.03E+38	1.13E+38	8.06E+37	9.65E+37	5.90E+37	2.45E+37	2.20E+37	…	…	4.53E+39
2455225.69	8.34E+38	3.28E+38	1.25E+38	6.52E+37	3.97E+37	4.15E+37	6.95E+37	2.06E+37	8.56E+36	7.69E+36	…	…	1.54E+39
2455226.66	4.62E+38	1.82E+38	5.36E+37	3.61E+37	1.85E+37	2.21E+37	2.70E+37	9.60E+36	3.98E+36	3.58E+36	…	…	8.19E+38
2455227.63	3.31E+38	1.30E+38	3.70E+37	2.59E+37	1.23E+37	1.36E+37	1.41E+37	6.41E+36	2.66E+36	2.39E+36	…	…	5.76E+38
2455228.59	2.37E+38	9.34E+37	2.56E+37	1.85E+37	8.24E+36	8.42E+36	7.36E+36	4.28E+36	1.78E+36	1.60E+36	…	…	4.06E+38
2455229.69	1.65E+38	6.50E+37	1.65E+37	1.29E+37	5.09E+36	5.00E+36	4.50E+36	3.00E+36	1.30E+36	1.12E+36	…	…	2.79E+38
2455230.68	1.23E+38	4.82E+37	1.34E+37	9.56E+36	3.69E+36	3.29E+36	3.15E+36	1.92E+36	8.36E+35	8.61E+35	…	…	2.08E+38
2455231.83	7.22E+37	2.84E+37	8.29E+36	5.63E+36	1.98E+36	1.77E+36	1.75E+36	1.15E+36	5.09E+35	5.13E+35	…	…	1.22E+38
2455232.83	5.65E+37	2.22E+37	5.10E+36	4.40E+36	1.15E+36	9.51E+35	1.07E+36	8.17E+35	3.66E+35	3.76E+35	…	…	9.29E+37
2455233.59	2.94E+37	1.16E+37	3.14E+36	2.29E+36	8.68E+35	7.10E+35	7.32E+35	5.79E+35	2.63E+35	2.75E+35	…	…	4.99E+37
2455234.60	2.60E+37	1.02E+37	3.08E+36	2.02E+36	7.84E+35	6.07E+35	6.24E+35	4.09E+35	1.89E+35	2.01E+35	…	…	4.41E+37
2455235.59	1.18E+37	4.65E+36	1.44E+36	9.13E+35	4.29E+35	3.15E+35	3.62E+35	2.89E+35	1.36E+35	1.47E+35	…	…	2.05E+37
2455236.84	1.05E+37	4.13E+36	1.20E+36	8.11E+35	4.19E+35	2.98E+35	3.41E+35	2.03E+35	9.68E+34	1.07E+35	…	…	1.81E+37
2455237.77	8.68E+36	3.74E+36	9.97E+35	8.57E+35	4.36E+35	2.93E+35	3.48E+35	1.92E+35	8.54E+34	8.99E+34	…	…	1.57E+37
2455238.43	8.15E+36	2.94E+36	8.29E+35	5.66E+35	2.99E+35	2.26E+35	2.61E+35	1.66E+35	7.67E+34	8.13E+34	…	…	1.36E+37
2455239.63	6.82E+36	3.34E+36	9.68E+35	6.05E+35	3.33E+35	2.38E+35	2.82E+35	1.44E+35	6.89E+34	7.34E+34	…	…	1.29E+37
2455240.51	8.68E+36	3.45E+36	8.05E+35	5.40E+35	2.96E+35	2.02E+35	2.35E+35	1.52E+35	6.63E+34	6.57E+34	…	…	1.45E+37
2455241.61	1.12E+37	3.93E+36	9.10E+35	5.83E+35	3.36E+35	2.31E+35	2.38E+35	1.35E+35	6.37E+34	5.88E+34	…	…	1.77E+37
2455242.54	9.11E+36	3.44E+36	8.42E+35	5.33E+35	2.99E+35	2.05E+35	2.70E+35	1.48E+35	6.76E+34	6.28E+34	…	…	1.50E+37
2455243.52	6.32E+36	2.84E+36	8.13E+35	5.34E+35	2.86E+35	1.94E+35	2.35E+35	1.25E+35	5.85E+34	5.13E+34	…	…	1.15E+37
2455244.45	6.69E+36	2.99E+36	7.85E+35	4.97E+35	2.73E+35	1.88E+35	2.29E+35	1.24E+35	6.09E+34	5.33E+34	…	…	1.19E+37
2455245.58	9.25E+36	3.45E+36	6.87E+35	4.88E+35	2.72E+35	1.82E+35	2.00E+35	1.23E+35	6.33E+34	5.54E+34	…	…	1.48E+37
2455246.49	1.17E+37	4.27E+36	8.97E+35	5.40E+35	2.86E+35	1.97E+35	2.19E+35	1.15E+35	5.61E+34	4.90E+34	…	…	1.83E+37
2455247.52	1.03E+37	3.71E+36	7.95E+35	4.98E+35	2.69E+35	1.87E+35	2.13E+35	1.08E+35	4.96E+34	4.33E+34	…	…	1.61E+37
2455248.58	8.75E+36	2.95E+36	7.56E+35	4.99E+35	2.75E+35	1.73E+35	2.10E+35	1.02E+35	4.38E+34	3.82E+34	…	…	1.38E+37
2455249.58	8.25E+36	2.85E+36	7.19E+35	3.99E+35	2.36E+35	1.57E+35	1.79E+35	9.19E+34	4.02E+34	4.12E+34	…	…	1.30E+37
2455250.54	9.75E+36	2.76E+36	5.56E+35	3.63E+35	1.99E+35	1.34E+35	1.63E+35	8.29E+34	3.69E+34	4.44E+34	…	…	1.41E+37
2455251.66	7.45E+36	2.54E+36	5.99E+35	3.91E+35	2.00E+35	1.44E+35	1.76E+35	8.23E+34	3.77E+34	2.76E+34	…	…	1.17E+37
2455252.32	4.27E+36	1.82E+36	5.82E+35	3.80E+35	2.02E+35	1.36E+35	1.66E+35	8.15E+34	3.86E+34	2.98E+34	2.68E+34	3.93E+33	7.73E+36
2455253.61	3.96E+36	1.80E+36	5.66E+35	3.69E+35	2.03E+35	1.28E+35	1.56E+35	8.06E+34	3.94E+34	3.22E+34	2.75E+34	4.52E+33	7.37E+36
2455254.78	4.63E+36	1.72E+36	4.76E+35	3.10E+35	1.72E+35	1.10E+35	1.35E+35	6.95E+34	3.30E+34	2.51E+34	…	…	7.68E+36
2455255.66	4.13E+36	1.46E+36	3.99E+35	2.60E+35	1.45E+35	9.38E+34	1.16E+35	5.97E+34	2.76E+34	1.95E+34	…	…	6.71E+36
2455256.66	3.02E+36	1.15E+36	3.35E+35	2.18E+35	1.23E+35	8.01E+34	1.00E+35	5.12E+34	2.29E+34	1.50E+34	…	…	5.12E+36
2455257.35	1.88E+36	1.02E+36	2.86E+35	1.87E+35	1.04E+35	6.80E+34	8.39E+34	4.20E+34	1.90E+34	1.21E+34	…	…	3.70E+36
2455258.50	2.58E+36	8.94E+35	2.45E+35	1.59E+35	8.88E+34	5.75E+34	7.00E+34	3.42E+34	1.57E+34	9.61E+33	…	…	4.15E+36
2455259.75	1.62E+36	7.43E+35	2.01E+35	1.31E+35	7.32E+34	4.49E+34	5.44E+34	2.52E+34	1.08E+34	1.33E+34	…	…	2.92E+36
2455260.47	1.16E+36	5.00E+35	1.57E+35	1.02E+35	5.69E+34	3.64E+34	4.52E+34	2.18E+34	9.45E+33	1.02E+34	…	…	2.10E+36
2455261.85	1.00E+36	4.23E+35	1.22E+35	7.92E+34	4.37E+34	2.92E+34	3.73E+34	1.88E+34	8.26E+33	7.60E+33	…	…	1.77E+36
2455262.76	1.04E+36	4.41E+35	1.29E+35	8.32E+34	4.58E+34	2.55E+34	3.21E+34	1.87E+34	7.18E+33	8.01E+33	…	…	1.83E+36
2455263.69	1.03E+36	4.36E+35	1.02E+35	6.60E+34	3.74E+34	2.21E+34	2.80E+34	1.45E+34	6.20E+33	6.37E+33	…	…	1.75E+36
2455264.63	6.53E+35	2.54E+35	8.06E+34	5.19E+34	3.02E+34	1.91E+34	2.43E+34	1.10E+34	5.31E+33	4.98E+33	…	…	1.13E+36
2455265.63	4.79E+35	1.72E+35	5.50E+34	3.51E+34	1.96E+34	1.24E+34	1.62E+34	6.98E+33	3.03E+33	2.92E+33	…	…	8.03E+35
2455266.56	3.14E+35	1.40E+35	3.61E+34	2.27E+34	1.17E+34	7.41E+33	1.01E+34	3.78E+33	1.34E+33	1.40E+33	…	…	5.49E+35
2455267.64	4.02E+35	1.66E+35	6.24E+34	4.00E+34	2.29E+34	1.38E+34	1.75E+34	6.63E+33	3.17E+33	3.56E+33	…	…	7.38E+35
2455268.58	4.48E+35	1.65E+35	5.56E+34	3.55E+34	1.82E+34	1.04E+34	1.21E+34	5.57E+33	1.96E+33	2.65E+33	…	…	7.55E+35
2455269.55	4.22E+35	1.46E+35	2.70E+34	1.68E+34	8.96E+33	5.77E+33	7.24E+33	4.72E+33	1.77E+33	8.64E+32	…	…	6.41E+35
2455270.39	5.27E+35	1.81E+35	3.15E+34	1.97E+34	1.02E+34	6.35E+33	8.00E+33	3.93E+33	1.59E+33	1.10E+33	…	…	7.90E+35
2455271.72	7.37E+35	2.34E+35	3.63E+34	2.29E+34	1.15E+34	6.96E+33	8.80E+33	3.17E+33	1.42E+33	1.36E+33	…	…	1.06E+36

Table 5
(Continued)

HJD	*Swift w*2	*Swift w*1	*U*	*B*	*V*	R_c	I_c	*J*	*H*	*K*	*WISE W*1	*WISE W*2	$L_{\rm total}$
2455272.75	3.60E+35	1.44E+35	4.09E+34	2.59E+34	1.50E+34	9.29E+33	1.21E+34	4.32E+33	2.01E+33	2.04E+33	…	…	6.15E+35
2455273.77	4.94E+35	2.14E+35	4.72E+34	3.00E+34	1.52E+34	8.86E+33	1.08E+34	2.96E+33	1.29E+33	2.08E+33	…	…	8.26E+35
2455274.86	3.86E+35	2.03E+35	6.64E+34	4.26E+34	2.31E+34	1.37E+34	1.61E+34	5.71E+33	3.17E+33	3.60E+33	…	…	7.64E+35
2455275.62	3.84E+35	1.93E+35	4.00E+34	2.53E+34	1.26E+34	7.52E+33	1.06E+34	4.10E+33	1.52E+33	1.57E+33	…	…	6.80E+35
2455276.47	4.03E+35	2.20E+35	4.49E+34	2.85E+34	1.44E+34	8.54E+33	1.16E+34	4.21E+33	1.50E+33	1.93E+33	…	…	7.38E+35
2455277.33	4.23E+35	2.50E+35	4.36E+34	2.77E+34	1.40E+34	8.28E+33	1.14E+34	4.18E+33	1.51E+33	1.84E+33	…	…	7.85E+35
2455278.52	3.54E+35	1.69E+35	4.40E+34	2.79E+34	1.41E+34	8.34E+33	1.14E+34	4.19E+33	1.50E+33	1.86E+33	…	…	6.37E+35
2455279.72	2.96E+35	1.13E+35	6.23E+34	3.99E+34	2.08E+34	1.20E+34	1.51E+34	4.55E+33	1.44E+33	3.15E+33	…	…	5.68E+35
2455280.67	2.85E+35	1.35E+35	5.65E+34	3.61E+34	1.92E+34	1.17E+34	1.38E+34	4.60E+33	2.33E+33	2.85E+33 t	…	…	5.67E+35
2455281.73	2.20E+35	9.88E+34	3.63E+34	2.29E+34	1.20E+34	7.10E+33	8.85E+33	2.63E+33	1.52E+33	1.46E+33	…	…	4.12E+35
2455282.79	1.68E+35	7.14E+34	2.17E+34	1.33E+34	6.60E+33	3.60E+33	4.93E+33	9.37E+32	8.17E+32	4.07E+32	…	…	2.91E+35
2455283.72	1.82E+35	7.81E+34	2.00E+34	1.22E+34	6.18E+33	2.88E+33	3.75E+33	7.70E+32	2.49E+31	3.25E+32	…	…	3.06E+35
2455284.70	1.97E+35	8.52E+34	2.02E+34	1.23E+34	5.04E+33	3.09E+33	3.99E+33	7.05E+32	2.96E+32	1.03E+32	…	…	3.28E+35
2455285.73	1.56E+35	7.34E+34	2.36E+34	1.45E+34	5.62E+33	2.83E+33	4.16E+33	4.70E+33	1.28E+33	2.16E+32	…	…	2.86E+35
2455286.61	1.22E+35	6.30E+34	1.36E+34	8.02E+33	3.12E+33	1.58E+33	2.65E+33	2.08E+33	5.70E+32	0.00E+00[a]	…	…	2.16E+35
2455287.50	9.34E+34	5.39E+34	6.02E+33	3.07E+33	1.01E+33	4.76E+32	1.30E+33	0.00E+00	0.00E+00	0.00E+00	…	…	1.59E+35
2455288.75	2.01E+35	8.00E+34	1.12E+34	6.46E+33	2.72E+33	1.50E+33	2.02E+33	0.00E+00	0.00E+00	0.00E+00	…	…	3.05E+35
2455289.75	1.61E+35	6.43E+34	6.44E+33	3.35E+33	2.80E+33	1.21E+33	1.36E+33	0.00E+00	0.00E+00	0.00E+00	…	…	2.41E+35
2455290.75	1.55E+35	6.18E+34	5.69E+33	2.86E+33	1.28E+33	6.91E+32	6.59E+32	0.00E+00	0.00E+00	0.00E+00	…	…	2.28E+35
2455291.74	1.49E+35	5.94E+34	4.97E+33	2.39E+33	0.00E+00	2.01E+32	1.72E+19	0.00E+00	0.00E+00	0.00E+00	…	…	2.16E+35
2455292.74	1.43E+35	5.71E+34	4.27E+33	1.93E+33	0.00E+00	0.00E+00	0.00E+00	0.00E+00	0.00E+00	0.00E+00	…	…	2.06E+35
2455293.74	1.28E+35	5.14E+34	2.51E+33	7.82E+32	0.00E+00	0.00E+00	5.32E+31	0.00E+00	0.00E+00	0.00E+00	…	…	1.83E+35

Note.
[a] 0.00E+00 entries denote values so small they are essentially equal to 0.

6. CONCLUSIONS

The 2010 eruption of U Sco was the all-time best observed nova eruption at the time. (In sheer number of observations, U Sco has since been eclipsed by the 2011 eruption of the RN T Pyxidis (Schaefer 2012), but U Sco still has the most comprehensive overall coverage.) The early discovery, fast notification, and regular observations by our collaboration of professional and amateur astronomers allowed us to define the entire eruption light curve from shortly after peak until the return to quiescence 67 days later. For previous eruptions there are a few isolated points late in the tail of the decline, but this was the first time U Sco was intentionally monitored for more than 30 days after peak (Schaefer 2010). This systematic coverage allows us to describe the overall shape of the light curve, starting with the fast decline (days 0–14), and continuing through the first plateau (days 14–32) which is caused by the supersoft X-ray source as described by Hachisu et al. (2008) and coincides with the return of the optical eclipses. The first plateau falls off starting on day 32, and our long-term coverage of the eruption allowed us to discover the second plateau in the light curve, which lasts from days 41 to 54 and is as yet unexplained, but occurs at the same time as the aperiodic optical dips that have been linked to transient vertical structure in the accretion disk as it reforms after being blown away during the eruption (Pagnotta et al. 2010; Schaefer et al. 2011). Following the second plateau, U Sco undergoes a jittery return to quiescence (days 54–67), where it will remain until the next eruption, which should occur around 2020.

We were able to combine our comprehensive *V*-band coverage with our Strömgren *y* observations to show that U Sco is nearly consistent (within 1σ errors) with the universal decline law of Hachisu & Kato (2006). We were unable to obtain a high-enough cadence in *y*-band to use it exclusively as recommended, but our multiple Strömgren *y* observations at different epochs allow us to compare it with the *V*-band light curve and see that they track each other nearly identically, giving us confidence that we can use the *V*-band data to test the universal decline law. We calculate power law indices of -1.71 ± 0.02 for the first phase and -3.36 ± 0.14 for the second, and a break time of $T = \mathrm{HJD}\ 2455255.38 \pm 1.01$ days. Our fits our nearly consistent with the template values from Hachisu & Kato (2006) of -1.75 and -3.5 for the first and second power laws, respectively, with the first power law falling just outside the 1σ range of our fit, and the second falling just on the edge. This is likely due to the fact that U Sco does not have a smooth light curve shape, but instead has the unusual features detailed above, which slightly skew the light curve away from the model, since it is constructed for novae with smoother, more regular declines.

Our full multi-wavelength coverage confirmed the predicted temporal correlation between the (first) optical/near-IR plateau, the return of the eclipses, and the detection of the supersoft X-rays. The simultaneity of these three events is due to the shell becoming optically thin at that time, revealing the inner binary, which allows us to see both the X-rays and the reestablishment of the eclipses. The high cadence UV coverage shows for the first time how well the UV light curve tracks the optical one, including showing the primary eclipses and possibly the secondary eclipses as well.

We were also able, for the first time, to construct daily SEDs of a nova eruption covering an average wavelength range of 193 nm (*Swift* UVOT *w2*) to 2200 nm (*K*-band). Using this unique data set, we were able to calculate the total radiated energy from the eruption, $E_{\mathrm{rad}} = 6.99^{+0.83}_{-0.57} \times 10^{44}$ erg, which we then used to estimate the amount of mass ejected, $m_{\mathrm{ej}} = 2.05^{+0.26}_{-0.18} \times 10^{-6}\,M_{\odot}$, following Shara et al. (2010). This calculation would not have been possible without the exceptional amount of data that was collected for U Sco throughout the entire eruption over many wavelengths. Unfortunately, the measurements of the total mass accreted since the last eruption, m_{acc}, are not precise enough to allow us to determine whether the U Sco WD is gaining or losing mass over the course of a full eruption cycle. In spite of this, the Shara et al. (2010) method is an improvement upon previous methods and should be tested on and applied to future nova eruptions whenever enough observations can be made. Early UV coverage is particularly important to this computation, and this can best be obtained from the *Swift* UVOT as soon as possible after the eruptions are detected.

This is the most comprehensive multi-wavelength light curve of a nova eruption, covering more wavelengths over a longer time period than ever before. With this unprecedented data set we discovered three new phenomena and tested some of the theoretical predictions that have been made for novae in general and U Sco in particular. We encourage future similar campaigns whenever possible to determine whether these new phenomena are unique to U Sco or are in fact common among novae or recurrent novae, and to continue to find unexpected phenomena as we open new time and wavelength regimes.

This research was supported by NSF Grant AST-0708079, the Louisiana Space Consortium and NASA through Grant NNX10AI40H, as well as the Kathryn W. Davis Postdoctoral Scholar program, which is supported in part by the New York State Education Department and by the National Science Foundation under grant numbers DRL-1119444 and DUE-1340006. A.U.L. acknowledges support from NSF Grant AST-0803158. K.L.P. and J.P.O. acknowledge support from the UK Space Agency. G.H. acknowledges partial financial support from the Austrian FWF grant P20526-N16 and encouragement from Patrick Woudt.

We heartily thank all members of the USCO2010 collaboration, whose observations were critical to our successful campaign. We acknowledge with many thanks the variable star observations from the AAVSO International Database contributed by observers worldwide and used in this research, as well as the observers of the Center for Backyard Astrophysics. This publication makes use of data products from the *Wide-field Infrared Survey Explorer*, which is a joint project of the University of California, Los Angeles, and the Jet Propulsion Laboratory/California Institute of Technology, funded by the National Aeronautics and Space Administration. This research has made use of the NASA/IPAC Infrared Science Archive, which is operated by the Jet Propulsion Laboratory, California Institute of Technology, under contract with the National Aeronautics and Space Administration.

REFERENCES

Anupama, G. C., & Dewangan, G. C. 2000, AJ, 119, 1359
Cardelli, J. A., Clayton, G. C., & Mathis, J. S. 1989, ApJ, 345, 245
Duschl, W. J., Livio, M., & Truran, J. W. 1990, ApJ, 360, 232
Hachisu, I., & Kato, M. 2006, ApJS, 167, 59
Hachisu, I., Kato, M., Kato, T., & Matsumoto, K. 2000, ApJL, 528, L97

Hachisu, I., Kato, M., Kiyota, S., et al. 2008, in ASP Conf. Ser. 401, RS Ophiuchi (2006) and the Recurrent Nova Phenomenon, ed. A. Evans, M. F. Bode, T. J. O'Brien & M. J. Darnley (San Francisco, CA: ASP), 206
Kato, M. 1990, ApJ, 355, 277
Manousakis, A., Revnivtsev, M., Krivonos, R., & Bozzo, E. 2010, ATel, 2412, 1
Ness, J.-U., Schaefer, B. E., Dobrotka, A., et al. 2012, ApJ, 745, 43
Orio, M., Behar, E., Gallagher, J., et al. 2013, MNRAS, 429, 1342
Osborne, J. P., Page, K. L., Wynn, G., et al. 2010, ATel, 2442, 1
Page, M. J., Kuin, N. P. M., Breeveld, A. A., et al. 2013, MNRAS, 436, 1684
Pagnotta, A., Schaefer, B. E., Handler, G., et al. 2010, ATel, 2507, 1
Roming, P. W. A., Kennedy, T. E., Mason, K. O., et al. 2005, SSRv, 120, 95
Schaefer, B. E. 2005, ApJL, 621, L53
Schaefer, B. E. 2010, ApJS, 187, 275
Schaefer, B. E. 2011, ApJ, 742, 112
Schaefer, B. E. 2012, American Astronomical Society Meeting Abstracts, 219, 348.21
Schaefer, B. E. 2013, American Astronomical Society Meeting Abstracts, 221, 233.06
Schaefer, B. E., Harris, B. G., Dvorak, S., Templeton, M., & Linnolt, M. 2010a, IAUC, 9111, 1
Schaefer, B. E., & Patterson, J. 1983, ApJ, 268, 710
Schaefer, B. E., Pagnotta, A., LaCluyze, A. P., et al. 2011, ApJ, 742, 113
Schaefer, B. E., Pagnotta, A., Osborne, J. P., et al. 2010c, ATel, 2477, 1
Schaefer, B. E., Pagnotta, A., Xiao, L., et al. 2010b, AJ, 140, 925
Schlegel, E. M., Schaefer, B. E., Pagnotta, A., et al. 2010d, ATel, 2419, 1
Shara, M. M., Yaron, O., Prialnik, D., & Kovetz, A. 2010, ApJL, 712, L143
Shen, K. J., & Bildsten, L. 2007, ApJ, 660, 1444
Simonson, M., & MacRobert, A. 2010, Sky & Telescope May 2010, 18
Starrfield, S., Sparks, W. M., & Shaviv, G. 1988, ApJL, 325, L35
Thoroughgood, T. D., Dhillon, V. S., Littlefair, S. P., Marsh, T. R., & Smith, D. A. 2001, MNRAS, 327, 1323
Webbink, R. F., Livio, M., Truran, J. W., & Orio, M. 1987, ApJ, 314, 653
Wright, E. L., Eisenhardt, P. R. M., Mainzer, A. K., et al. 2010, AJ, 140, 1868
Yaron, O., Prialnik, D., Shara, M. M., & Kovetz, A. 2005, ApJ, 623, 398